DESIGN AND SIMULATION OF AN INTELLIGENT MEDICAL VENTILATOR SYSTEM FOR PATIENT-VENTILATOR SYNCHRONY AND LUNG PROTECTION

WANZALA JIMMY NABENDE

2021/PhD/028/PS

A THESIS SUBMITTED TO FACULTY OF SCIENCE IN FULFILLMENT OF THE REQUIREMENTS LEADING TO THE AWARD OF THE DEGREE OF DOCTOR OF PHILOSOPHY IN PHYSICS OF MBARARA UNIVERSITY OF SCIENCE AND TECHNOLOGY

JANUARY, 2024

DECLARATION

I, WANZALA JIMMY NABENDE, declare that the work presented in this thesis is my original work and it has never been presented at any institution for any academic award. Where I have used the works of others, due acknowledgement and sources are provided.

Date : JANUARY 30, 2024

Signature : 

APPROVAL

This research has been done under our supervision and submitted with our approval:

Date : 30/01/2024

Signature :

Dr. Michael Robson Atim

Department of Physics,

Faculty of Science,

Mbarara University of Science and Technology.

Date : 30/01/2024

Signature :

Dr. Johnes Obungoloch

Department of Biomedical Engineering,

Faculty of Applied Science and Technology,

Mbarara University of Science and Technology.

ACKNOWLEDGEMENTS

First and foremost, I thank God for the gifts of wisdom, knowledge, understanding, faith, and good health; before, during, and after the degree of Doctor of Philosophy in Physics.

I gratefully appreciate my supervisors; Dr. Michael Robson Atim and Dr. Johnes Obungoloch, for the all-round support given to me during the study that enabled me to learn how to better conduct research, present results, and contribute to academia through publication of original research.

I greatly thank the Physics department at Mbarara University of Science and Technology, for the social and academic guidance during the course of this study.

Finally, my family (parents, brothers, sisters, and relatives) and friends contributed a big part in the achievement of the doctoral degree. I thank them. They kept me going especially during the academic challenges. It is through them that I was motivated and disciplined to make sure that I am result oriented.

DEDICATION

In loving memory of my late sister (Namono Slyvia) and to my entire family.

Contents

Declaration i

Approval ii

Acknowledgement iii

Dedication iv

List of Figures viii

List of Tables xiii

Acronyms xiv

Publications xvii

Abstract xviii

1 Introduction 1

1.1 Background 1

1.2 Problem Statement 5

1.3 Aim of the Study 5

1.4 Objectives of the Study 5

1.5 Scope 6

1.6 Significance 6
1.7 Thesis Outline 7
1.7.1 Chapter Two 7
1.7.2 Chapter Three 7
1.7.3 Chapter Four 7
1.7.4 Chapter Five 8

2 Theoretical Background and Literature Review 9
2.1 Electrical Analogy of Respiratory System and the Physics of Breathing . . 9
2.2 Fuzzy Logic 12
2.2.1 Crisp Inputs: 13
2.2.2 Fuzzification and Membership Functions: 13
2.2.3 Expert Fuzzy System/ Rule base: 14
2.2.4 Defuzzification and Membership Functions: 15
2.2.5 Crisp Outputs: 16
2.3 Berlin Definition of ARDS 16
2.4 Mechanical Ventilators 17
2.4.1 Pressure Support Ventilation 17
2.4.2 Proportional Assist Ventilator 18
2.4.3 Neurally Adjusted Ventilator Assist 19

3 Materials and methods 24
3.1 Materials 24
3.2 Methods 26
3.2.1 Design and Simulation of a Physician Based Fuzzy Logic System for Ventilator Adjustments in Acute Respiratory Distress Syndrome (ARDS) Patients to Ensure Lung Protection 26

3.2.2 Design and Simulation of a Physician Based Fuzzy Neural System for Ventilator Adjustments in ARDS Patients to Ensure Lung Protection 41
3.2.3 Build a Feed-in Imaging Model to Detect Lung and Brain Scans using Convolutional Neural Network 50
3.2.4 Design and Simulation of an Intelligent System to Test and Validate Patient Ventilator Synchrony and Lung Protection using Real-time Medical Imaging and Fuzzy Expert System 56

4 Results and Discussion 68
4.1 Design and Simulation of a Physician Based Fuzzy Logic System for Ventilator Adjustments in Acute Respiratory Distress Syndrome (ARDS) Patients to Ensure Lung Protection 68
4.1.1 Decremental PEEP Algorithm 68
4.1.2 Incremental PEEP Algorithm 75
4.2 Design and Simulation of a Physician Based Fuzzy Neural System for Ventilator Adjustments in ARDS Patients to Ensure Lung Protection . . . 85
4.3 Build a Feed-in Imaging Model to Detect Lung and Brain Scans using Convolutional Neural Network 94
4.4 Design and Simulation of an Intelligent System to Test and Validate Patient Ventilator Synchrony and Lung Protection using Real-time Medical Imaging and Fuzzy Expert System 100

5 Conclusions and recommendations 106
5.1 Conclusion 106
5.2 Recommendations 108

Appendix 128

List of Figures

2.1 Electrical representation of the lung 11

2.2 Brainstem signals driving the respiratory rhythm 20

3.1 The ventilator logic system architecture 27

3.2 Fuzzy logic designer showing FiO_2 membership functions 31

3.3 Fuzzy logic designer showing high-PEEP membership functions 32

3.4 Fuzzy logic designer showing low-PEEP membership functions 33

3.5 Fuzzy logic designer showing change-in-PEEP membership functions 34

3.6 Membership function for FiO_2 input 36

3.7 Membership function for high-PEEP input 37

3.8 Membership function for low-PEEP input 38

3.9 Membership function for change in PEEP output 39

3.10 Neuro-Fuzzy Designer structure with two inputs, 20 membership functions for each input; and one output 41

3.11 Fuzzified ARDS Berlin definition of ARDSNet PEEP table 43

3.12 Fuzzy based ARDS Berlin definition 44

3.13 Input-Output logic for patient subsystem 45

3.14 FiO_2 and PEEP input subsystem 47

3.15 FiO_2 and PEEP fuzzy subsystem 49

3.16 Conditions of the lung: (a) COVID-19, (b) healthy, and (c) pneumonia . . 51

3.17 Conditions of the brain: (a) acute ischemic stroke, (b) healthy, and (c) hemorrhagic stroke 53
3.18 General MATLAB/ Simulink schematic system showing the image input, processing of images using convolutional neural network, positive end expiratory pressure, and values passed through the lung transfer function 58
3.19 Convolutional neural network Simulink subsytem for the brain and lung images 59
3.20 Fuzzy logic based PEEP subsystem containing the trained four fuzzy logic PEEP algorithms 62
3.21 Neural based PEEP subsystem containing the trained two neural fuzzy algorithms 63
3.22 Electrical circuit of the respiration system 64
3.23 Lung transfer function subsystem with ventilator screen to display pressure, volume, and flow graphs 67

4.1 Rule viewer: decremental high-PEEP algorithm 1; two crisp inputs: FiO_2 = 0.3 and high-PEEP = 5 giving a crisp output: change in PEEP = 0 . . 69
4.2 Rule viewer: decremental low-PEEP algorithm 1; two crisp inputs: FiO_2 = 0.3 and low-PEEP = 5 giving a crisp output: change-in-PEEP = 5×10^{-17} 70
4.3 3D surface view for decremental high-PEEP algorithm, with two inputs: FiO_2 and high-PEEP; and one output: change-in-PEEP 74
4.4 3D surface view for decremental low-PEEP algorithm, with two inputs: FiO_2 and low-PEEP; and one output: change-in-PEEP 75
4.5 Rule viewer: incremental high-PEEP algorithm 1; two crisp inputs: FiO_2 = 0.3 and high-PEEP = 5 giving a crisp output: change-in-PEEP = 3.52×10^{-16} 76

4.6 Rule viewer: incremental low-PEEP algorithm; two crisp inputs: FiO_2 = 0.3 and low-PEEP = 5 giving a crisp output: change-in-PEEP = 1.7 . . . 77
4.7 3D surface view for incremental high-PEEP algorithm, with two inputs: FiO_2 and high-PEEP; and one output: change-in-PEEP 81
4.8 3D surface view for incremental low-PEEP algorithm, with two inputs: FiO_2 and low-PEEP; and one output: change-in-PEEP 82
4.9 A graph showing the relationship between the FiO_2, ARDSNet high PEEP, fuzzified high PEEP with fewer linguisitc terms, and fuzzified high PEEP with more linguisitc terms 83
4.10 A graph showing the relationship between the FiO_2, ARDSNet low PEEP, fuzzified low PEEP with fewer linguisitc terms, and fuzzified low PEEP with more linguisitc terms 84
4.11 High-PEEP rule viewer for FiO_2 = 0.3 and non-fuzzified PEEP = 5, giving an output of fuzzified PEEP = 5 86
4.12 Graph showing the relationship between the two input parameters: FiO_2 (yellow in colour) and general range of PEEP (blue in colour), with one output: fuzzified high-PEEP (orange in colour) 88
4.13 Surface view for the two inputs: FiO_2 and non-fuzzified high-PEEP, and one output: fuzzified high-PEEP 89
4.14 Low-PEEP rule viewer for FiO_2 = 0.3 and non-fuzzified PEEP = 5, giving an output of fuzzified PEEP = 5 90
4.15 Graph showing the relationship between the two input parameters: FiO_2 (yellow in colour) and general range of PEEP (blue in colour), with one output: fuzzified low-PEEP (orange in colour) 92
4.16 Surface view for the two inputs: FiO_2 and non-fuzzified low-PEEP, and one output: fuzzified low-PEEP 93
4.17 Accuracy and error graph key 96

4.18 Accuracy and loss curves for three lung conditions 97
4.19 Accuracy and loss curves for three brain conditions 99
4.20 Ventilator waveforms for healthy lungs with PEEP of 5 cm H_2O 101
4.21 Ventilator waveforms for healthy lungs with PEEP of 15 cm H_2O 101
4.22 Ventilator waveforms for sick lungs with PEEP of 5 cm H_2O 102
4.23 Ventilator waveforms for sick lungs with PEEP of 15 cm H_2O 103
4.24 Ventilator waveforms for recovering lungs with PEEP of 5 cm H_2O 104
4.25 Ventilator waveforms for recovering lungs with PEEP of 15 cm H_2O 104

List of Tables

2.2 ARDS Berlin definition PEEP adjustments 23

3.1 FiO_2 input membership function parameters for algorithm 1 fuzzy system . 30
3.2 High-PEEP input membership function parameters for algorithm 1 fuzzy system 32
3.3 Low-PEEP input membership function parameters for algorithm 1 fuzzy system 33
3.4 Change-in-PEEP output membership function parameters for algorithm 1 system 34
3.5 FiO_2 linguistic terms used 35
3.6 High-PEEP linguistic terms used 37
3.7 Low-PEEP linguistic terms used 38
3.8 Change-in-PEEP output membership function parameters for algorithm 1 system 39
3.9 Lung CNN algorithm parameters 52
3.10 Brain CNN algorithm parameters 54

4.1 Comparison between physician based high-PEEP definition and fuzzified decremental high-PEEP 72
4.2 Comparison between physician based low-PEEP definition and fuzzified decremental low-PEEP 73

4.3 Comparison between physician based high-PEEP and fuzzified incremental high-PEEP 79
4.4 Comparison between physician based low-PEEP and fuzzified incremental low-PEEP 80
4.5 Comparison between non-fuzzified high-PEEP and fuzzified high-PEEP . . 87
4.6 Comparison between non-fuzzified low-PEEP and fuzzified low-PEEP . . . 91
4.7 Lung CNN confusion matrix 94
4.8 Lung CNN performance measurement values 95
4.9 Brain CNN confusion matrix 97
4.10 Brain CNN performance measurement values 99

1 FiO_2 and low-PEEP Fuzzy set rules 129
2 FiO_2 and low-PEEP Fuzzy set rules continuation 130
3 FiO_2 and low-PEEP Fuzzy set rules continuation 131
4 FiO_2 and high-PEEP Fuzzy set rules 131
5 FiO_2 and high-PEEP Fuzzy set rules continuation 132
6 FiO_2 and high-PEEP Fuzzy set rules continuation 133
7 Rules for high-PEEP algorithm 1 system 134
8 Rules for low-PEEP algorithm 1 system 135

ABBREVIATIONS AND ACRONYMS

ARDS	Acute Respiratory Distress Syndrome
ARDSNet	Acute Respiratory Distress Syndrome Network
CNN	Convolutional Neural Network
COVID-19	Corona Virus Disease 2019
CRF	Chronic Respiratory Failure
FiO_2	Fraction of Inspired Oxygen
FIS	Fuzzy Inference System
FLC	Fuzzy Logic Controller
FP	False Positive
FN	False Negative

ABBREVIATIONS AND ACRONYMS

ICU	Intensive Care Unit
IDE	Integrated Development Environment
MF	Membership Function
MV	Mechanical Ventilation
NAVA	Neurally Adjusted Ventilatory Assist
PaO_2	Partial pressure of Oxygen
PAV	Proportional Assist Ventilation
PEEP	Positive End Expiratory Pressure
pH	Potential of Hydrogen
P_{pl}	Pleural pressure

ABBREVIATIONS AND ACRONYMS

P_{plat}	Plateau pressure
PSV	Pressure Support Ventilator
ResNet-50	Residual Network with 50 layers
RV	Residual Volume
SpO2	Saturation of Peripheral Oxygen
TCT	Total Cycle Time
TLC	Total Lung Capacity
TN	True Negative
TP	True Positive
V_T	Tidal volume

PUBLICATIONS

(1) Wanzala, J.N., Atim, M.R. & Obungoloch, J. Design of Fuzzy Logic-Based ARDS Berlin Definition for Ventilator Adjustments to Ensure Lung Protection. Int. J. Fuzzy Syst., Springer, 25, 1935–1951 (2023). https://doi.org/10.1007/s40815-023-01485-y

(2) Wanzala, J.N., Atim, M.R. & Obungoloch, J., "Design and Simulation of a Physician-Based *Fuzzy System for Ventilator Adjustments in ARDS Patients to Ensure Lung Protection*" Advances in Fuzzy Systems, vol. 2023, Article ID 3252763, 15 pages, 2023. https://doi.org/10.1155/2023/3252763

ABSTRACT

Respiratory failure can be life threatening for patients with hypoxemic and hypercapnic conditions, and the failure requires fast medical response to save the patient(s). Respiratory diseases such as acute respiratory distress syndrome (ARDS), pneumonia, and corona virus disease 2019 (COVID-19) have increased the need for mechanical ventilation (MV). Mechanical ventilators are devices that support patients in delivering oxygen to the lungs during inspiration and removing the carbondioxide during expiration. The ventilators are mostly controlled manually by physicians, in changing the ventilator settings, such as positive end expiratory pressure (PEEP). Physicians in most hospitals are few and the number of patients with respiratory failures is on the rise due to viruses, smoke inhalation, and injuries that cause fluids to collect in the air sacs of the lungs. The manual control of the ventilators comes with human errors caused by some physicians especially when they are overwhelmed with lots of work, which may lead to inaccurancy or delay in the adjustments made on the mechanical ventilators; hence, resulting into delay in recovering of the patient or to the worst, increasing the death rate due to inaccurate ventilator setting adjustments. In this study, firstly, fuzzy logic method was used to develop a computer aided decision making to improve on the accuracy of the reasoning done during the ventilator setting adjustments. The ARDS Network (ARDSNet) PEEP values were used in building the fuzzy rules of the fuzzy algorithm and four algorithms were trained, that is: incremental high PEEP, decremental high PEEP, incremental low PEEP, and decremental low PEEP. The need for use of the fuzzy logic method to guide the physicians was with a purpose of reducing the physician's time spent in thinking on what

parameters to adjust on the ventilator, especially during an emergency. Secondly, the fuzzy neural network model was further trained to increase the accuracy and reduce the time spent comparing the fuzzy logic algorithm output and the ARDSNet PEEP values. Thirdly, the convolutional neural network (CNN) was then used to classify the different brain and lung conditions, so as to add a variable and alarm to already existing ventilator variables and alarms respectively. Finally, a single lung compartment transfer function was derived and used to test the simulation of the fuzzy-image based system, with trained fuzzified PEEP and CNN algorithms connected to the derived lung transfer function. On testing the system, the first consideration was based on healthy brains after the brain medical scans, whereby the incremental high PEEP algorithm was selected for patients with pneumonia, and decremental high PEEP algorithm was selected for patients with COVID-19. The second consideration was based on healthy lungs after the lung medical scans in which incremental low PEEP algorithm was selected for patients with intracranial hemorrhage or acute ischemic stroke, and a decremental low PEEP algorithm was selected for patients with normal/ healthy brains. This guides the doctors in determining other causes of respiratory failure, hence, acting as an alarm on the ventilator. The neural fuzzy algorithm was able to mimic the ARDSNet PEEP values for high and low PEEP. The CNN algorithm had 97% validation accuracy for the three lung conditions, and 98% validation accuracy for the three brain conditions. Three lung transfer functions were used in the simulation, that is: transfer functions for healthy lung, sick lung, and recovering lung. The lung residual volume (RV) and total lung capacity (TLC) values indicate that for healthy lungs, lower PEEP is desirable. For sick lungs, more PEEP is required to attain the recommended lung RV and TLC ranges. For recovering lungs, lower PEEP is required to balance the lung protection and oxygenation. The intelligent ventilator system can therefore, be applied as a physician-ventilator interface to guide the physician during the ventilation, so as to reduce on the human errors; ensure lung protection; and reduce on the time spent by physicians in making decisions. This can be achieved by the

system, when it guides the physicians on what parameters to adjust at minimal possible time during the ventilation, and increase the possibility of patient survival. The efficiency of physicians that operate on the mechanical ventilators, especially during emergency times, can now be improved by not necessarily increasing the number of the physicians controlling one ventilator, but by adding the fuzzy-image reasoning to the mechanical ventilator systems, to help in providing suggestions to the physician(s).

Chapter 1

Introduction

This chapter outlines the general background information about the medical ventilators. The different types of medical ventilators are articulated with their challenges in regards to balancing lung protection and delivering the right amount of oxygen. The last part of this chapter articulates the specific aspects of research; the problem, the aim and objectives, the scope, and the significance of the study.

1.1 Background

Pulmonary ventilation which is a process of inhaling oxygen and exhaling carbondioxide is very important in sustaining human lives through different respiratory mechanisms [Urfy and Suarez, 2014, Del-Negro et al., 2018, Mortola, 2019]. Every system in the body depends on oxygen to burn fuel (sugars and fatty acids) in the cells to produce energy [Ortiz-Prado et al., 2019]. The mechanism of pulmonary ventilation involves various respiratory structures that enable breathing to take place, such as: nose, windpipe, and lungs [Hage and Brinkman, 2016, Lewith and Pandit, 2020]. The respiratory structures are however affected by diseases and/ or disorders that lead to difficulty or shortage of breath, for example: chronic respiratory failure (CRF) that is caused by health issues like

anesthesia (this is when the patient temporarily losses sensation or becomes unconscious due to the drugs administered through a tube or mask before a surgery), corona virus disease 2019 (COVID-19) which is an infection that generates fluids and mucus into the lungs blocking oxygenation of lung tissue, hindering the natural respiration [Amin, 2006, Forman and Chin, 2008, Joynt, 2008, Yuki et al., 2020].

When faced with breathing problem, patients require mechanical ventilators which are devices that support them with breathing until their immune system and treatment clear the infection, and the natural respiratory mechanism is restored [Cawley, 2007, Chatburn et al., 2014, Chatburn and Mireles-Cabodevila, 2016, Pham et al., 2017, Tobin and Manthous, 2017, Tobin, 2018]. COVID-19 patients put on ventilators, according to Yang et al., are 56% of the admitted COVID-19 patients, that actually require mechanical ventilation (MV) [Yang et al., 2020]. The results of COVID-19 patients on MV show that COVID-19 patients requiring MV had a reasonable chance for recovery [King et al., 2020].

The mechanical ventilators are of three types, namely: manual, automatic, and intelligent ventilators. During the manual operation, the operator squeezes a bag with air, as it delivers oxygen of certain volume [Sassoon, 2011]. For the automatic MV, the operator changes the ventilator parameters physically by monitoring the respiratory rate (RR) of the patient and changing the settings required to deliver the right amount of oxygen. For the intelligent MV, the operator changes the parameters depending on the patient's requirement after monitoring/ taking the readings such as: RR, lung compliance, airway resistance; and adjust the parameters based on the individual needs [Kacmarek, 2011]. Intelligent type is the current one that uses artificial intelligence in the decision making of adjustments of the MV settings [Kacmarek, 2011, Kumar et al., 2022]. The intelligent MV uses patient-ventilator synchrony in triggering the ventilator, with the use of sensors and feedback mechanisms. The synchrony is not well achieved in manual and automatic

types, since the operator has to frequently adjust the parameters of the ventilator. This is however, time consuming and in case of any error, the patient suffers from not having the right/ synchronised ventilation; which is the main goal for the intelligent systems, though, they do not focus on the lung protection, simultaneously with oxygen synchronisation [Hao et al., 2020].

The different modes of MV include: pressure support ventilator (PSV), an automatic ventilator which assists the patient in breathing by delivering oxygen at set pressure level that is determined by the operator [Sinha and Donn, 2006]. The pressure remains the same until the operator changes the respiratory parameters such as tidal volume, peak pressure, positive end expiratory pressure (PEEP), inspiratory time, inspiratory flow, inspiratory to expiratory ratio, time of pause [Carrillo and López-Herce, 2003]. The manual control of the ventilator attributes to inaccurate patient-ventilator synchrony, and the better modes (intelligent ventilators) of MV are: proportional assist ventilation (PAV) and neurally adjusted ventilatory assist (NAVA), which were developed to help improve the synchrony [Schulze, 2006, Lellouche and Brochard, 2009]. In these modes, the respiratory readings taken from the patient determine the parameters to be set, triggers, and cycles the breath [Aguirre-Bermeo et al., 2014]. Depending on the patient, the ventilators can fully work with no patient's effort, or can work alongside with the patient by compensating for what the patient may not achieve to have a full breath, or the ventilator may stop working and the patient does the breathing [Bristle et al., 2014].

In coventional MV, there are more shortcomings that come with use of high tidal volumes irrespective of the improved patient-ventilator synchrony [Allison et al., 2015]. The modern ventilators have been developed and they focus on the lung-protective strategies that use low tidal volumes [Sud et al., 2021]. High tidal volumes, higher driving pressures (ΔP) and plateau pressures (Pplat) are more dangerous to patients with acute respiratory

distress syndrome (ARDS) and non-ARDS patients [Jamil and Spragg, 2008, Sahetya et al., 2019]. There is need for early intervention for ARDS patients, since the early stages of lung injury are very crucial in reducing mortality rates, which can be achieved with low tidal volume and adequate airway PEEP [Bein et al., 2016].

Intelligent ventillators have been designed, in addition to the manual and automatic ventilators. Intelligent ventilators do include: INTELLiVENT-ASV that adapts to the patient's needs based on the respiratory mechanics. These systems however are limited to patients with ARDS, as they are personalised to patients' needs without considering the different adjustments needed to treat a patient with ARDS conditions; AMV + IntelliCycle Pro is able to reduce the time of ventilation for patients with mild to moderate ARDS, however, it is unable to track the recovery of the lungs [Bialais et al., 2016, Arnal et al., 2020, Liu et al., 2020]. Fuzzified systems have been developed; such as: Lozano et al. [2007] who focus on the automation of the ventilators using autopilot technique; they however, do not focus on how to balance the patient-ventilator synchrony and lung protection. Zhu and Moller [2008] study the uses of fuzzy neural network to mainly adjust the flow of the ventilator. Furthermore, Guler and Ata [2014] focus on using fuzzy logic to adjust the pneumatic system, while maintaining the use of manual adjustment; the system does not however tend towards the furtherance of balancing the patient ventilator synchrony and lung protection. Mehedi et al. [2021] focuses on using fuzzy sliding to adjust only pressure, without the furtherance of balancing the synchrony and lung protection. This therefore, leads to the need of real-time imaging of the lung and brain to diagnose the respiratory failure cause, such that physicians do not adjust the ventilator parameters blindly; hence, reducing the time patients are on the ventilator, so that the VILI is minimal or avoided, as the lungs are protected during the ventilation.

1.2 Problem Statement

The assisted breathing is very crucial during the support of a life especially in intensive care unit (ICU). The mechanical ventilators have been designed and implemented into different modes. These modes damage the patients' lung muscles or do not provide the patient-ventilator synchrony. In order to mitigate the aforementioned shortcoming, there is need for an intelligent mechanical ventilator system that uses medical scans, fuzzy logic, fuzzy neural network, and convolutional neural network to balance the lung protection and patient-ventilator synchrony.

1.3 Aim of the Study

This study aimed at designing and simulating an intermediate intelligent system, for balancing the lung protection and patient-ventilator synchrony in ventilators, using fuzzy logic for parameter adjustment, fuzzy neural network to mimic the ARDSNet Berlin protocol, and convolutional neural network (CNN) technique in machine learning to track the recovery of the lungs during the ventilation, and to add an alarm to already existing ventilator alarms.

1.4 Objectives of the Study

This research was guided by the following objectives:

1. Design and simulation of a physician based fuzzy logic system for ventilator adjustments in acute respiratory distress syndrome (ARDS) patients to ensure lung protection
2. Design and simulation of a physician based fuzzy neural system for ventilator adjustments in ARDS patients to ensure lung protection

3. Build a feed-in imaging model to detect lung and brain scans using convolutional neural network

4. Design and simulation of an intelligent system to test and validate patient ventilator synchrony and lung protection using real-time medical imaging and fuzzy expert system

1.5 Scope

Medical images used were for the brain(s) and lungs; brain images had three conditions: intracranial hemorrhagic stroke, acute ischemic stroke, and control images; and the lung images were of three conditions: corona virus disease 2019 (COVID-19), pneumonia, and normal images. The images were trained using the CNN in MATLAB R2021b software, and transfer learning was done using RESNET-50 architecture. Fuzzy algorithms were trained using fuzzy logic designer and neural fuzzy designer applications.

1.6 Significance

This research provides the following benefits:

i) **Knowledge addition**: The study adds more knowledge on a body of existing knowledge on the MV, by using images as a ventilator variable to support in balancing the patient-ventilator synchrony and patient-lung protection, using convolutional neural network.

ii) **Patient health-driven ventilatory assist**: The intelligent intermediate system relies on the patient's lung and brain health to adjust the ventilation parameters, while balancing with the ventilation synchrony.

iii) **Accuracy in parameter adjustment**: Fuzzy logic techniques improve the accuracy of the ventilator parameter feedback, supporting the life of the patient as well as protecting the lungs.

iv) **Added ventilator alarm**: There is an incorporated alarm using the medical scans to the existing ventilator alarms, to notify the physician in case the patient's lungs are healthy but the brain-stem responsible for breathing functions is damaged.

.

1.7 Thesis Outline

The remainder of this thesis is organised in four chapters as briefly described in subsections 1.7.1 to 1.7.4.

1.7.1 Chapter Two

This chapter discusses the theoretical background of mechanical ventilators and literature review on the electrical analogy of the lung, fuzzy logic, fuzzy neural network (FNN), CNN, and lung transfer function.

1.7.2 Chapter Three

This chapter decribes the materials and methods used in design and simulation of fuzzy based mechanical ventilator system using real-time medical imaging.

1.7.3 Chapter Four

This chapter presents the results and discussion on the fuzzy based mechanical ventilator system, using a real-time medical imaging with the aid of a lung transfer function, for testing of the effectiveness of the fuzzy and CNN algorithms.

1.7.4 Chapter Five

This chapter draws the conclusion from chapter four and further highlights the limitations and recommendations of this research.

Chapter 2

Theoretical Background and Literature Review

2.1 Electrical Analogy of Respiratory System and the Physics of Breathing

Lungs are organs that are responsible for receiving oxygen in the body (inspiration) through the nose or mouth, oxygen is then passed through the tranchea, then bronchi, then transfered to the lungs and further in the blood through the bronchioles and alveoli. Lungs then support the removing of carbondioxide from the blood during expiration [Murray, 2010]. Once lungs are affected by a disease or disorder, they hinder proper respiration, leading to respiratory distress or pneumonia or heart failure [Martinez-Pitre et al., 2023]. The respiratory rate may increase to compensate for the loss in the lung full function of exchanging the oxygen and carbondioxide; it is therefore, an important factor to determine the condition of the lungs so as to diagnose the cause, for example shortness of breath, unconsciousness [Uchida, 2023].

The two chosen diseases/ disorder that affect the respiratory system, are; firstly, COVID-19 that is brought about by the severe acute respiratory syndrome coronavirus 2 (SARS-CoV-2) which affects the respiratory epithelium, causing the damage of the lung tissue; secondly, if the damage is severe, it causes pneumonia, which is caused by air sacs (alveoli) in the lungs being filled with fluid and pus, leading to difficulty in breathing [Purohit et al., 2021].

Brain controls the nervous system, and is responsible for regulation of the respiratory functionality, by sending the signals to the diaphragm. The diaphragm sends signals to the brain as feedback to help the brain in determining the amount of oxygen to receive and carbondioxide to release [Juventin et al., 2023]. Respiration can however be difficult to regulate due to neural illness or injury, leading to the shortness of breath, irrespective of normal functioning lungs. This therefore is an important factor to consider during the medical ventilation of patients [Mao et al., 2022].

In this study, two brain diseases were used for training of the algorithm, that is: acute ischemic stroke which is caused by interrupted blood flow in the brain, leading to damage of brain cells due to the blockage of the blood vessel by blood clot [MEYER, 1963]. The second condition considered was hemorrhagic stroke, caused by rupture of the blood vessel leading to brain bleeding [Kessinger and Rigby, 1970]. These are both emergency conditions that need to be treated as early as the conditions are identified, by either removing the clots or repairing the damaged blood vessels while the patient is on oxygen support machine [MEYER, 1963, Kessinger and Rigby, 1970].

A ventilator uses resistance (ΔPressure/ Flow) and compliance (ΔVolume/ ΔPressure) variables to change the airway pressures [Guttmann et al., 1992, Wilson and DiFiore, 2012]. The pulmonary mechanics involves principles of Physics that promote oxygenation in the respiratory system [Srivastava et al., 2009]. Electrical analogies of the lung compartmer

are: double and single lung compartments [Carvalho and Zin, 2011]. Figure 2.1 displays the double lung compartment; it consists of the tranchea airway resistance, bronchi airway resistance, and lung compliance, represented by R_{aw}, R (R_1 and R_2), and C (C_1 and C_2) respectively. The double lung compartment focuses on the airway resistance and lung compliance of the chest walls and lungs respectively. The single lung compartment focuses on only the lungs [Jaber et al., 2020]. Since the medical scans focus on the lungs, then, the single lung compartment was chosen for the study. The airflow from the ventilator

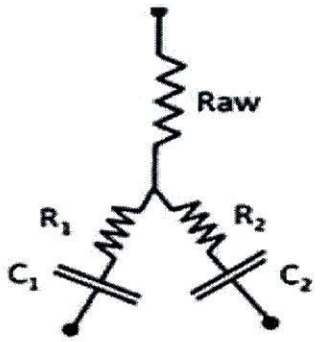


Figure 2.1: Electrical representation of the lung [Carvalho and Zin, 2011]

to the lungs through the airways is measured by resistance, while compliance which is inversely proportional to the alveolar pressure inflating the lung, as shown in Equation 2.1 determines how much the lungs and chest wall can stretch [Olsen et al., 1969, Guerin and Richard, 2007]. The higher the compliance, the more the volume of the lungs can increase with low alveolar pressure. This in turn, avoids respiratory disorders, such as barotrauma that increases with increase in the lung pressure [Frank et al., 1957].

$$C = \frac{V}{P} \tag{2.1}$$

Where, C is compliance, V is the air volume, P is the intra-alveolar pressure.

The electrical representation of the respiratory system guides in deriving the transfer function of the lung respiration function [Bachmann et al., 2018]. In a lung system, using a single compartment model, V_{in} is the input variable of the lung system during inspiration since voltage creates a potential that allows current to flow, hence, current, i is the output variable of the lung system during expiration, and transfer function uses the formular in Equation 2.2 [Campbell and Brown, 1963].

$$H_{(s)} = \frac{I_{(s)}}{V_{in(s)}} \tag{2.2}$$

where, $H_{(s)}$ is the transfer function, s is the s-domain of the transfer function.

2.2 Fuzzy Logic

Fuzzy logic system uses fuzzy sets to represent knowledge, and decision making, that could have been represented using mathematical formulars, by using degrees of membership [Zadeh, 1965, John, 2000, Kacprzyk, 2000, Bai Y., 2006, Bobillo et al., 2012, Cleophas and Zwinderman, 2012, Gonzalez-De La Fuente et al., 2022, Roldan Lopez de Hierro et al., 2022]. Defining a fuzzy set: it is a pair of elements with fuzzy boundaries [Roldan Lopez de Hierro et al., 2022]; if we assume X is the universe of the discourse containing x elements, a fuzzy set A, in X is defined by its membership function in Equation 2.3 [Zadeh, 1965]:

$$\mu_A(x) : X \rightarrow [0, 1], \tag{2.3}$$

From equation 2.3, $\mu_A(x)$ represents how x changes within the fuzzy set A, in the [0,1] range.

Fuzzy logic consists of the crisp input, fuzzification, membership functions, rule base, defuzzification, and crisp output as explained in subsection 2.2.1 to subsection 2.2.5 [Zadeh, 1965].

2.2.1 Crisp Inputs:

Crisp inputs by definition in the fuzzy system, represent the raw parameter inputs from the control system [Buckley and Hayashi, 1993].

2.2.2 Fuzzification and Membership Functions:

The crisp input values are then converted into fuzzy values through membership functions (MF) such as: triangular, trapezoidal, among others; which convert the raw crisp inputs into the degree of truth, that is, between zero (0) and one (1) and including zero (0) and one (1), as fuzzy values [Rondeau et al., 1997]. The fuzzification maps crisp input values $x \in X$ to fuzzy set $A \in X$. The fuzzy input values are then applied in the rule base [Sinha and Dougherty, 1993, Rondeau et al., 1997, Straszecka, 2000, Ross, 2000, Thaker and Nagori, 2018]. The mapping process considers MF such as: triangular and trapezoidal MF, as they provide accurate and fast response in mapping of inputs to outputs [Jin and Bose, 2002, Monicka et al., 2011, Omar et al., 2015], which profusely supports the aim of the objective of this research, to have an accurate and fast responding algorithm to both reduce human errors so as to increase the lung protection of the patients, and ventilate as many patients as possible. Since they are fast, they help in reducing on the time needed by the physician to make a decision during the ventilation parameter adjustment.

The triangular MF is defined by Equation 2.4; where a is the lower limit, b is an upper limit, and m is the peak value. The trapezoidal MF is defined by Equation 2.5; where a is the lower limit, b is a lower support limit, c is the upper support limit, and d is the upper limit.

$$\mu_A(x) = \begin{cases} 0 & x \leq a \\ \frac{x-a}{m-a} & a < x \leq m \\ \frac{b-x}{b-m} & m < x \leq b \\ 0 & x \geq b \end{cases} \tag{2.4}$$

$$\mu_A(x) = \begin{cases} 0 & (x < a)\, or\, (x > b) \\ \frac{x-a}{b-a} & a \leq x \leq b \\ 1 & b \leq x \leq c \\ \frac{d-x}{d-c} & c \leq x \leq d \end{cases} \tag{2.5}$$

2.2.3 Expert Fuzzy System/ Rule base:

The fuzzy values are then interpreted using the expert fuzzy system. The expert fuzzy system contains a set of rules or knowledge that maps the fuzzy inputs to the fuzzy outputs [Rondeau et al., 1997]. The set of fuzzy rules were used to guide and/ or limit the range in which: PEEP and inspired fraction of oxygen (FiO_2) are to be safely attained during the ventilation while protecting the lungs from damage or further damage.

The Equation 2.6 and Equation 2.7 are used in building the fuzzy rules of the fuzzy system. Equation 2.6 uses the "or" fuzzy operator, and Equation 2.7 uses the "and" fuzzy operator in setting the "If-then" fuzzy rules, by combining the inputs for fuzzification [Zadeh, 1965];

$$B \cup C \cup D \cup E = \{x, max(\mu_B(x), \mu_C(y), \mu_D(z), \mu_E(q))\} \tag{2.6}$$

$$B \cap C \cap D \cap E = \{x, min(\mu_B(x), \mu_C(y), \mu_D(z), \mu_E(q))\} \tag{2.7}$$

for $x \in X, y \in Y, z \in Z, q \in Q$.

A general fuzzy rule method used in building the rules is in the form of:

"If x_i = B $\cup/\cap$ y_i = C $\cup/\cap$ z_i = D $\cup/\cap$ q_i = E then m_i = F $\cup/\cap$ n_i is G"

where;

$x \in X$, $y \in Y$, $z \in Z$, $q \in Q$, $m \in M$, $n \in N$,
F and G are the output fuzzy sets,
$i = 1 ... n$, where n represents the number of linguistic values of the respective linguistic variables/ fuzzy sets.

2.2.4 Defuzzification and Membership Functions:

The fuzzy output values are then mapped to the crisp outputs using the defuzzification methods [Rondeau et al., 1997, Ross, 2000]. The centroid defuzzification method determines the center of the area of the fuzzy set and returns the crisp value (Z) [Sameena et al., 2011, Marlena et al., 2018]. It maps a continuous and smooth change of the input crisp values to the crisp outputs; hence, accurate for fuzzy reasoning [Mogharreban and Dilalla, 2006]. The centroid defuzzification method is helpful in this study to increase on the accuracy of the ventilator parameter adjustments. The expression that mathematically describes the centroid method is shown in Equation 2.8, where $\mu(x_i)$ is the membership value for the element x_i, in the universe of the discourse [Zadeh, 1965].

$$Crisp\ output, Z = \frac{\sum_i x_i \mu(x_i)}{\sum_i \mu(x_i)} \tag{2.8}$$

The centroid method considers the fact that if a body is balancing perfectly, then its concentrated mass is at the centre of gravity or centre of mass. This is attained by dividing the summation of the product of each element in the universe of the discourse and its membership value ($\sum_i x_i \mu(x_i)$) by the summation of its membership value alone ($\sum_i \mu(x_i)$) [Mitsuishi, 2022]. In the process, the center of area of the fuzzy set is converted into the correlating crisp output [Figueroa García et al., 2022].

2.2.5 Crisp Outputs:

The crisp outputs are the values that manage the control system [Buckley and Hayashi, 1993]. The crisp outputs are values that are precise, unlike the fuzzy values that are approximate. The crisp outputs are: ΔV_t and $\Delta PEEP$, which are displayed for the physician's guidance on how to adjust the ventilator parameters based on the patient's demand (process under control), minimising the human errors. The process repeats continuously using the closed feedback loop to help the algorithms to adjust parameter settings. A closed-loop ventilation increases on the lung-protective strategy and provide right amount of oxygenation while reducing on the operational errors during the ventilator setting adjustments, which according to, is very key during the ventilation [Garcia et al., 2021].

2.3 Berlin Definition of ARDS

The ventilation of patients with acute respiratory distress syndrome (ARDS) according to Berlin definition, starts with ensuring ventilation synchrony and then titrating the positive end expiratory pressure (PEEP) [Force et al., 2012b, Sahetya et al., 2017a, Gattinoni et al., 2010, Collino et al., 2019]. The plateau pressure (P_{plat}) is measured with inspiratory pause, and the PEEP is gradually increased; then, P_{plat} is re-measured after 20 seconds; if the driving pressure reduces, the lowest PEEP is captured; otherwise, the previous PEEP is

recorded. P_{plat} is again measured, and if it is less than 30 mm Hg, potential of hydrogen (pH) is recorded and respiratory rate (RR) and tidal volume (V_T) readings adjusted until pH is greater than 7.2. If P_{plat} is greater than 30 mm Hg, V_T is reduced upto 4 cc/ kg; and if P_{plat} remains less than 30 mm Hg, then a call for a physician is passed on as an alarm. From parameters discussed, the Fi_2O and PEEP were chosen for parameter adjustments since the Fi_2O looks at the amount of oxygen in the blood, very crucial for patient-ventilator synchrony [Hoofs et al., 2018]; and PEEP is important in the alveoli recruitment, affecting the lung protection [Riforgiato et al., 2022].

2.4 Mechanical Ventilators

2.4.1 Pressure Support Ventilation

Pressure Support Ventilation (PSV) is a mechanical ventilator mode that partially supports in ventilation, by pressure triggering of the ventilation based on a positive-pressure boost, synchronized with patient inspiratory effort [Nafday et al., 2005]. This ventilator is used on patients who are not deeply sedated and have an adequate respiratory drive. The pressure in the airway is increased to match the pressure from the ventilator when the inspires the gas, until the expiration phase, which is triggered by the decay of the inspiratory flow. PSV is therefore: patient-initiated (pressure or flow), pressure-targeted, flow-cycled mode of mechanical ventilation [Tobin, 2013].

The challenge that comes with PSV is that it delivers the set pressure, set by the operator and continues with insufflation phase even when the patient has started exhaling. Furthermore, inadequate airway pressure in PSV does not initiate the ventilation [Tobin, 2013]. The inspiratory efforts by the patient fail in triggering of the ventilation at the third and sixth efforts. To improve on the synchrony of the PSV, the operator has to be on stand by to keep changing the pressure levels. The Proportional Assist Ventilator

(PAV) was later developed, which comes with improved patient-ventilator synchrony and stops the insufflation phase when the patient starts exhaling [Tobin, 2013].

2.4.2 Proportional Assist Ventilator

Proportional assist ventilator (PAV) is a synchronized mode in mechanical ventilators that changes or adapts to the levels of assistance to patient demand. This increases the patient comfort during the ventilation [Bureau et al., 2021]. Unlike PSV partial support, PAV does not have target flow, tidal volume, or ventilation or airway pressure. PAV operation is based on the equaton of motion of respiration in Equation 2.9 which states that the total pressure required to ventilate (P_{total}) is equal to tidal volume (V) times elastance (E) plus flow ($\dot{V}$) times airway resistance (R) [Tobin, 2013]:

$$P_{total} = (V)(E) + (\dot{V})(R) \tag{2.9}$$

The patient then supports breathing by triggering the inspiration, P_{total} in Equation 2.9 is then represented as shown in Equation 2.10

$$P_{total} = P_{mus} + P_{vent} \tag{2.10}$$

where, P_{mus} is the pressure generated by the patient's muscular effort and P_{vent} is the pressure generated by the ventilator. Therefore, Equation 2.10 turns to Equation 2.11:

$$P_{mus} + P_{vent} = (V)(E) + (\dot{V})(R) \tag{2.11}$$

In accordance with the equation 2.11, there is no pressure target in PAV, the total pressure increases; hence, flow increases too in response to patient effort as the patient inspires [Tobin, 2013]. For cycling of the breath, the patient effort starts to reduce; in turn, flow

reduces too until it reaches a set cycling level, the ventilator then starts to shift from inspiration to exhalation. The challenge that comes with the PAV, is that the patient has to initiate the ventilation by generating enough pressure to trigger the ventilator. This means that a patient having diseases like apnea breathing, may not be able to use the PAV [Bureau et al., 2021].

The Neurally Adjusted Ventilator Assist (NAVA) mode was developed to increase the triggering sensitivity. This mode uses a better signal (diaphragmatic electrical activity (Edi)) to trigger the ventilation [Lamouret et al., 2019].

2.4.3 Neurally Adjusted Ventilator Assist

Neurally Adjusted Ventilator Assist (NAVA) mode triggers the ventilator using the diaphragm signal [Sinderby et al., 2000]. NAVA works like PAV; it supports the patient based on the patient's need. The only difference is that it continuously gets the signal from the diaphragm. This therefore, makes the ventilator to mimic the human muscles in respiration, with the control coming the patient's central centre signal [Lamouret et al., 2019].

Furthermore, the PAV calculates the patient's muscle pressure to adjust the ventilator parameters, while the NAVA uses the signal from the diaphragm. This therefore, makes the NAVA system have better signal than the PAV. The modes, especially PAV and NAVA, improve the comfort of the patient during their assist, that depends on the patient's effort. The modes however, do not function depending on patient's brain and lung health. Mechanical ventilation applies physical stresses to the tissues of the lung and thus may give rise to Ventilator-Induced Lung Injury (VILI), particularly in patients with ARDS [Bates and Smith, 2018].

Figure 2.2 shows the signals used in triggering the ventilators. Initially, conventional MV used volume, airway pressure, and flow in a patient to trigger the ventilators [Nafday et al., 2005, Garcia et al., 2021]. This was then followed by the NAVA that uses respiratory muscles (specifically the diaphragm contraction) to trigger the ventilators [Lellouche and Brochard, 2009]. Future research is now looking at using more accurate signals from the

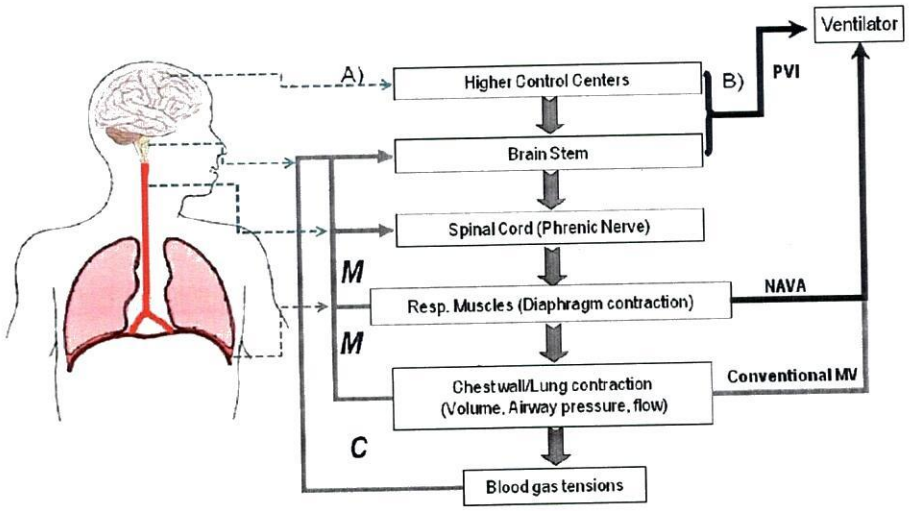


Figure 2.2: Brainstem signals driving the respiratory rhythm [Peralta et al., 2013]

brain stem and/ or higher control centers in the brain [Peralta et al., 2013].

ARDS is a deadly respiratory failure that is determined using: arterial blood gas levels (hypoxemia with a ration of partial pressure of oxygen (PaO_2) to fraction of inspired oxygen (FiO_2) being less than or equal to 300 mm Hg), and chest imaging of bilateral opacities [Jamil and Spragg, 2008]. Bilateral opacity is a type of pulmonary opacity (increased pulmonary attenuation where the amount of air in the lung airspaces decreases due to the airspaces being filled with fluid, that is leaked into the alveoli due to the lung damage) [Ferguson et al., 2012]. Therefore, since the fluid is leaked into the alveoli causing pulmonary edema, there is also an oxygen deficiency in the arterials.

The etiology of ARDS is a direct lung injury, due to mainly two causes: pulmonary ARDS, and extrapulmonary ARDS. For the case of the pulmonary ARDS, the lungs are damaged by factors within the lungs such as: lung contusion (bruise on the lung due to chest blow), smoke inhalation, viral pneumonia (when a lung tissue is swollen due to a virus), fat embolism (when fats from a bone slide into the blood vessels). For the case of extrapulmonary ARDS, the lungs are affected by external factors such as: head injury, trauma, cardiopulmonary bypass (use of an artificial ventilator during surgery to help in blood circulation and maintaining of the oxygen content in the patient's blood). The two etiological ways are inconsistent to different MV; implying that there is a need of chest scan to determine the causes of the ARDS, such that effective settings are implemented by the operator as well as use of the lung injury preventive methods [Fan et al., 2018]. There is a similarity in the treatment of neonatal ARDS and COVID-19 ARDS [Grasselli et al., 2020, Bhatt et al., 2021, Batah and Fabro, 2021]. There is also a similarity of respiratory distress syndrome (not ARDS) and COVID-19 [Koumbourlis and Motoyama, 2020]. This means that a designed single treatment protocol algorithm can be used for patients of the different diseases/ disorders: neonatal ARDS, respiratory distress syndrome (not ARDS), COVID-19 ARDS, and COVID-19.

There has been a developed procedure on ventilating the patients with ARDS, called the ARDS Berlin definition [Force, 2012]. Berlin definition of ARDS was defined from Berlin, as ARDS that is discovered one week after respiratory failure with presence of bilateral opacities on chest scans. The Berlin definition protocols are the guidelines to the physician on what adjustments to make on the ventilator system while ventilating a patient with ARDS. The severity of the ARDS is a big factor when determining the deviation from the studied 6 ml/ kg tidal volume [Ney and Kuebler, 2000, Network, 2000, Laffey and Kavanagh, 2000]. The ARDS Berlin definition of ARDS severity is shown in

Table 2.1.

Table 2.1: Severity of ARDS [Ferguson et al., 2012]

ARDS severity	**PaO_2/ FiO_2 (mm Hg)**
Mild	$200 < PaO_2/\ FiO_2 \leq 300$
Moderate	$100 < PaO_2/\ FiO_2 \leq 200$
Severe	$PaO_2/\ FiO_2 \leq 100$

The severity of ARDS depends on the degree of the hypoxemia that is calculated based on the ratio of PaO_2 to FiO_2. Table 2.1 classifies the severity of ARDS with PEEP $\geq$ 5 cm H_2O [Ferguson et al., 2012]. The high-PEEP and low-PEEP do not significantly affect mortality for patients with ARDS and without ARDS [Meade et al., 2008, Pettenuzzo et al., 2021]. There is however no significant change for mortality, but the higher the PEEP levels, the higher the chances of survival of patients with ARDS [Briel et al., 2010].

The ARDS Berlin definition on high-PEEP and low-PEEP adjustments with respect to the FiO_2 is shown in Table 2.2. Furthermore, manually setting ventilators produces MV errors [Dennison et al., 2007]. There is also a need to incorporate a lung transfer function of different health conditions of patients, to test for the effectiveness of the fuzzy algorithms [Bernstein et al., 2013, Nguyen et al., 2014].

Table 2.2: ARDS Berlin definition PEEP adjustments [Brower et al., 2004, Sahetya et al., 2017b]

Input variable	Output variables	
FiO_2	**Low-PEEP**	**High-PEEP**
0.3	5	5-14
0.4	5-8	14-16
0.5	8-10	16-18
0.6	10	18-20
0.7	10-12	18-20
0.8	12-14	20-22
0.9	18	22
1.0	18-24	22-24

Chapter 3

Materials and methods

3.1 Materials

The following materials were used for this research:

- MATLAB R2021b software: widely applied in data analysis of the positive end expiratory pressure (PEEP) and inspired fraction of oxygen (FiO_2), 2D visualization of the ventilator graphs, simulation of the single lung model/ compartment, and algorithm training of the convolutional neural network (CNN).
- Simulink toolbox: to simulate the trained algorithms and designed control systems, so as to study the behavior of the designed lung transfer function, that is based on the output of the algorithms.
- Fuzzy logic designer application: design of the algorithm to predict and fine-tune the uncertainty and imprecision of the PEEP and FiO_2 values, by applying the linguistic variables and membership functions to serve as the ventilator settings.
- Neuro fuzzy designer application: advancing of the fuzzy logic by applying neural network to enhance the effectiveness of the algorithm.

- RESNET-50 architecture: a CNN architecture to classify images used in the study.
- Brain images: to identify the different brain conditions that may lead to respiratory failure.
- Lung images: to identify the different lung conditions that may lead to respiratory failure.
- Scope block: display of the output of the algorithms.
- MATLAB function block: to employ the different programming language to enable the running of the control system based on its intended code.
- Image classifier block: to accomodate the brain and lung CNN models, and giving an output label/ score with respect to the image input.
- Fuzzy logic controller block: to run the built fuzzy logic and neural fuzzy models.
- Transfer function block: to represent the single lung compartment model relating the input and output of the control system.
- Ventilator graphical user interface: the flow, volume, and pressure graphs are displayed on the ventilator screen to monitor and analyse the patient's responses.

3.2 Methods

3.2.1 Design and Simulation of a Physician Based Fuzzy Logic System for Ventilator Adjustments in Acute Respiratory Distress Syndrome (ARDS) Patients to Ensure Lung Protec

The designed system starts with the use of the fuzzy logic rule base, to determine the range in which the settings can be adjusted, to provide the right amount of oxygen while protecting the lungs. Fuzzy logic designer toolbox in MATLAB R2021b software was used to design the fuzzy logic algorithms, which was implemented in the adjustments of the parameter settings, using the acute respiratory distress syndrome (ARDS) Network (ARDSNet) protocol. Figure 3.1 displays the fuzzy logic architecture showing the: crisp/ reference input, fuzzification, expert fuzzy system/ rule base, aggregation, defuzzification, crisp output, process under control; which cover the process to achieve the fuzzy logic based ventilator adjustment system.

A) **Fuzzy Logic System Architecture**

From Figure 3.1, the reference point was the point at which the feedback algorithm was based, when adding or subtracting the error. The inputs used were the parameters changed on the mechanical ventilators during the ventilation of the patient by the physicians, that is: x_1, x_2, ... x_i. Crisp inputs used were: positive end-expiratory pressure (PEEP), and fraction of inspired oxygen (FiO_2).

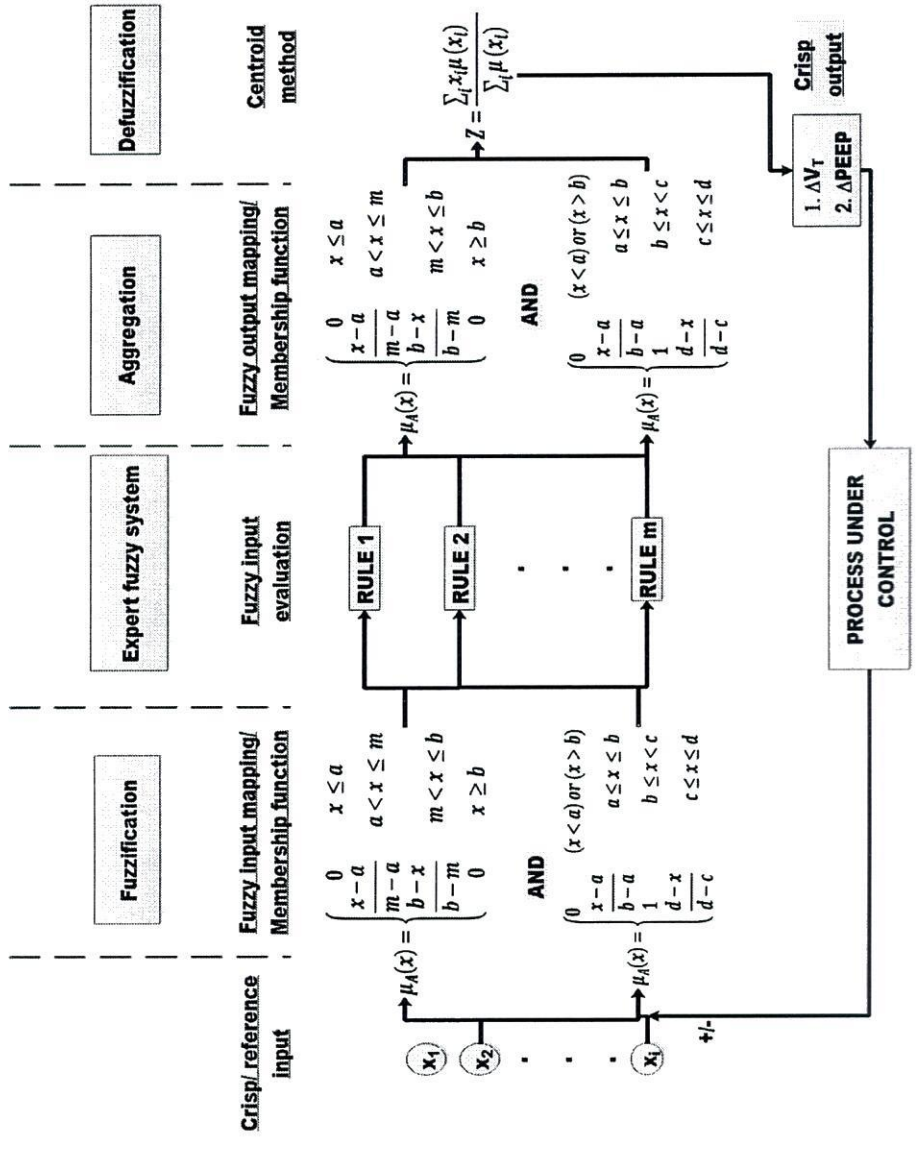


Figure 3.1: The ventilator logic system architecture

The mapping process for this study considered two MF; triangular and trapezoidal MF, as they provide accurate and fast response in mapping of inputs to outputs [Jin and Bose, 2002, Monicka et al., 2011, Omar et al., 2015]. This profusely supports the objective of this research, targeting the accuracy and fast response of the algorithm, to reduce human errors so as to increase the lung protection of the patients; and hence, ventilating as many patients as possible. Since they are fast, they help in reducing the time needed by the physician to make a decision during the ventilation parameter adjustment.

Process under control is the stage where the patient's physiology signals such as: amount of oxygen in the blood, severity of the diseases through medical imaging of the chest, are exported to the algorithm for processing. The ventilator then adjusts the settings to match the amount of oxygen delivered to a patient's lung and the pressure at which the gas flows. Fuzzy output values from the fuzzy logic designer trigger signals that are used to determine the patient's health conditions.

B) **Design of the ARDSNet Based Fuzzy Logic Rules:**

The rules built for the fuzzy high-PEEP algorithm 1 are shown in Table 7. It consists of two crisp inputs, that is: FiO_2 and high-PEEP; and one crisp output: change-in-PEEP. The two crisp inputs are operated on using the "and" fuzzy operator. Linguistic values of the FiO_2 linguistic terms: F1, F2, F3, F4, F5, F6, F7, F8, F9, and F10 are: 0.1, 0.2, 0.3, 0.4, 0.5, 0.6, 0.7, 0.8, 0.9, and 1 respectively; linguistic meaning of the high-PEEP linguistic terms: HP1, HP2, HP3, HP4, HP5, HP6, HP7, and HP8 are: 0-24 scale, as shown in Table 2.2. The Mamdani fuzzy inference system (FIS) is used for this research due to its accuracy while using the min-max operations [Lambat et al., 2021, Tamiloli et al., 2021, F. Shukri, 2021].

For aggregation, the mapping of the fuzzy input values into fuzzy output values using the rule base is done using the triangular and trapezoidal MF. The fuzzy output values are then passed on for defuzzification.

Table 7 displays the fuzzy set rule linguistic terms used for: FiO_2, high-PEEP, change in PEEP; for patients that require high-PEEP intervention. For rule numbers 1 to 8, F10 linguistic term is related to the linguistic terms HP1 to HP8; the "Increase" linguistic term is used to denote need of PEEP increase for high-PEEP, by increasing HP1 to HP8 linguistic term. PEEP is then maintained at HP8. For rule numbers 9 and 10, FiO_2 is fixed at F9 linguistic term; and for HP8, high-PEEP is decreased, changing it to HP7; and F10 to F9. The high-PEEP is then maintained.

The rules built for the fuzzy low-PEEP algorithm 1 are shown in Table 8, which consists of two crisp inputs, that is: FiO_2 and low-PEEP; and one crisp output: change-in-PEEP. The two crisp inputs are operated on using the "and" fuzzy operator. Table 8 displays the fuzzy set rule linguistic terms used for: FiO_2, low-PEEP, and change in PEEP; for patients that require low-PEEP ventilation. For rule numbers 1 to 8, F10 linguistic term is related to the linguistic terms LP1 to LP8; the "Increase" linguistic term is used to denote need of PEEP increase, for low-PEEP, by increasing LP1 to LP8 linguistic term. PEEP is then maintained at LP8 linguistic term. Rule numbers 9 and 10, FiO_2 is fixed at F9 linguistic term. For LP8, low-PEEP in decreased, changing it to LP7 and low-PEEP is then maintained.

The rules generated are inserted in the rule editor of the MATLAB's fuzzy logic toolbox of the mamdani FIS, which maps the fuzzy inputs to the fuzzy outputs. Using the linguisitic terms in the linguistic rules, the crisp inputs are mapped to the crisp outputs, which are the results of the fuzzy system.

C) **MATLAB code: Algorithm 1 fuzzy system with decremental ARDSNet protocol**

The input membership function (MF) and output MF parameters used to design the fuzzy logic algorithm 1 are shown in Table 3.1 to Table 3.4 for FiO_2 input MF, high-PEEP input MF, low-PEEP input MF, and change-in-PEEP output MF respectively. In Table 3.1 as plotted in Figure 3.2, the MF parameters were attained by getting the average value from the ARDSNet PEEP table to represent the middle point of the lower and upper boundary points of the ARDSNet PEEP values. Linguistic terms: F1 to F10 have 0.1 to 1 as their peak value of the linguistic meaning. Their respective MF of 0.1 was subtracted from the peak value to attain the lower limit and 0.1 was added to the peak value to attain the upper limit.

Table 3.1: FiO_2 input membership function parameters for algorithm 1 fuzzy system

Linguistic term	**Linguistic meaning/ params**
F1	[0 0.1 0.2]
F2	[0.1 0.2 0.3]
F3	[0.2 0.3 0.4]
F4	[0.3 0.4 0.5]
F5	[0.4 0.5 0.6]
F6	[0.5 0.6 0.7]
F7	[0.6 0.7 0.8]
F8	[0.7 0.8 0.9]
F9	[0.8 0.9 1]
F10	[0.895 1 1]

From Table 3.2 as plotted in Figure 3.3, the mid-point of the ARDSNet high-PEEP was calculated to get the peak value of the triangular MF using Equation 3.1;

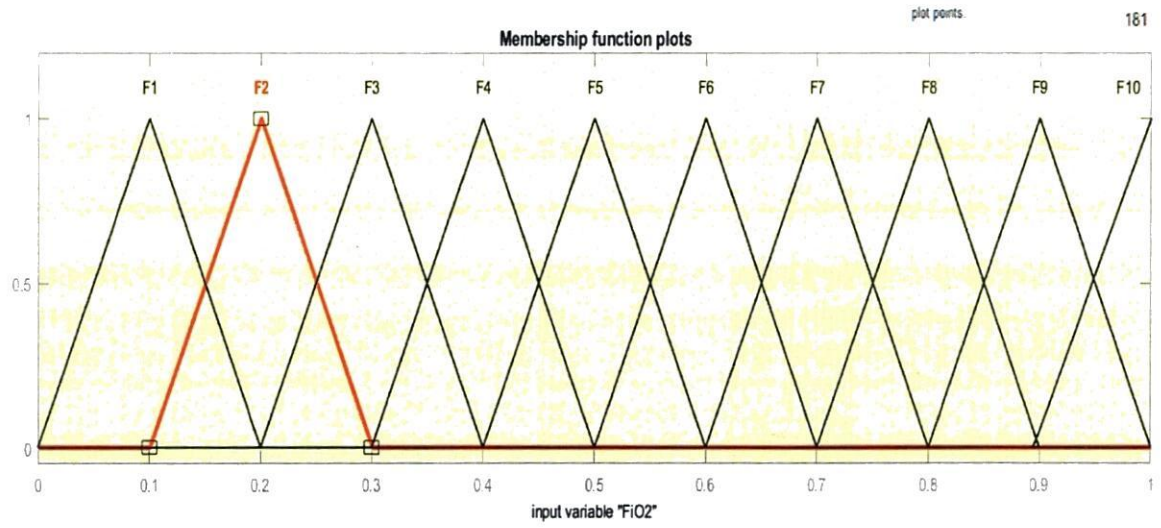


Figure 3.2: Fuzzy logic designer showing FiO_2 membership functions

$$peak\ value\ = \frac{x_1 + x_2}{2} \tag{3.1}$$

where;

x_1 and x_2 are the lower limit value and upper limit value of the high-PEEP range, respectively.

The ARDSNet suggests that the PEEP starts from 5, making it the lower limit of the HP1 linguistic term. For the proceeding linguistic terms, the lower limit of the triangular MF is the peak value of the previous PEEP range of a lower linguistic term. The upper limit is the peak value of the next PEEP range of the upper linguistic term. Linguistic term HP8 has however an upper limit of 24 since the ARDSNet PEEP table ends on 24th value for the PEEP readings.

Table 3.2: High-PEEP input membership function parameters for algorithm 1 fuzzy system

Linguistic term	Linguistic meaning/ params
HP1	[5 9.5 15]
HP2	[9.5 15 17]
HP3	[15 17 19]
HP4	[17 19 21]
HP5	[17 19 21]
HP6	[19 21 22]
HP7	[21 22 23]
HP8	[22 23 24]

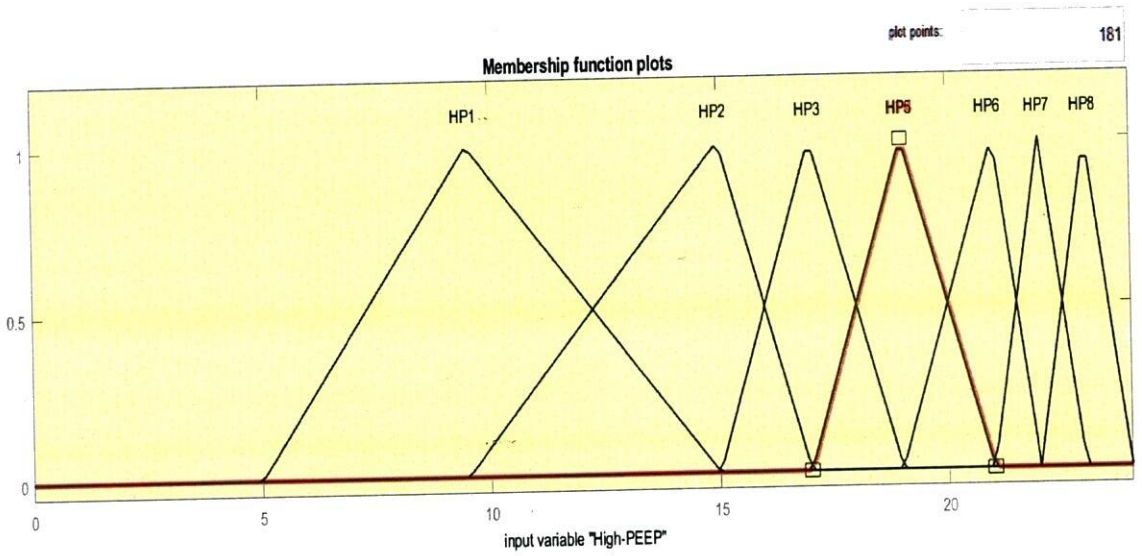


Figure 3.3: Fuzzy logic designer showing high-PEEP membership functions

For Table 3.3 as plotted in Figure 3.4, low-PEEP MF starts with 5 cm H_2O for PEEP as suggested by the ARDSNet PEEP table. The peak value of the MF was the calculated mid-point of the ranges. Lower limit and upper limit of the MF was the lower value and upper value of the low-PEEP ranges, respectively.

Table 3.3: Low-PEEP input membership function parameters for algorithm 1 fuzzy system

Linguistic term	**Linguistic meaning/ params**
HP1	[5 5 5]
HP2	[5 6.5 8]
HP3	[8 9 10]
HP4	[10 10 10]
HP5	[10 11 12]
HP6	[12 13 14]
HP7	[18 18 18]
HP8	[18.1 21.1 24.1]

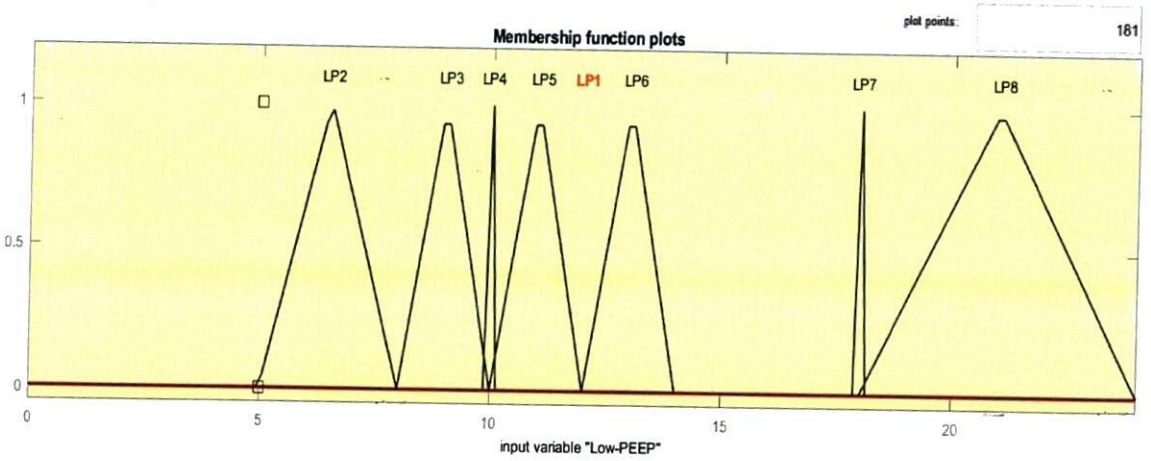


Figure 3.4: Fuzzy logic designer showing low-PEEP membership functions

Lastly, Table 3.4 as plotted in Figure 3.5, indicates the recommended adjustments in PEEP to be ± 4; therefore, "Decrease" linguistic term has got a peak value of - 2,

with lower limit and upper limit of - 4 and 0 (zero) respectively. "Maintain" linguistic term keeps the PEEP unchanged by having a peak value of 0 (zero), with lower and upper limits of - 2 and + 2, respectively. Finally, the "Increase" linguistic term allows an increase of PEEP up to + 4, with peak value of + 2 and lower limit of 0 (zero).

Table 3.4: Change-in-PEEP output membership function parameters for algorithm 1 system

Linguistic term	**Linguistic meaning/ params**
Decrease	[-4 -2 0]
Maintain	[-2 0 2]
Increase	[0 2 4]

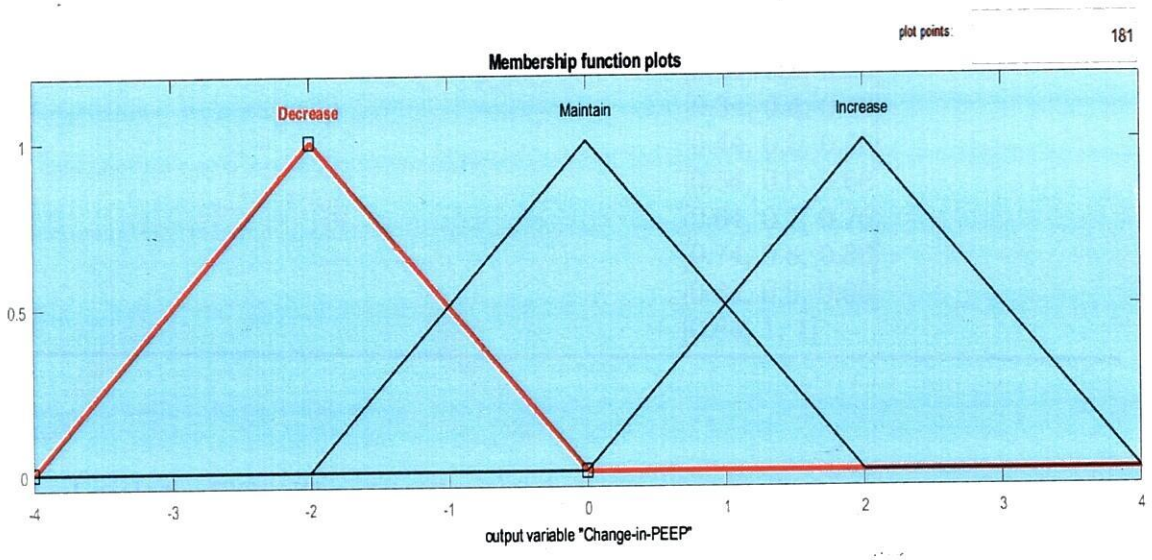


Figure 3.5: Fuzzy logic designer showing change-in-PEEP membership functions

D) **MATLAB code: Algorithm 1 fuzzy system with incremental ARDSNet protocol**

Linguistic terms were further increased to add incremental protocol of the algorithm. The "Linguistic meaning/ params" column are the membership function (MF) parameter of the "Linguistic term" column.

Table 3.5 as plotted in Figure 3.6 shows the parameters of the FiO_2 linguistic terms, ranging from F1 to F9. The MF that was used for FiO_2 was the triangular type for F1 to F9; ranging from zero (0) to one (1) since the ARDSNet protocol considers a

Table 3.5: FiO_2 linguistic terms used

Linguistic term	**Linguistic meaning/ params**
F1	[0, 0, 0.15, 0.26]
F2	[0.24, 0.3, 0.36]
F3	[0.34, 0.4, 0.46]
F4	[0.44, 0.5, 0.56]
F5	[0.54, 0.6, 0.66]
F6	[0.64, 0.7, 0.76]
F7	[0.74, 0.8, 0.86]
F8	[0.84, 0.9, 0.96]
F9	[0.84, 1, 1]

0.3 - 1 scale for FiO_2. The algorithm considers incremental FiO_2 from 0 to 1, with the first linguistic term (F1) having a peak value of 0.15. The following linguistic terms use the FiO_2 values in the ARDSNet table as the peak values. The lower limit of the MF was got by subtracting 0.01 from the mid-value of current MF peak value and peak value of the previous MF. The upper limit of the MF was attained by adding 0.01 to the mid-value of the current MF peak value and peak value of the proceeding MF.

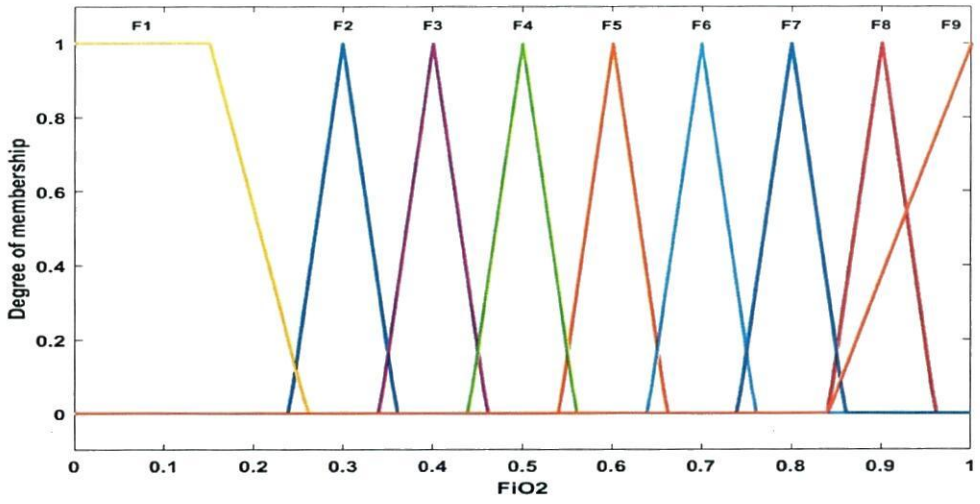


Figure 3.6: Membership function for FiO_2 input

Table 3.6 as plotted in Figure 3.7 shows the parameters of the high-PEEP linguistic terms, ranging from HP1 to HP8. The MF that were used for high PEEP were the trapezoidal type for HP1 and triangular type for HP2 to HP8; ranging from zero (0) to twenty four (24), since the ARDSNet protocol considers a 5 - 24 scale for high-PEEP adjustments.

The algorithm starts from 0 (zero), with the first trapezoidal MF having a lower limit and lower support limit as 0 (zero). 1.25 for upper support limit, which is a $\frac{1}{4}$ of 5 cm H_2O high-PEEP and the upper limit is 3.75 ($\frac{3}{4}$ of 5 cm H_2O high-PEEP). The following linguistic terms use triangular MF with peak value as the mid-point of the range of the high-PEEP values for respective FiO_2 values. The lower limit is attained by subtracting 0.5 from the mid-value of the current linguistic term and peak value of the previous linguistic term; the upper limit is calculated by adding 0.5 to mid-value of the current linguistic term and peak value of the next linguistic term.

Table 3.6: High-PEEP linguistic terms used

Linguistic term	Linguistic meaning/ params
HP1	[0, 0, 1.25, 3.75]
HP2	[2.5, 9.5, 14.5]
HP3	[13.5, 15, 16.5]
HP4	[15.5, 17, 18.5]
HP5	[17.5, 19, 20.5]
HP6	[19.5, 21, 22.5]
HP7	[21.5, 22, 22.5]
HP8	[21.5, 23, 24]

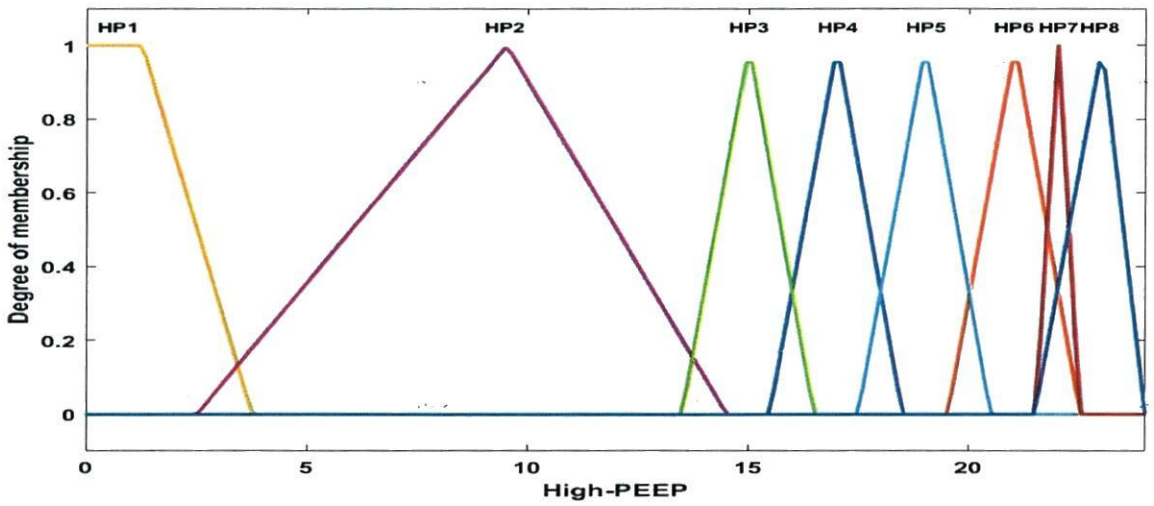


Figure 3.7: Membership function for high-PEEP input

Table 3.7 as plotted in Figure 3.8 shows the parameters of the low-PEEP linguistic terms, ranging from HP1 to HP9. The trapezoidal MF were used for HP1 low-PEEP and triangular type for HP2 to HP9, ranging from zero (0) to twenty four (24). The MF as well use peak values of mid-values of the respective linguistic terms.

Table 3.7: Low-PEEP linguistic terms used

Linguistic term	**Linguistic meaning/ params**
HP1	[0, 0, 1.275, 3.5]
HP2	[2.5, 5, 5.5]
HP3	[4.5, 6.5, 8.5]
HP4	[7.5, 9, 10.5]
HP5	[9.5, 10, 10.5]
HP6	[9.5, 11, 12.5]
HP7	[11.5, 13, 14.5]
HP8	[13.5, 18, 18.5]
HP9	[13.5, 21, 24]

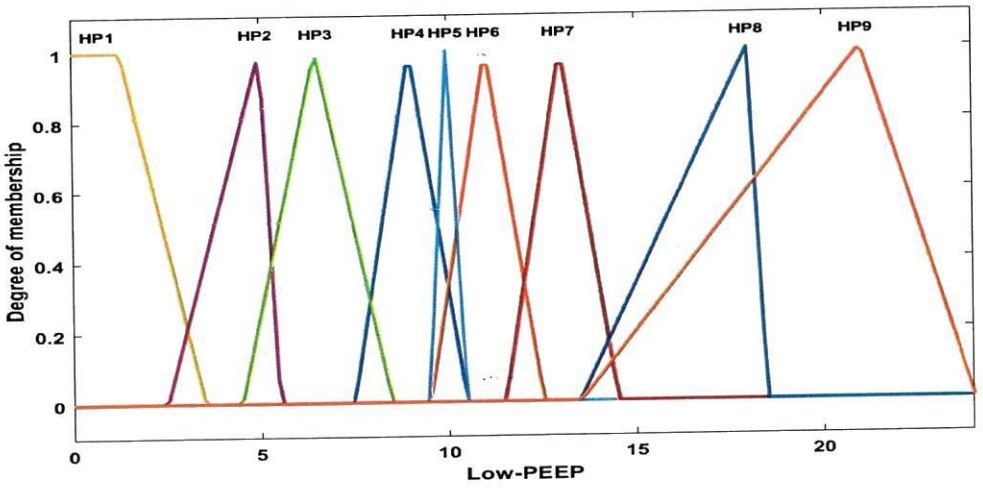


Figure 3.8: Membership function for low-PEEP input

Lastly, Table 3.8 as plotted in Figure 3.9, indicates the "Decrease" linguistic term with a peak value of - 4, with lower limit and upper limit of - 8 and 0 (zero) respectively. "Maintain" linguistic term keeps the PEEP unchanged by having a peak value of 0 (zero), with lower and upper limits of - 4 and + 4 respectively. Finally, the "Increase" linguistic term allows an increase of PEEP up-to + 8, with peak value of + 4 and lower limit of 0 (zero).

Table 3.8: Change-in-PEEP output membership function parameters for algorithm 1 system

Linguistic term	**Linguistic meaning/ params**
Decrease	[-8 -4 0]
Maintain	[-4 0 4]
Increase	[0 4 8]

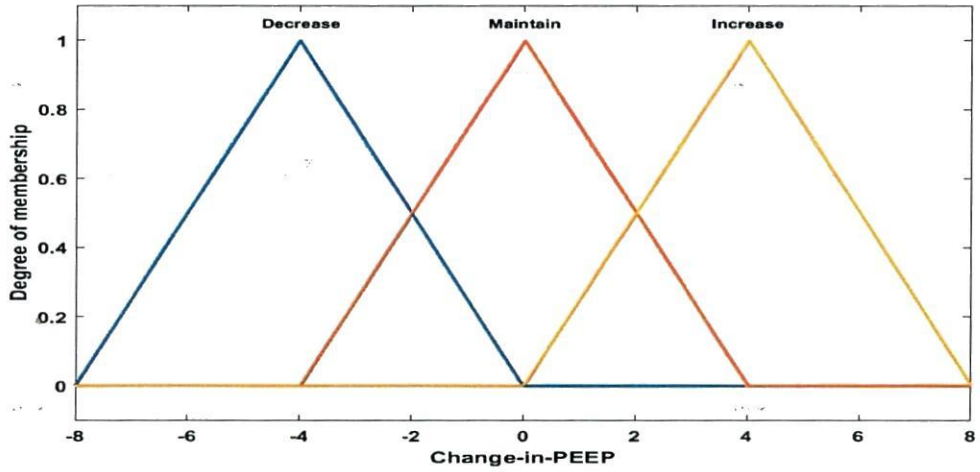


Figure 3.9: Membership function for change in PEEP output

The designed fuzzy logic based algorithms produce an output of "change-in-PEEP", and the PEEP adjusted by the ventilator (extrinsic PEEP) is calculated using the general Equation 3.2. The algorithms either increase or decrease the PEEP that is already in the patient's lungs (intrinsic PEEP), with respect to the FiO_2 measurement. The FiO_2 readings are increased as the PEEP values change until the optimal readings that protect the patient's lungs are attained.

$$Extrinsic\ PEEP = Intrinsic\ PEEP + (change - in - PEEP) \tag{3.2}$$

For decremental and incremental high-PEEP algorithm, Equation 3.3 particularly shows the formula used to calculate the extrinsic PEEP that is represented by the Fuzzy high PEEP; where physician high-PEEP is the intrinsic high-PEEP.

$$Fuzzy\ high\ PEEP = Physician\ high\ PEEP + (change - in - PEEP) \tag{3.3}$$

The fuzzy decremental and incremental low-PEEP in Equation 3.4 is the extrinsic low-PEEP, and physician low-PEEP is the intrinsic low-PEEP.

$$Fuzzy\ low\ PEEP = Physician\ low\ PEEP + (change - in - PEEP) \tag{3.4}$$

Fuzzy logic designer rules: The fuzzy set rules for low-PEEP are shown in Appendix, in Table 1 and continued in Table 2 and Table 3. For high-PEEP, the rules are shown in Table 4 and continued in Table 5 and Table 6.

3.2.2 Design and Simulation of a Physician Based Fuzzy Neural System for Ventilator Adjustments in ARDS Patients to Ensure Lung Protection

Neuro-Fuzzy Designer in MATLAB R2021b was used (since it is the only tool used to train the fuzzy neural network) to train the algorithm that detects the acute respiratory distress syndrome network (ARDSNet) protocol for positive end expiratory pressure (PEEP) ranges based on the inspired fraction of oxygen (FiO_2) values. Two inputs were considered during the training, that is: FiO_2 and PEEP, of which, Berlin definition of ARDS defines PEEP as high and low. The architecture design of the Neuro-Fuzzy Designer is shown in Figure 3.10, with which 20 membership functions (MFs) were chosen for the grid partition when generating the fuzzy inference system (FIS), 20 MFs were the optimal MFs to have

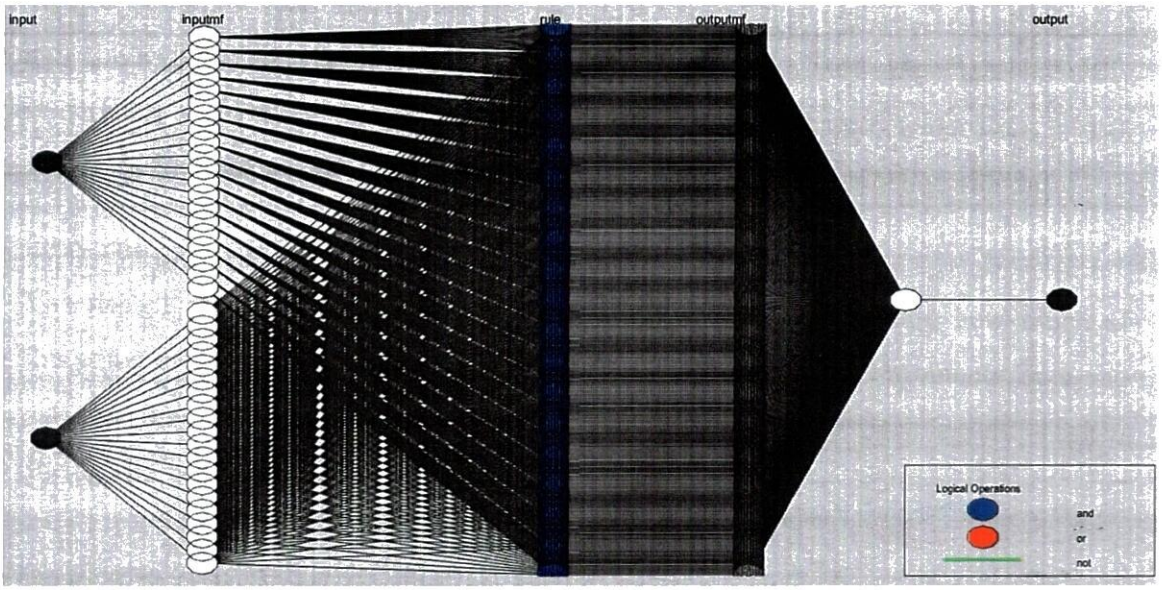


Figure 3.10: Neuro-Fuzzy Designer structure with two inputs, 20 membership functions for each input; and one output

the zero error. Hybrid optimatization method was selected at a zero error tolerance, and

20 epochs were used for the training, which was the optimal number to avoid the network from under-learning and over-learning.

Figure 3.11 shows the patient subsystem that entails the code to generate the FiO_2 and PEEP values that are fed into the fuzzy logic controller (FLC) for analysing. The output of the FLC is passed through the switch to generate the FiO_2 values greater than or equal to 0.3, as indicated in the Berlin ARDS definition. The values for PEEP are incremental, from 5 to 24, and then repeated for the different values of FiO_2.

From left to right of Figure 3.11, patient's respiratory system icon [Tamburrano et al., 2022] represents the measurements read from the patient; which are passed through the fuzzy logic controller (FLC) with electronic-brain icon [1], where the fuzzy logic algorithms and neural fuzzy network algorithms are stored. The output of the FLC was passed through the switch that considers values of $FiO_2 \geq 0.3$. FiO_2 values are incrementally added with 0.1 value for each full scale of PEEP values (≤ 24) upto when $FiO_2 = 1.0$. The values of FiO_2 and PEEP are then recorded to workspace file labelled as "data".

i) **General System:**

The design of the system is to guide the physician in determining how much of the adjustments to make during the ventilation after taking measurements from the patient. The system bases on the ARDS Berlin definition of the procedure taken during the ventilation of an ARDS patient.

Figure 3.12 shows a patient whose readings/ crisp inputs (inputs to the fuzzy system) are taken; that is, FiO_2, PEEP. The crisp inputs are fuzzified as shown in Figure 3.15. The "FiO_2 and PEEP input subsystem" is a subsystem that generates simulated FiO_2

[1] https://sciencebusiness.net/healthy-measures/news/artificial-intelligence-better-doctors-identifying-patients-risk-ventilator

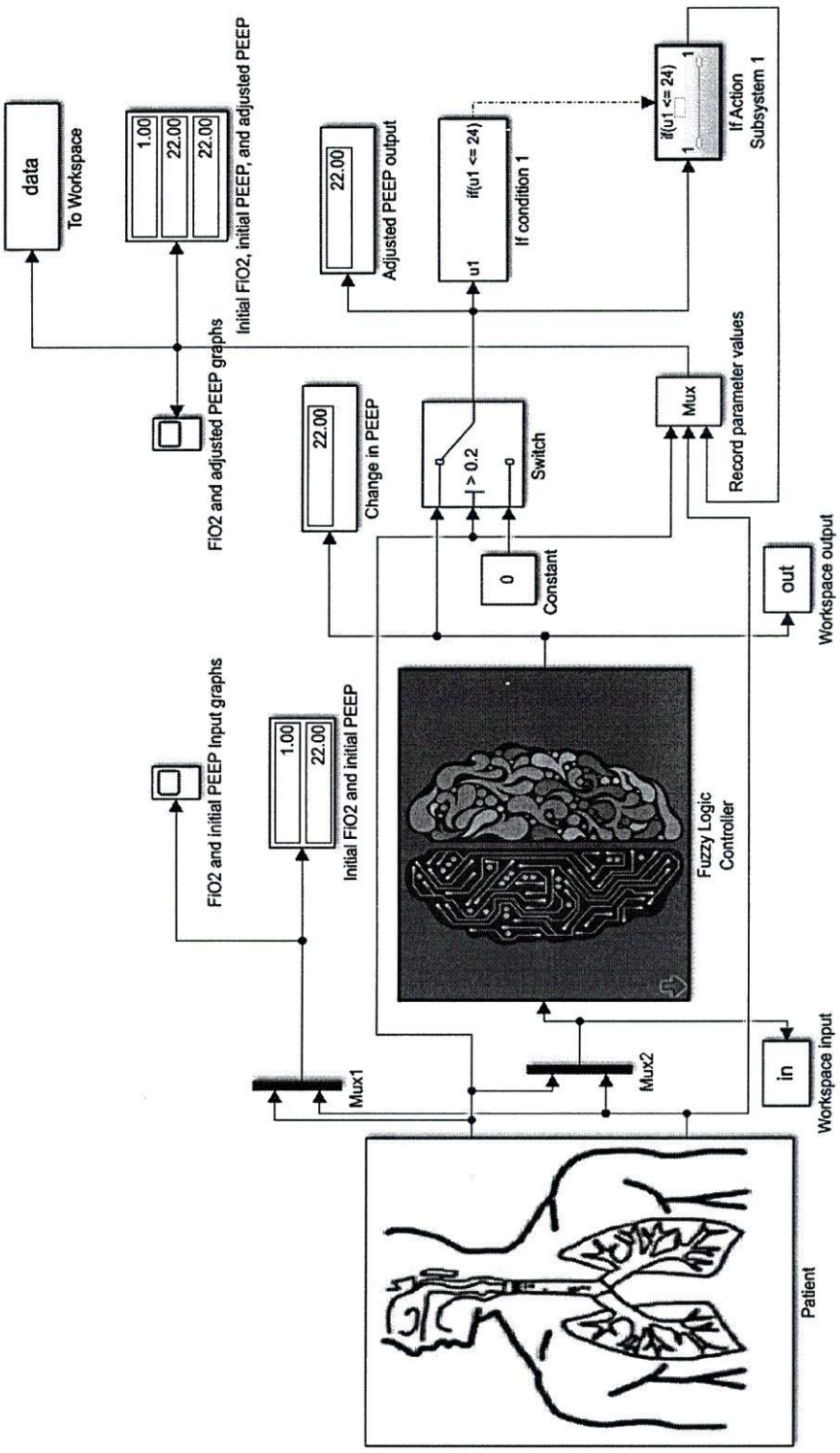


Figure 3.11: Fuzzified ARDS Berlin definition of ARDSNet PEEP table

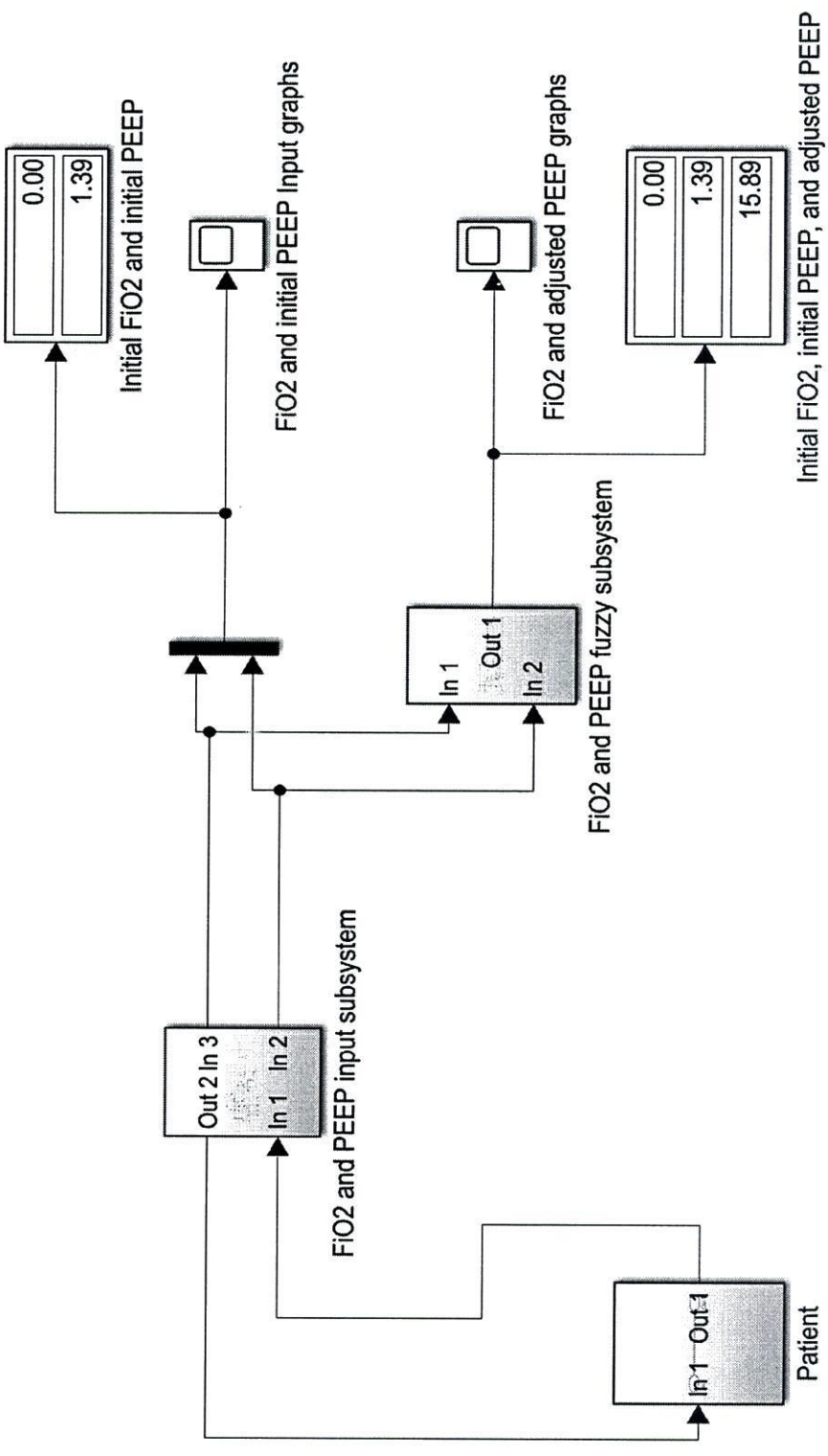


Figure 3.12: Fuzzy based ARDS Berlin definition

and PEEP data to be fed into "FiO2 and PEEP fuzzy subsystem". The readings are then taken using the Simulink display and simultaneously plotted using the Simulink scope.

ii) **Patient Subsystem:**The patient subsystem in Figure 3.13 is used as a loop path for the "FiO_2 and PEEP subsystem". The input 1 (In 1) connected to the output 1 (Out 1) is the FiO_2 and PEEP data from the patient input/ output subsystem to the "FiO2 and PEEP input subsystem" fuzzy system.

The Output 1 (Out 1) in Figure 3.13 connects to the Input 1 (In 1) in Figure 3.14. Output 3 (Out 2) in Figure 3.14 connects to the Input 1 (In 1) in Figure 3.13.



Figure 3.13: Input-Output logic for patient subsystem

iii) **FiO2 and PEEP Input Subsystem:**

The input 1 (In 1) is the FiO_2 data passed through the initial condition block (Initial FiO2) to initialise the signal during the simulation. The signal is set through the code clock (Initial input Code Block) whose purpose is to pause the loop after one second; input, u0 is connected to the output, y0.

The if-condition (if condition 3) triggers the signal from the code block output, y0; if the output, y1 from the code block is equal to zero (0), then the signal is sent from

output, y0 to memory 2, which is then added on a bias (Bias 3) of 0.1.

The if-condition (If condition 4) helps in triggering the PEEP. The initial PEEP is set to zero (0) and then sent to input, u1 of the code block which is connected to output, y1. The signal from the output, y1 is added on a bias (Bias 1) of 1, then the signal is sent to memory 1. The signal is then fed into the code block (Loop Code Block) that contains an If-condition; if input, u1 is less than 25, then output, y0 is connected to input, u1; otherwise, the output, y0 is connected to input, u0. The simulation stops if the FiO_2 input is greater than 0.9.

The action subsystems ("If Action Subsystem 1.1", "If Action Subsystem 1.2", "If Action Subsystem 3", and "If Action Subsystem 4") are used to relay the original signal since the signal sent from the If-condition block is a trigger signal.

The Output 1 (In 3) in Figure 3.14 connects to the Input 1 (In 1) in Figure 3.15; Output 2 (In 2) in Figure 3.14 connects to the Input 2 (In 2) in Figure 3.15.

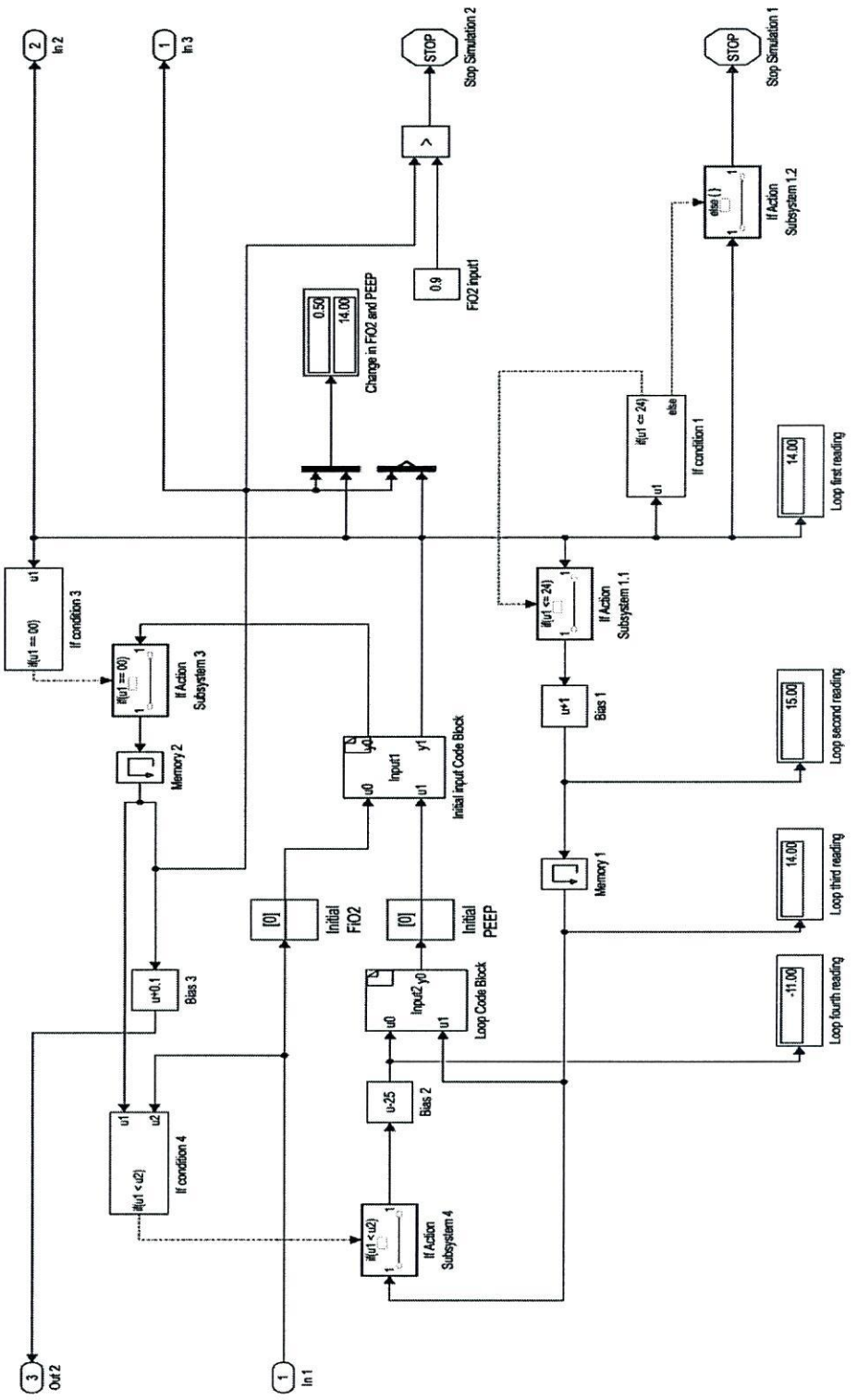


Figure 3.14: FiO_2 and PEEP input subsystem

iv) **FiO2 and PEEP Fuzzy Subsystem:**

The inputs (In 1 and In 2) are fed into the Fuzzy Logic Controller (FLC) as crisp inputs and then output as crisp output which is the change in the PEEP to be made. The output (change in PEEP) is then added to the initial PEEP. The output 1 (Out 1) in Figure 3.15 is then displayed and plotted using the Simulink display and scope respectively.

The If-condition (If condition 1) is used to generate the PEEP data for as long as the PEEP is less than or equal to 24. The membership functions used in designing the FLC are in Figure 3.9, Figure 3.6, Figure 3.7, and Figure 3.8.

The fuzzy logic and fuzzy neural network approaches designed were used to protect the lungs by; firstly, using fuzzy logic in fuzzy logic designer for adjustment of the parameters within the Berlin ARDS protocol limit of 4 cm H_2O; secondly, the neural network in neural fuzzy designer was used to mimic the values before adjustments. With this, the lungs are protected within the limits suggested in the Berlin ARDS protocol.

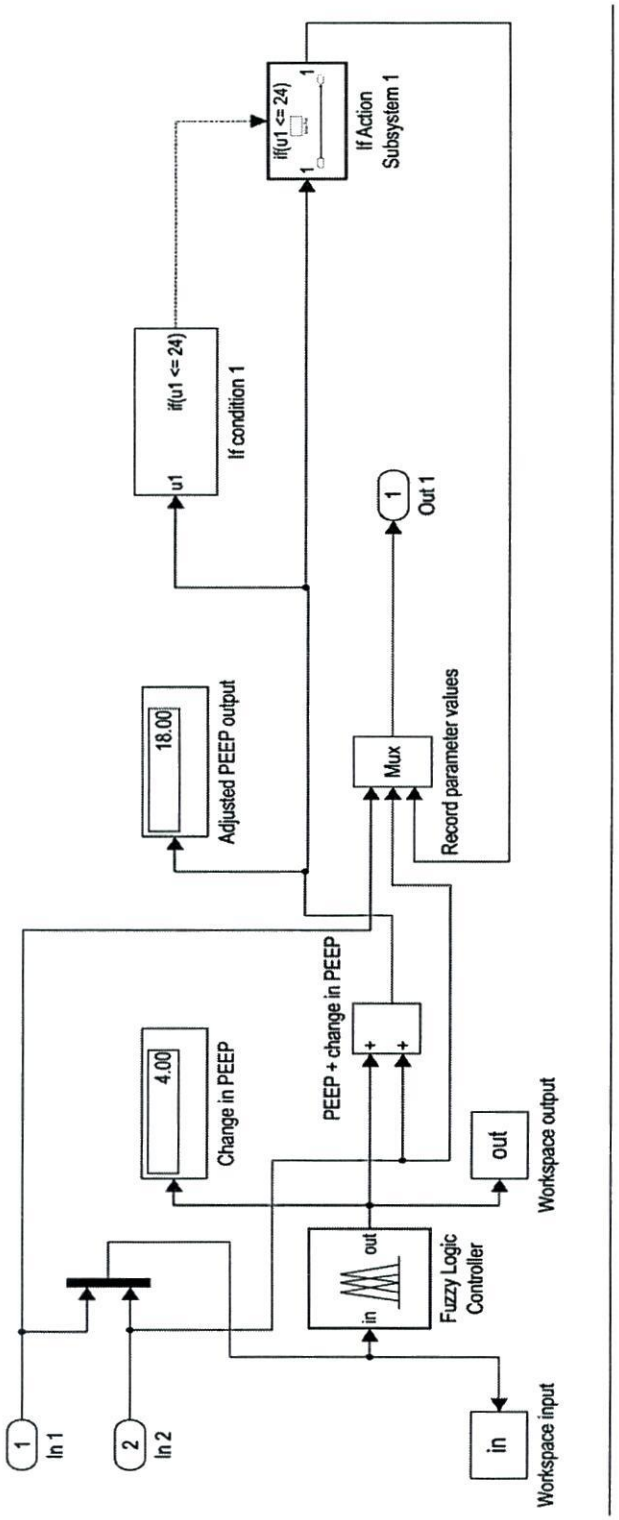


Figure 3.15: FiO_2 and PEEP fuzzy subsystem

3.2.3 Build a Feed-in Imaging Model to Detect Lung and Brain Scans using Convolutional Neural Network

The training of medical images using the neural network was done with convolutional neural network (CNN), that identifies and extracts features from images for classification. The trained algorithm uses the inputs of the CNN that has 3-dimensional tensor of shape [width, height, channel] = [224, 224, 3]. The width and height are the dimensions of the images of the different lung conditions, in pixels, and the channel represents the three colors of the image, that is: red, green, and blue. The output of the classification was the probability distribution over a set of brain and lung classes.

The residual network with 50 layers (ResNet-50) is a type of CNN which was used to support the training of new images, by changing the input parameters and output classes. ResNet-50 was chosen because of: the many layers that deeply extract the many features from the medical images; it was trained on a big image database, making it faster to extract features using the transfer learning method. The training parameters that were set for the algorithm training are explained under the lung and brain sections:

A) **Lung:**

Two types of lung diseases that were considered during the study were: corona virus disease 2019 (COVID-19), pneumonia, and during the training, images of normal/ healthy patients were used as control method. The different conditions are displayed in Figure 3.16. Images (a), (b), (c) display COVID-19, healthy lung, and pneumonia, respectively.

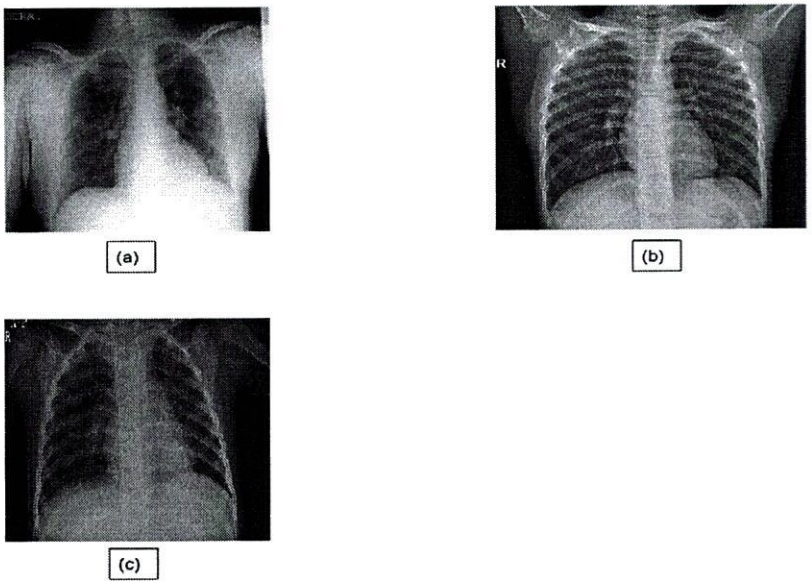


Figure 3.16: Conditions of the lung: (a) COVID-19, (b) healthy, and (c) pneumonia

3,616 COVID-19 images, 4,265 pneumonia images, and 11,767 healthy/ normal lung images were got from Xiaosong et al. [2017], Kermany et al. [2018], Chowdhury et al. [2020], Rahman et al. [2021]. The authors stored their published image dataset in kaggle repository [1]. 752 COVID-19 images, 1,584 pneumonia images, and 1,639 healthy/ normal lung images were got from Bhowal et al. [2021]. The published dataset was stored in kaggle repository [2]. 12,544 healthy/ normal lung images were got from Bhowal et al. [2021]. The published dataset was stored in kaggle repository [3]. Therefore, this gave a total number of 4,368 COVID-19 images, 11,767 pneumonia images, and 4,265 healthy/ normal lung images.

The number of test images were subtracted from the total number of images before the training of the lung CNN algorithm. 100 COVID-19 images, 100 pneumonia images, and 150 healthy lung images were used for testing. To attain the number of images

for training and validation, the code;
$[trainingSet, validationSet] = splitEachLabel(imds, 0.7, 'randomize')$; was used. 70% of the total number of images with test image data subtracted, was used for training and 30% for validation. The summary of the image dataset is indicated in Table 3.9.

Table 3.9: Lung CNN algorithm parameters

	COVID-19	**Pneumonia**	**Normal**	**Reference**
Source 1[1]	3,616	4,265	11,767	[Xiaosong et al. [2017], Kermany et al. [2018], Chowdhury et al. [2020], Rahman et al. [2021]]
Source 2[2]	752	1,584	1,639	Bhowal et al. [2021]
Source 3[3]			12,544	Ahishali et al. [2021]
Total images	4,368	13,351	25,950	
Test dataset	100	100	150	
Train dataset	2,988	4,024	18,060	
Validation dataset	1280	1725	7,740	

[1]https://www.kaggle.com/datasets/donjon00/covid19-detection
[2]https://www.kaggle.com/datasets/subhankarsen/novel-covid19-chestxray-repository
[3]https://www.kaggle.com/datasets/aysendegerli/qatacov19-dataset

B) **Brain:**

Two types of brain disorder that were considered during the study were: acute ischemic stroke and hemorrhagic stroke. The different conditions are displayed in Figure 3.17. Images (a), (b), (c) display acute ischemic stroke, control/ healthy brain, and hemorrhagic stroke, respectively.

1,002 acute ischemic stroke images were got from Tasci and Tasci [2022]. The image data was acquired from kaggle repository [1]. 1,037 hemorrhagic stroke images were got from Hssayeni [2019]. The image data was acquired from kaggle repository [2]. 1,008 healthy images were got from kaggle repository [3]. The number of test images were

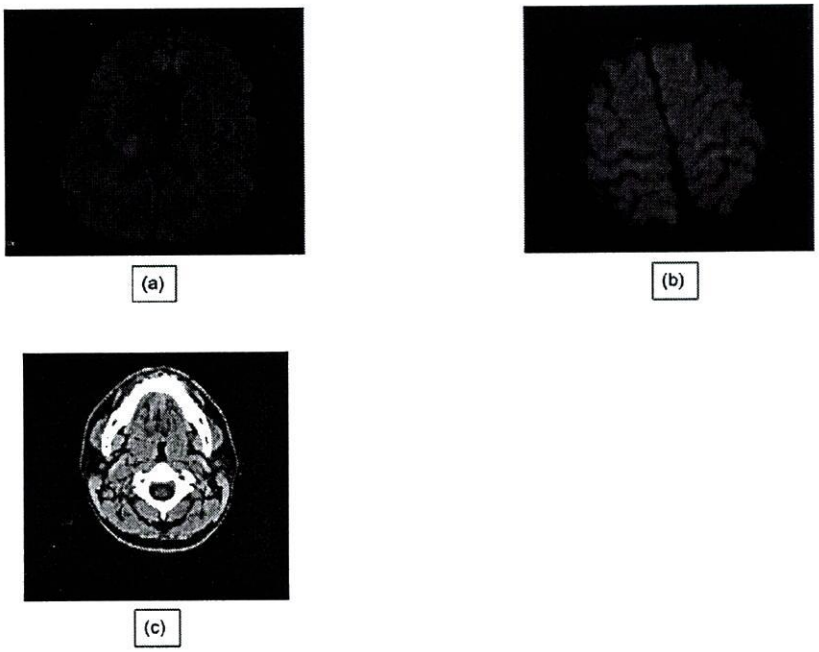


Figure 3.17: Conditions of the brain: (a) acute ischemic stroke, (b) healthy, and (c) hemorrhagic stroke

subtracted from the total number of images before the training of the brain CNN algorithm. 50 acute ischemic stroke images, 50 hemorrhagic stroke images, and 50 healthy lung images were used for testing. The summary of the image dataset is indicated in Table 3.10.

Table 3.10: Brain CNN algorithm parameters

	Acute ischemic stroke	**Intracranial hemorrhage**	**Control**
Source 1[1]	1,002 [Tasci and Tasci [2022]]		
Source 2[2]		1037 [Hssayeni [2019]]	
Source 3[3]			1,008
Total images	1,002	1,037	1,008
Test dataset	50	50	50
Train dataset	666	691	671
Validation dataset	296	261	287

To calculate the accuracies of the algorithms, the formulas of precision, recall/ sensitivity, F1-score, and accuracy shown in Equation 3.5, Equation 3.6, Equation 3.7, and

[1]https://www.kaggle.com/datasets/buraktaci/mri-stroke?select=Acute+Ischemic+Stroke-Control
[2]https://www.kaggle.com/datasets/vbookshelf/computed-tomography-ct-images
[3]https://www.kaggle.com/datasets/afridirahman/brain-stroke-ct-image-dataset

Equation 3.8 respectively, were used [Powers, 2011].

$$Precision = \frac{TP}{TP + FP} \tag{3.5}$$

$$Recall/sensitivity = \frac{TP}{TP + FN} \tag{3.6}$$

$$F1 - score = 2\,\frac{Precision\ \times\ Recall}{Precision + Recall} = \frac{2TP}{2TP + FP + FN} \tag{3.7}$$

$$Accuracy_{model} = \frac{TP + TN}{TP + TN + FP + FN} * 100\% \tag{3.8}$$

where, TP, FP, FN, and TN are True Positive, False Positive, False Negative, and True Negative respectively.

3.2.4 Design and Simulation of an Intelligent System to Test and Validate Patient Ventilator Synchrony and Lung Protection using Real-time Medical Imaging and Fuzzy Expert System

A) **General MATLAB/ Simulink Schematic System**

The general Simulink simulation of fuzzified ventilator system in MATLAB software is shown in Figure 3.18. From left to right of the figure, the brain and lung images are passed through the CNN model; the predictions, scores and labels are then displayed. The outputs of the PEEP algorithm system are displayed on the screen of the system as suggestions for physicians to adjust on the ventilator.

The algorithm starts with the lung imaging section. If the patient has pneumonia, the signal is sent to the incremental high PEEP fuzzy algorithm. For a patient with COVID-19, the signal is sent to the decremental high PEEP fuzzy algorithm. In case the patient on ventilation has healthy lungs, that is: normal, the signal is sent to "switch 1" to turn on the brain scan.

The brain imaging section is then activated and the algorithms are selected. If the patient has intracranial hemorrhage or acute ischemic stroke, the signal is sent to the incremental low PEEP fuzzy algorithm. For a patient with a healthy/ control brain scan, the signal is sent to the decremental low PEEP fuzzy algorithm.

B) **Convolutional Neural Network Subsystem**

Figure 3.19 displays a subsystem of the general ventilator schematic system. The

brain and lung scans are passed to the the MATLAB function block that contains a conversion code. The code converts 2-dimensional input images into 3-dimensional output images and leaves the 3-dimensional input images unchanged.

The signal is then sent to the MATLAB resize block that adjusts the size of the input images to [224, 224, 3]. This is done to make all input scans uniform so as to align with the image input size of the MATLAB CNN based image classifier. The image signal is then passed through the CNN classifier, and the results are displayed as prediction, scores, and labels.

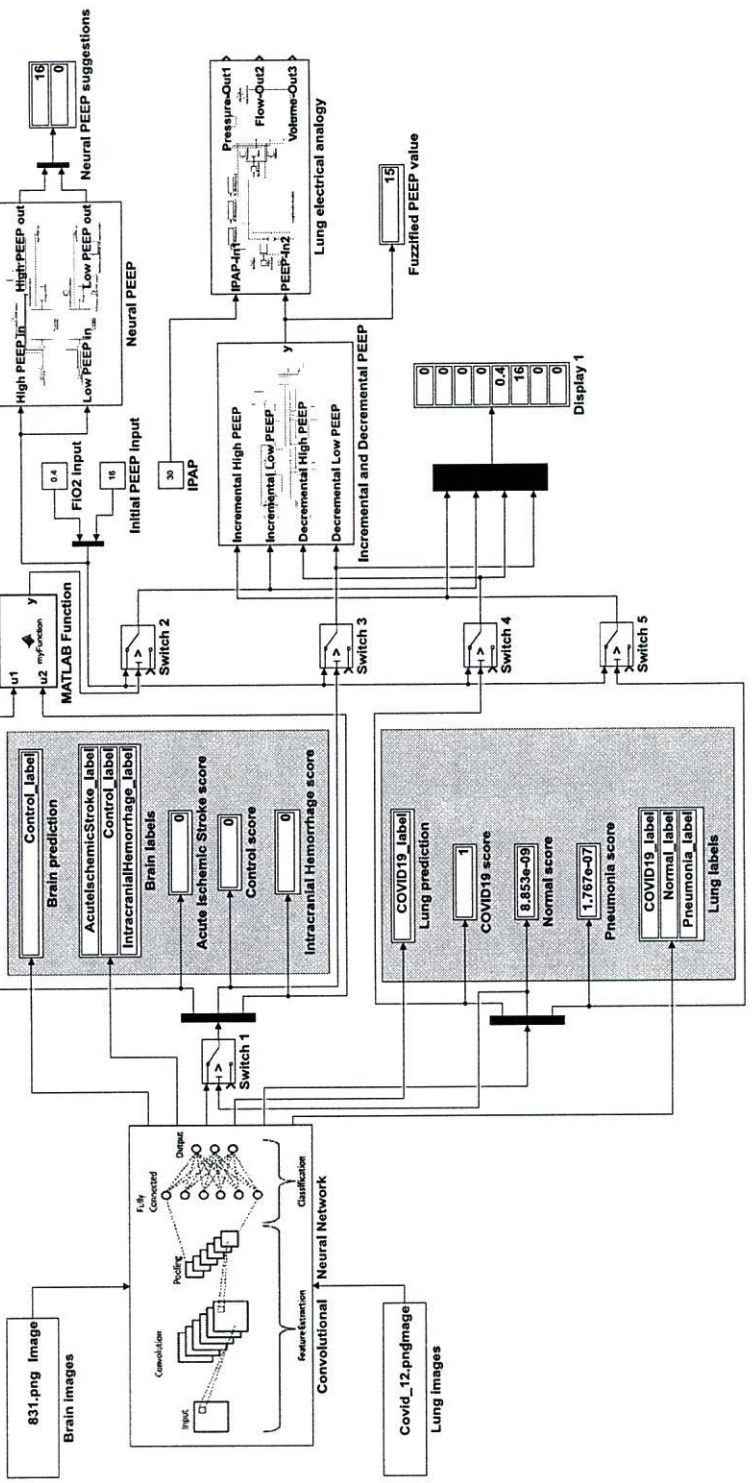


Figure 3.18: General MATLAB/ Simulink schematic system showing the image input, processing of images using

Figure 3.19: Convolutional neural network Simulink subsytem for the brain and lung images

C) **Fuzzy Logic Based PEEP Subsystem**

There are four fuzzy logic algorithms designed as shown in Figure 3.20. Fuzzy Logic Controller, Fuzzy Logic Controller1, Fuzzy Logic Controller2, and Fuzzy Logic Controller3; containing the incremental high PEEP fuzzy algorithm, incremental low PEEP fuzzy algorithm, decremental high PEEP fuzzy algorithm, and decremental low PEEP fuzzy algorithm, respectively.

The input of the system is selected by the condition of the lung and/or brain, and the output is the fuzzified PEEP value that is suggested to the physician. For a patient with pneumonia, the signal is passed through the incremental high PEEP fuzzy algorithm input (1) of the subsystem. For a patient with COVID-19, the signal is passed through the decremental high PEEP fuzzy algorithm input (3) of the subsystem. A patient on ventilation with healthy lungs/ normal, with intracranial hemorrhage or acute ischemic stroke, the signal is passed through the incremental low PEEP fuzzy algorithm input (2) of the subsystem. For a patient with a healthy/ control brain scan, with a healthy lung, the signal is passed through the decremental low PEEP fuzzy algorithm input (4) of the subsystem.

The values from the four PEEP algorithms are passed through the MATLAB function block to output the predicted value, to the output (1) of the subsystem. The value is then passed to the lung electrical analogy subsystem.

D) **Neural Based PEEP Subsystem**

Figure 3.21 displays the subsystem for PEEP algorithms built using the fuzzy neural

designer. The inputs of the subsystem (1) and (2) are the fraction of inspired oxygen (FiO_2) and PEEP read from the patient. The outputs (High PEEP out and Low PEEP out) mimic the acute respiratory distress syndrome Network (ARDSNet) PEEP table values.

The Fuzzy Logic Controller contains the fuzzified high PEEP neural algorithm and Fuzzy Logic Controller2 contains the fuzzified low PEEP neural algorithm. The outputs are to guide the physicians to evaluate the difference between the fuzzy logic suggested PEEP values and the ARDSNet PEEP values (neural algorithm output values).

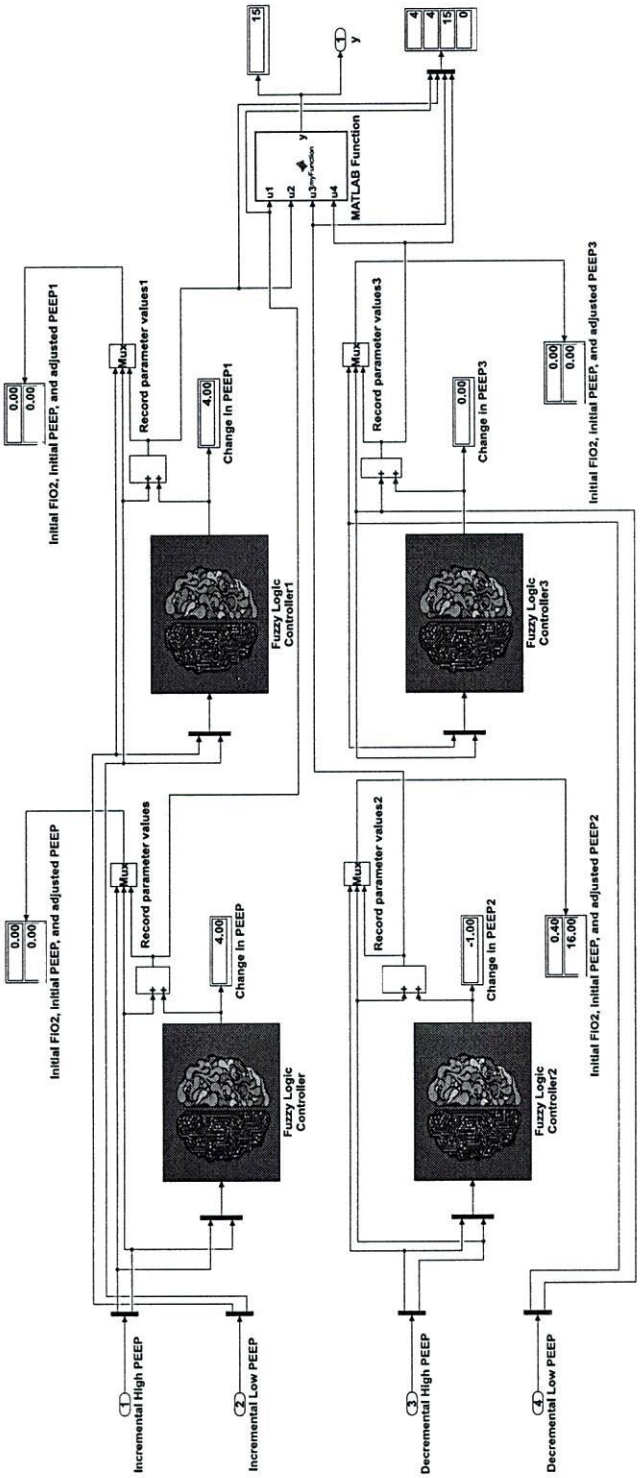


Figure 3.20: Fuzzy logic based PEEP subsystem containing the trained four fuzzy logic PEEP algorithms

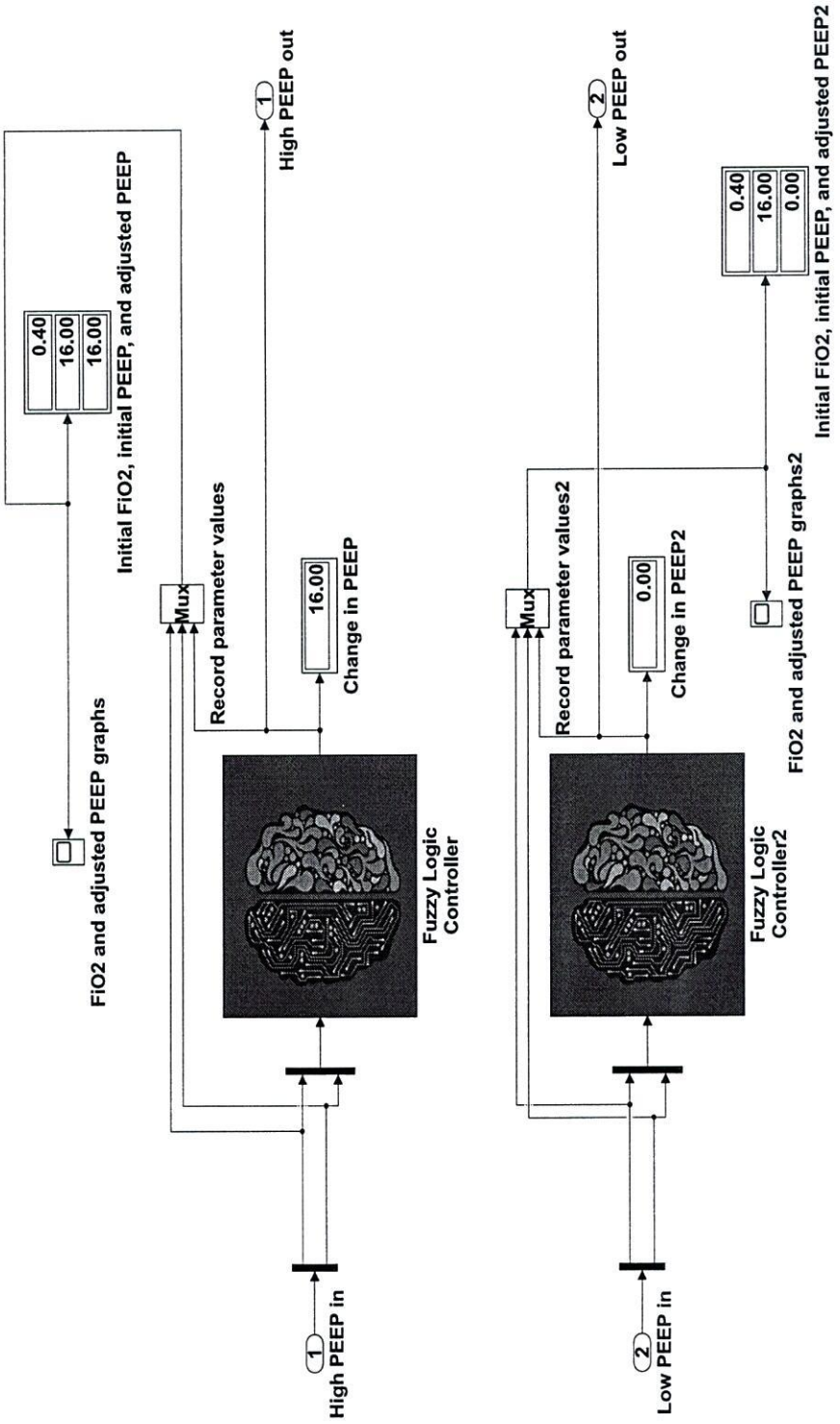


Figure 3.21: Neural based PEEP subsystem containing the trained two neural fuzzy algorithms

E) **Lung compartment subsystem**

Lung transfer function was derived using the electrical analogy. The purpose of the lung transfer function was to test the efficiency of the developed algorithms using the lung transfer function as a patient. Different lung conditions were tested using different lung transfer conditions.

In a lung system, there is an input variable during the inspiration and an output variable during the expiration. For this study, the current, i was considered as the output variable of the lung system and voltage, V_{in} as the input variable of the lung system, for a single lung compartment of the respiratory system shown in Figure 3.22. Resistor, R represents the airway resistance; capacitor, C represents the compliance of the lung. The voltage input variable creates a potential difference that causes

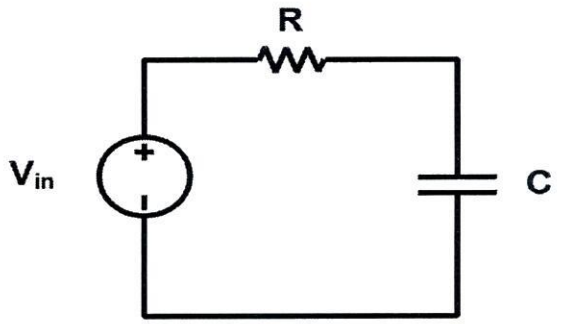


Figure 3.22: Electrical circuit of the respiration system

a proportional electric current to flow through the circuit, as per Ohm's law. The electric current is therefore the output variable of the system.

From Figure 3.22, derivation of the single lung transfer function, $H_{(s)}$ was attained

starting with the Ohm's formula of the system, as shown in Equation 3.9.

$$V_{in} = iR + \frac{1}{C}\int i(t)dt \tag{3.9}$$

Laplace transforms of the parameters in Equation 3.9 were then attained as shown in Equations 3.9a to 3.9c;

$$V_{in(s)} = I_{(s)}R + \frac{I_{(s)}}{Cs} \tag{3.9a}$$

$$= I_{(s)}(R + \frac{1}{Cs}) \tag{3.9b}$$

$$= I_{(s)}(\frac{RCs+1}{Cs}) \tag{3.9c}$$

$$H_{(s)} = \frac{I_{(s)}}{V_{in(s)}} = \frac{Cs}{RCs+1} \tag{3.10}$$

Equation 3.10 indicates the lung transfer function of the lung that was used in this study. Different values of capacitance and resistance were used to come up with the different lung conditions (sick and healthy lungs). Simulink settings for the lung compartment used in the study are;

(1) Amplitude/ Inspiratory positive airway pressure (IPAP) = 30 cm H_2O was used as per the ARDSNet PEEP protocol.

(2) Total cycle time (TCT) = 3 s (1 s inspiration and 2 s expiration)

(3) Pulse width = 33.33 % of TCT = inspiration time. This was to limit the inspraition to 1 second and expiration to 2 seconds.

(4) Formula in Equation 3.11 was used to show that for a healthy lung, if the patient inspires for 1 second and expires for 2 seconds, then there should be 20 breathes

in each minute, as shown in Equations 3.12 and 3.13;

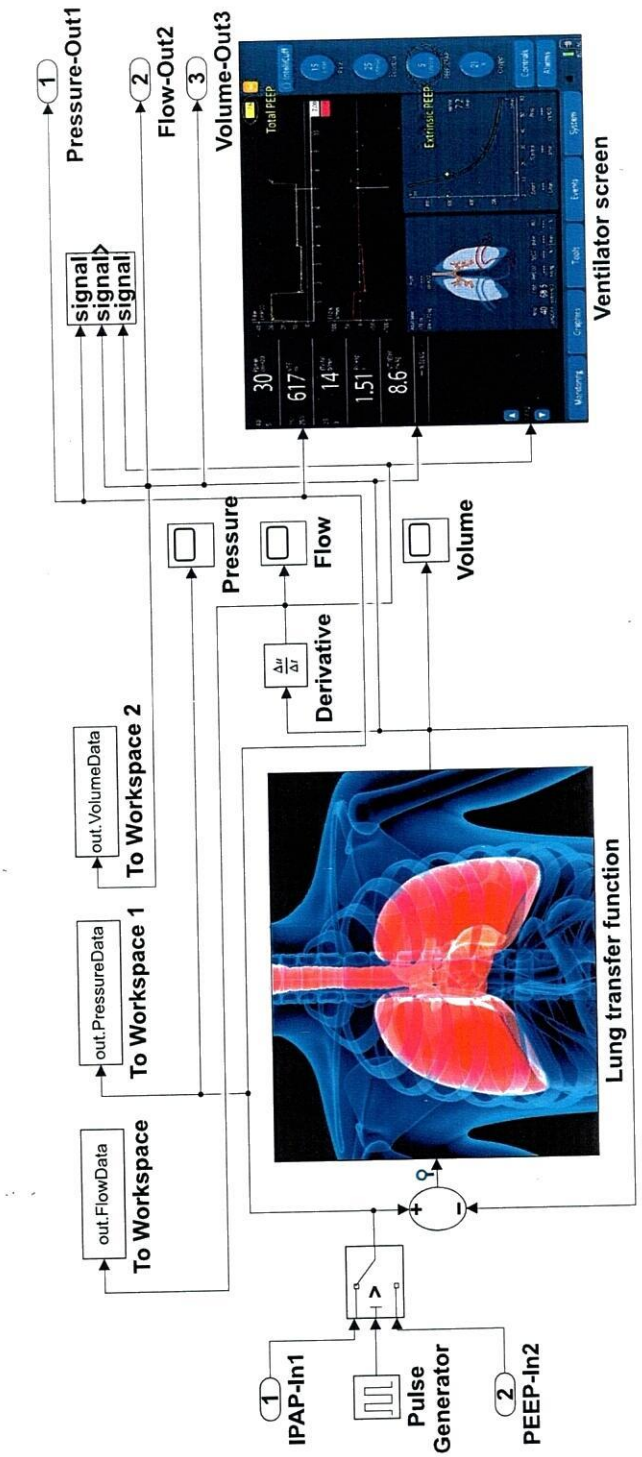
$$Breaths\ per\ minute = \frac{1\ min}{TCT} \tag{3.11}$$

$$Breaths\ per\ minute = \frac{60\ s}{3\ s} \tag{3.12}$$

$$Breaths\ per\ minute = 20\ breaths\ per\ minute. \tag{3.13}$$

The fuzzified PEEP values were then passed through the lung transfer function of the electrical analogy operation of the lung, as shown in Figure 3.23, as input (PEEP-In2). The output of the lung transfer function was then passed through the screen to display the pressure, volume, and flow graphs of the air in the lungs.

The fuzzy algorithms concentrate on the lung protection as they have the adjustments and Berlin ARDSNet values within the recommended 4 cm H_2O limits. The imaging is able to track the lung recovery during the ventilator parameters, improving the patient-ventilator synchrony, since the triggering is done based on the patient's health feedback.


1
Pressure-Out1
2
Flow-Out2
3
Volume-Out3
signal
signal
signal
Ventilator screen
Pressure
Flow
Volume
Derivative
out.VolumeData
To Workspace 2
out.PressureData
To Workspace 1
out.FlowData
To Workspace
Lung transfer function
1
IPAP-In1
Pulse Generator
2
PEEP-In2

and high-PEEP set to 5, giving a crisp output (change-in-PEEP) of 0 (zero); that is, the extrinsic high-PEEP is the same as the intrinsic high-PEEP, implying that no change in PEEP was required. That is, the ventilator PEEP does not need to be adjusted.

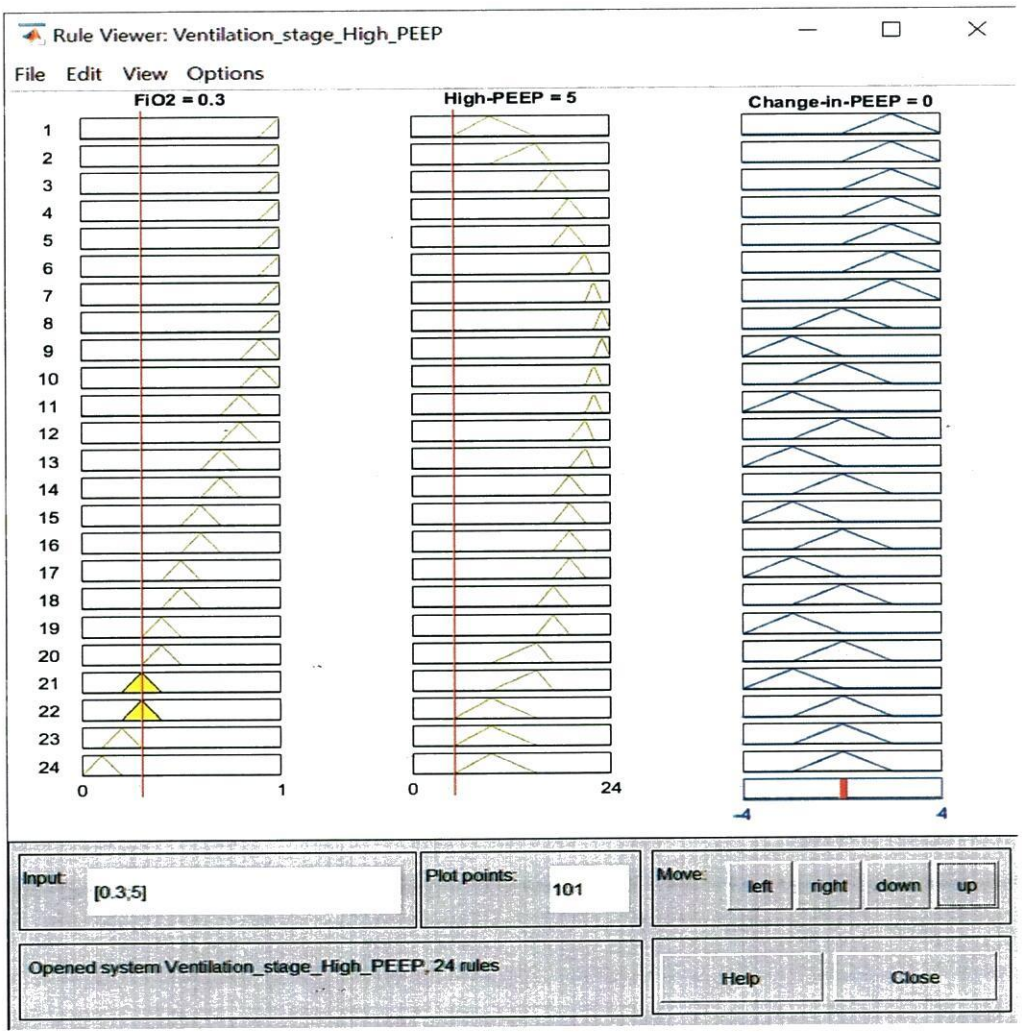


Figure 4.1: Rule viewer: decremental high-PEEP algorithm 1; two crisp inputs: FiO_2 = 0.3 and high-PEEP = 5 giving a crisp output: change-in-PEEP = 0

Figure 4.2 displays the decremental low-PEEP algorithm, with two crisp inputs: FiO_2

set to 0.3 and low-PEEP set to 5. Giving a crisp output (change-in-PEEP) of 5×10^{-17}; that is, the extrinsic low-PEEP is $5 + 5 \times 10^{-17}$. The results were calculated using the Equation 3.4.

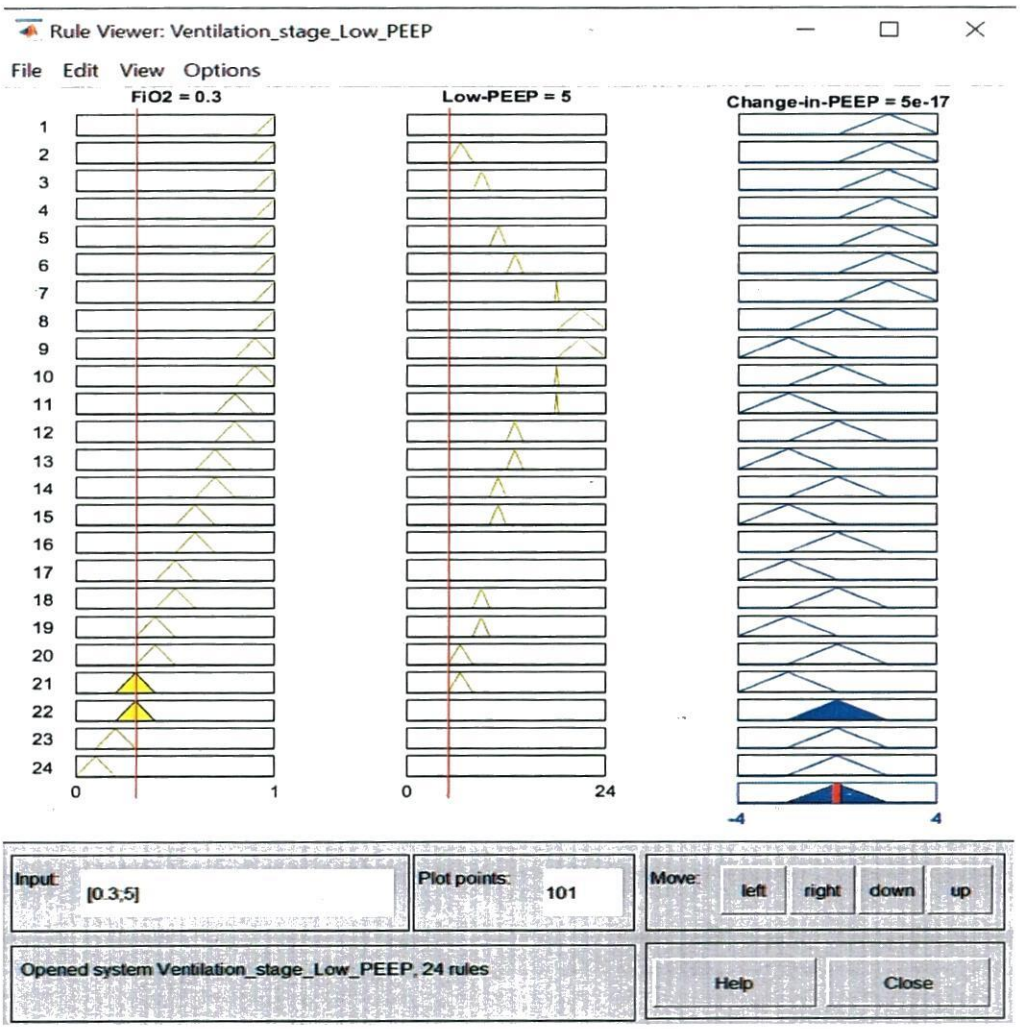


Figure 4.2: Rule viewer: decremental low-PEEP algorithm 1; two crisp inputs: FiO_2 = 0.3 and low-PEEP = 5 giving a crisp output: change-in-PEEP = 5×10^{-17}

Table 4.1 and Table 4.2 show the summary of the calculations of the extrinsic readings of the high-PEEP and low-PEEP, respectively, using the decremental high-PEEP algorithm. The calculations compare the fuzzy based Berlin definition of ARDS (system designed in this study) and the physician based mechanical ventilation (MV) protocol using the original high levels of PEEP [Brower et al., 2004]. The fuzzified values of the PEEP indicate the PEEP adjustments to be made during the ventilation. For patient PEEP values close to the respective Physician PEEP, with respect to the FiO_2 value, the adjustment is zero or close to zero. While values of PEEP from the patients higher than the respective Physician PEEP, with respect to the FiO_2 value, the adjustment is a decremental one. This follows the fuzzy rules set for the decremental PEEP.

The physician based PEEP adjustments for MV protocol as shown in Table 2.2 [Brower et al., 2004, Sahetya et al., 2017b], have whole numbers for PEEP adjustments; however, the fuzzified system of this research, has PEEP adjustments with detailed variation in change of the PEEP. This implies that the fuzzy based Berlin definition of ARDS system is more accurate, improving on the accuracy of the decision making during the MV.

Table 4.1: Comparison between physician based high-PEEP definition and fuzzified decremental high-PEEP [Brower et al., 2004, Sahetya et al., 2017b]

Input variables	Output variables	
FiO_2	**Physician PEEP**	**Fuzzy high-PEEP**
0.3	5	$5 + 0$
0.3	6	$6 + 1.94 \times 10^{-16}$
0.3	7	$7 + 9.8 \times 10^{-17}$
0.3	8	$8 + 1.36 \times 10^{-17}$
0.3	9	$9 + 5.06 \times 10^{-17}$
0.3	10	10 + -0.244
0.3	11	11 + -0.621
0.3	12	12 + -0.927
0.3	13	13 + -1.22
0.3	14	14 + -1.55
0.4	14	$14 + -2.18 \times 10^{-17}$
0.4	15	$15 + 5 \times 10^{-17}$
0.4	16	16 + -1
0.5	16	$16 + 1.93 \times 10^{-17}$
0.5	17	$17 + 5 \times 10^{-17}$
0.5	18	18 + -1
0.6	18	18 + -1
0.6	19	19 + -1
0.6	20	20 + -1
0.7	18	$18 + 1.93 \times 10^{-17}$
0.7	19	$19 + 5 \times 10^{-17}$
0.7	20	20 + -1
0.8	20	$20 + 1.93 \times 10^{-17}$
0.8	21	$21 + 5 \times 10^{-17}$
0.8	22	22 + -2
0.9	22	22 + 0.134
1.0	22	22 + 2
1.0	23	$23 + 5 \times 10^{-17}$
1.0	24	$24 + 0$

Table 4.2: Comparison between physician based low-PEEP definition and fuzzified decremental low-PEEP [Brower et al., 2004, Sahetya et al., 2017b]

Input variables	**Output variables**	
FiO_2	**Physician PEEP**	**Fuzzy low-PEEP**
0.3	5	$5 + 5 \times 10^{-17}$
0.4	5	$5 + 0$
0.4	6	$6 + 1.36 \times 10^{-16}$
0.4	7	$7 + 1.36 \times 10^{-16}$
0.4	8	$8 + 0$
0.5	8	$8 + 0$
0.5	9	$9 + 5 \times 10^{-17}$
0.5	10	10 + -2
0.6	10	$10 + 5 \times 10^{-17}$
0.7	10	$10 + 0$
0.7	11	$11 + 5 \times 10^{-17}$
0.7	12	$12 + 0$
0.8	12	$12 + 0$
0.8	13	$13 + 5 \times 10^{-17}$
0.8	14	$14 + 0$
0.9	18	$18 + 0.134$
1.0	18	$18 + 2$
1.0	19	$19 + -4.24 \times 10^{-17}$
1.0	20	$20 + -2.46 \times 10^{-17}$
1.0	21	$21 + 5.01 \times 10^{-17}$
1.0	22	$22 + -2.31 \times 10^{-17}$
1.0	23	$23 + 5.28 \times 10^{-17}$
1.0	24	$24 + 8.73 \times 10^{-17}$

B) **Results in MATLAB (Surface View)**

There are two inputs: FiO_2 and PEEP and one output: change-in-PEEP. The X Mesh points are 11 to accomodate the 0 - 1 scale of FiO_2 values. The Y Mesh points are 25 considering the 24 adjustments made for PEEP. Figure 4.3 displays the surface view of the decremental high-PEEP algorithm, showing that the changes in PEEP

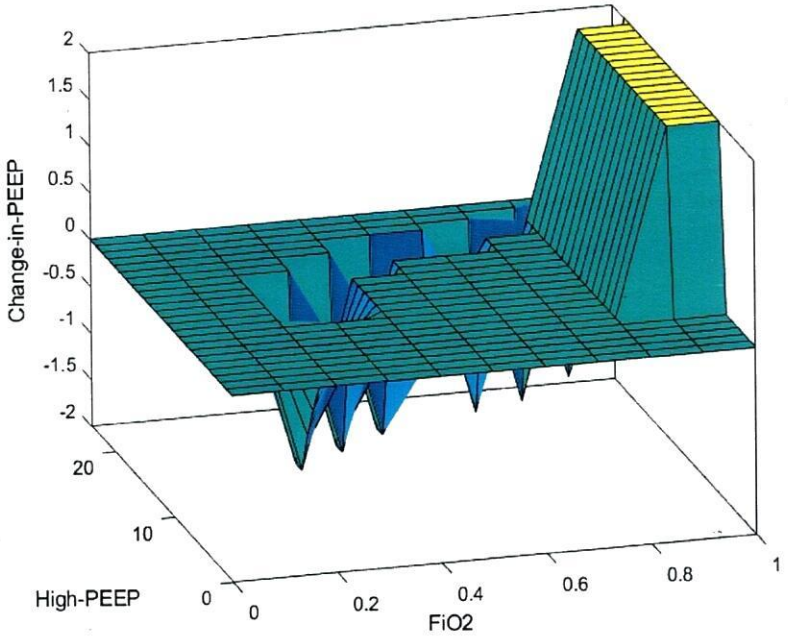


Figure 4.3: 3D surface view for decremental high-PEEP algorithm, with two inputs: FiO_2 and high-PEEP; and one output: change-in-PEEP

are mainly maintained based on the rules of the algorithm. It only decreases when reaching the optimal PEEP value. It is only for 0.8 - 1 values of FiO_2 that the PEEP is increased to meet the optimal PEEP value. The PEEP changes are seen more towards the upper PEEP scale of 0 - 24, due to higher PEEP values shown in Table 2.2. The PEEP changes tend towards the lower PEEP scale of 0 - 24 for Figure 4.4, due to lower PEEP values shown in Table 2.2.

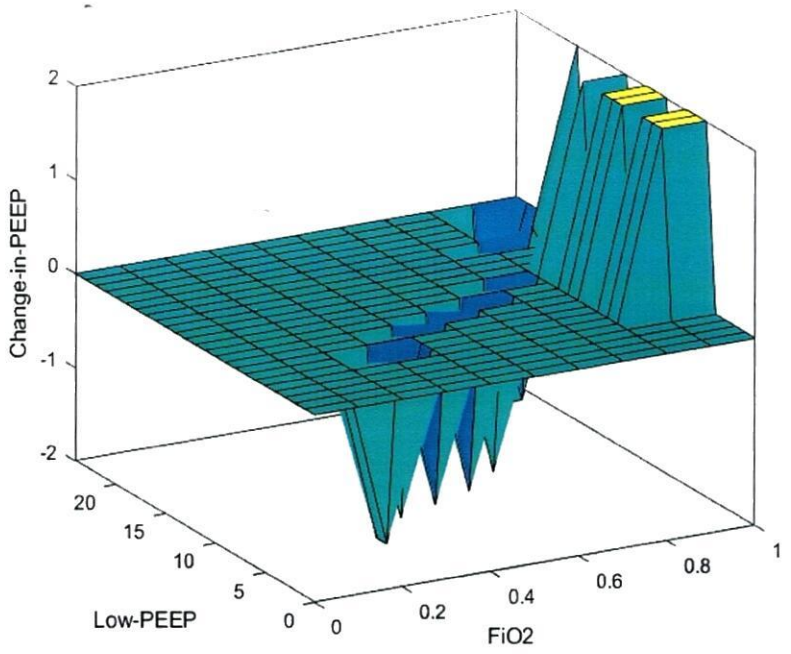


Figure 4.4: 3D surface view for decremental low-PEEP algorithm, with two inputs: FiO_2 and low-PEEP; and one output: change-in-PEEP

4.1.2 Incremental PEEP Algorithm

A) **Results in MATLAB (Rule Viewer)**

Figure 4.5 displays the incremental high-PEEP algorithm with two crisp inputs, FiO_2 set to 0.3 and low-PEEP set to 5. Giving a crisp output, change-in-PEEP of 3.52×10^{-16}; that is, the extrinsic PEEP is $5 + 3.52 \times 10^{-16}$. The extrinsic PEEP is calculated using Equation 3.3.

Figure 4.5 displays the incremental low-PEEP algorithm with two crisp inputs, FiO_2 set to 0.3 and low-PEEP set to 5. Giving a crisp output (change-in-PEEP) of 1.7; that is, the extrinsic PEEP is 5 + 1.7, using Equation 3.4.

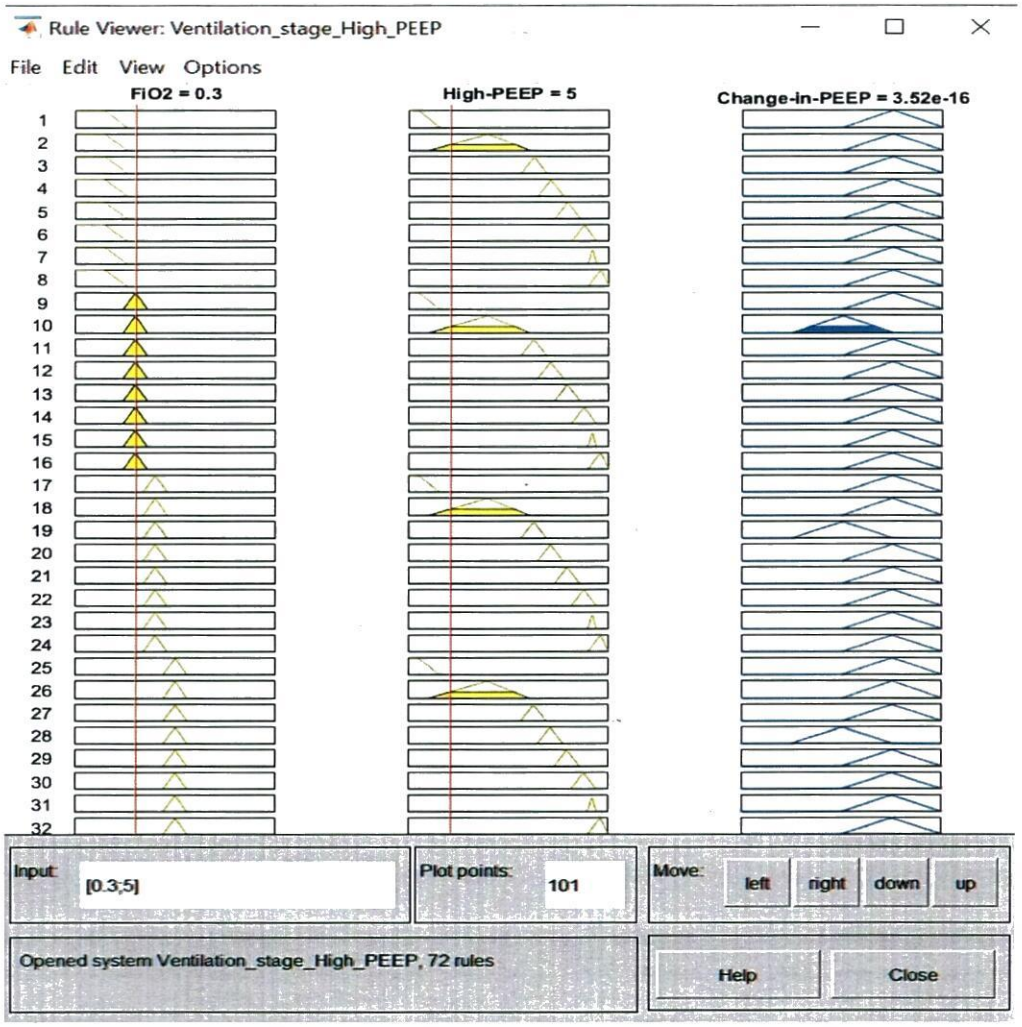


Figure 4.5: Rule viewer: incremental high-PEEP algorithm 1; two crisp inputs: FiO_2 = 0.3 and high-PEEP = 5 giving a crisp output: change-in-PEEP = 3.52×10^{-16}

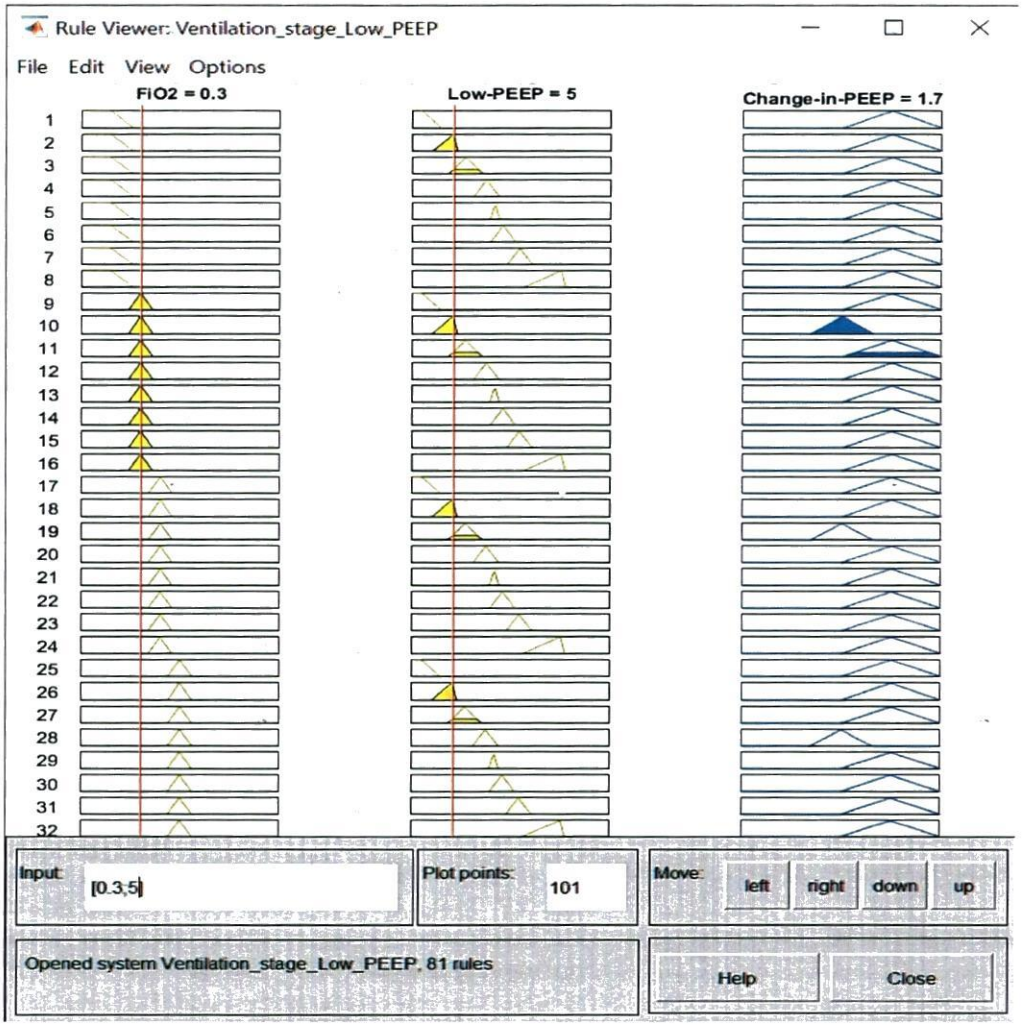


Figure 4.6: Rule viewer: incremental low-PEEP algorithm; two crisp inputs: $FiO_2 = 0.3$ and low-PEEP = 5 giving a crisp output: change-in-PEEP = 1.7

Tables 4.3 and 4.4 show the comparison between the physician based Berlin definition of ARDS using the ARDSNet protocol and the fuzzy based Berlin definition of ARDS. The protocol requires that there is a PEEP adjustment of 2 to 4 during the ventilation. This is why the adjustments in the Tables 4.3 and 4.4 do not exceed 4 in value adjustment. It is noticed that the physician based Berlin definition of ARDS have whole numbers compared to fuzzified system of Berlin definition of ARDS. The fuzzified values of the PEEP indicate the PEEP adjustments to be made during the ventilation. For patient PEEP values close to the respective Physician PEEP, with respect to the FiO_2 value, the adjustment is zero or close to zero. While values of PEEP from the patients, that are higher than the respective Physician PEEP, with respect to the FiO_2 value, the adjustment is an incremental one. This follows the fuzzy rules set for the incremental PEEP.

The triangular and trapezoidal membership functions were found fit for the fuzzy system since they are based on linear fit function capability; hence, they were approriate to define the ventilator setting values and represent the ARDSNet PEEP parameter ranges. In comparison with the non-linear membership functions such as: gaussian function, sigmoidal function, the linear fit functions need less computational power and time, making it convenient to adjust the ventilator parameters in shortest time possible, as well as having accurate crisp outputs during the emergency ventilation intervention.

Table 4.3: Comparison between physician based high-PEEP and fuzzified incremental high-PEEP [Brower et al., 2004, Sahetya et al., 2017b]

Input variables	**Output variables**	
FiO_2	**Physician PEEP**	**Fuzzy high-PEEP**
0.3	5	$5 + 3.52 \times 10^{-16}$
0.3	6	$6 + 3.85 \times 10^{-17}$
0.3	7	$7 + -4.84 \times 10^{-17}$
0.3	8	$8 + 1.05 \times 10^{-16}$
0.3	9	$9 + 1 \times 10^{-16}$
0.3	10	$10 + -4.26 \times 10^{-17}$
0.3	11	$11 + -4.64 \times 10^{-17}$
0.3	12	$12 + 3.85 \times 10^{-17}$
0.3	13	$13 + 2.66 \times 10^{-16}$
0.3	14	$14 + 3.12$
0.4	14	$14 + 0.884$
0.4	15	$15 + 9.99 \times 10^{-17}$
0.4	16	$16 + 2$
0.5	16	$16 + 2$
0.5	17	$17 + 9.99 \times 10^{-17}$
0.5	18	$18 + 2$
0.6	18	$18 + 2$
0.6	19	$19 + 9.99 \times 10^{-17}$
0.6	20	$20 + 2$
0.7	18	$18 + 2$
0.7	19	$19 + 9.99x10^{-17}$
0.7	20	$20 + 2$
0.8	20	$20 + 2$
0.8	21	$21 + 9.99 \times 10^{-17}$
0.8	22	$22 + 2.67$
0.9	22	$22 + 1.43$
1.0	22	$22 + 2.67$
1.0	23	$23 + 9.99 \times 10^{-17}$
1.0	24	$24 + 0$

Table 4.4: Comparison between physician based low-PEEP and fuzzified incremental low-PEEP [Brower et al., 2004, Sahetya et al., 2017b]

Input variables	Output variables	
FiO_2	Physician PEEP	Fuzzy low-PEEP
0.3	5	$5 + 1.7$
0.4	5	$5 + 3.31$
0.4	6	$6 + 7.69 \times 10^{-17}$
0.4	7	$7 + 7.69 \times 10^{-17}$
0.4	8	$8 + 2.89$
0.5	8	$8 + 2.39$
0.5	9	$9 + 7.21 \times 10^{-17}$
0.5	10	$10 + 3.14$
0.6	10	$10 + 1.96$
0.7	10	$10 + 3.14$
0.7	11	$11 + 7.21 \times 10^{-17}$
0.7	12	$12 + 2.64$
0.8	12	$12 + 2.64$
0.8	13	$13 + 7.21 \times 10^{-17}$
0.8	14	$14 + 1.55$
0.9	18	$18 + 2.39$
1.0	18	$18 + 2.75$
1.0	19	$19 + 7.76 \times 10^{-17}$
1.0	20	$20 + 7.34 \times 10^{-17}$
1.0	21	$21 + 7.21 \times 10^{-17}$
1.0	22	$22 + 8.11 \times 10^{-17}$
1.0	23	$23 + -2.6 \times 10^{-17}$
1.0	24	$24 + 0$

B) **Results in MATLAB (Surface View)**

Figure 4.7 displays the surface view of the incremental high-PEEP algorithm, showing that the changes in PEEP are mainly incremental based on the rules of the algorithm. It is maintained only when it has reached the PEEP value that matches with the

respective $\hat{F}iO_2$ indicated in the Berlin PEEP table. The PEEP changes are seen more towards the upper PEEP scale of 0-24.

Figure 4.8 displays the surface view of the decremental low-PEEP algorithm. The

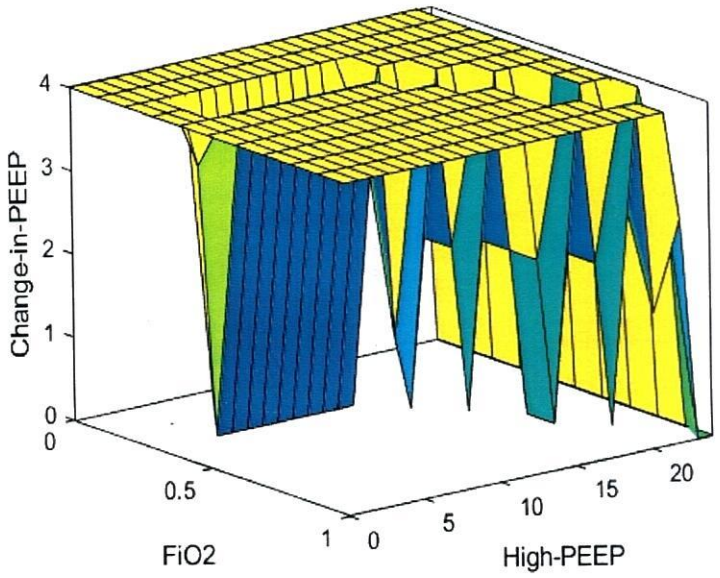


Figure 4.7: 3D surface view for incremental high-PEEP algorithm, with two inputs: FiO_2 and high-PEEP; and one output: change-in-PEEP

PEEP changes tend towards the lower PEEP scale of 0-24 for Figure 4.8, due to lower PEEP values shown in Table 2.2.

Comparison between Decremental and Incremental High-PEEP

Figure 4.9 displays FiO_2 (graph in blue colour) on the x-axis/ horizontal scale which adjusts by 0.1. ARDSNet high-PEEP (graph in brown colour) that is indicated in the ARDSNet PEEP table in Table 2.2. The fuzzified high-PEEP designed in this study is shown as the yellow colored graph. The graph shows the comparison between the decremental high-PEEP and incremental high-PEEP. The graph indicates

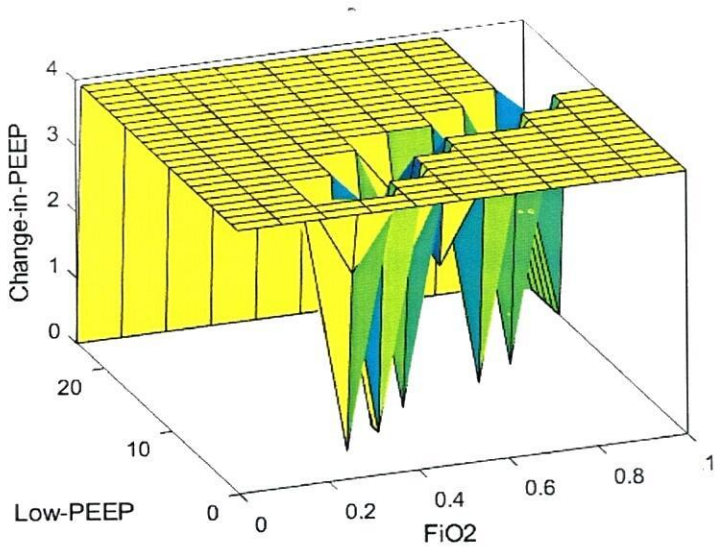


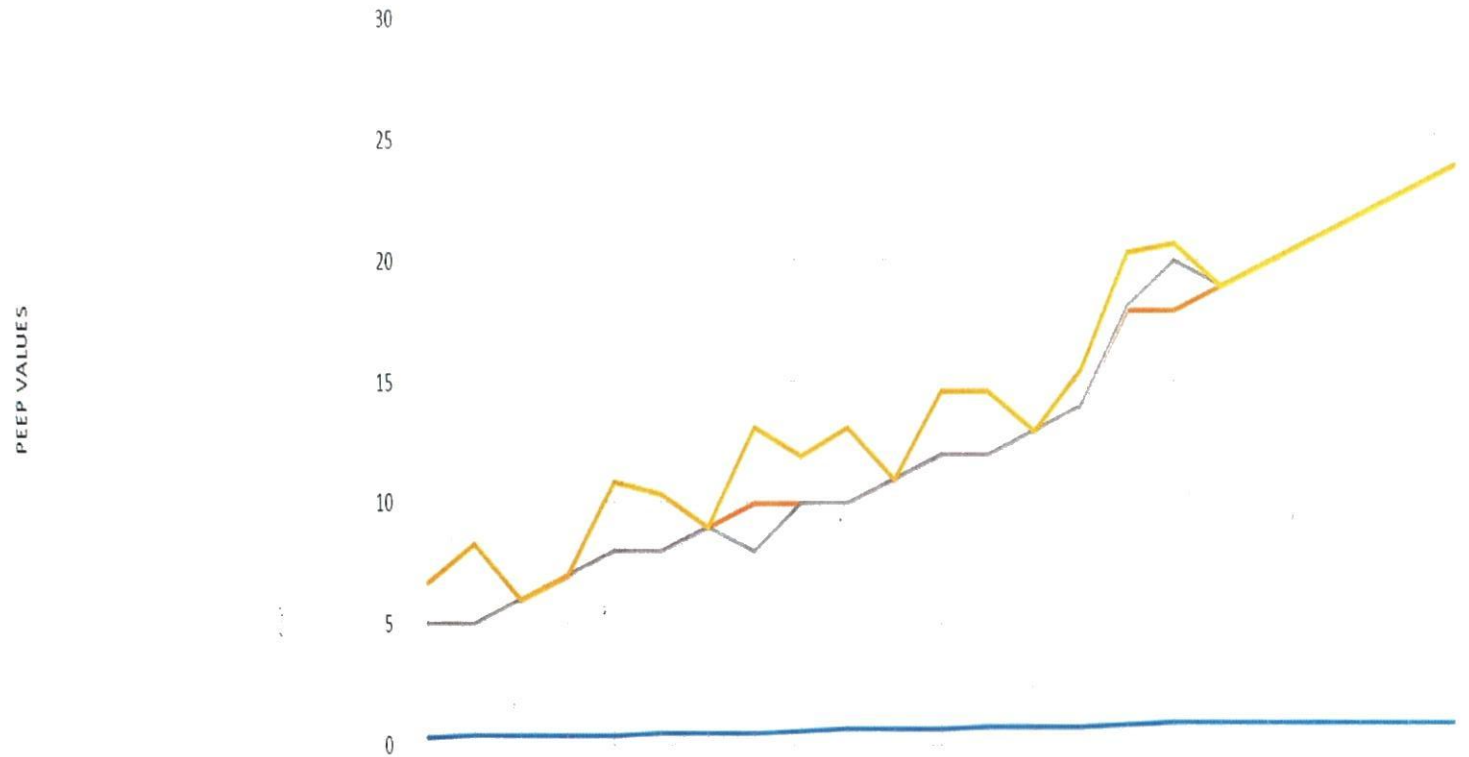
Figure 4.8: 3D surface view for incremental low-PEEP algorithm, with two inputs: FiO_2 and low-PEEP; and one output: change-in-PEEP

that the incremental high-PEEP algorithm creates an upper boundary to PEEP adjustments since the algorithm was designed with incremental PEEP protocol. The decremental high-PEEP algorithm creates a lower boundary to PEEP adjustments since the algorithm was designed with decremental PEEP protocol.

Comparison between Decremental and Incremental Low-PEEP

Figure 4.10 displays FiO_2 (graph in blue colour) on the x-axis/ horizontal scale which adjusts by 0.1. ARDSNet low-PEEP (graph in brown colour) that is indicated in the ARDSNet PEEP table in Table 2.2. The fuzzified low-PEEP designed in this study is colored yellow in the graph. The graph shows the comparison between the decremental low-PEEP and incremental low-PEEP. The graph indicates that the incremental low-PEEP algorithm creates an upper boundary to PEEP adjustments since the algorithm was designed with incremental PEEP protocol. The decremental low-PEEP algorithm creates a lower boundary to PEEP adjustments.

Figure 4.9: A graph showing the relationship between the FiO_2, ARDSNet high PEEP, fuzzified high PEEP with fewer linguisitc terms, and fuzzified high PEEP with more linguisitc terms



	1	2	3	4	5	6	7	8	9	10	11	12	13	14	15	16	17	18	19	20	21	22	23
FiO2	0.3	0.4	0.4	0.4	0.4	0.5	0.5	0.5	0.6	0.7	0.7	0.7	0.8	0.8	0.8	0.9	1	1	1	1	1	1	1
ARDSNet low PEEP	5	5	6	7	8	8	9	10	10	10	11	12	12	13	14	18	18	19	20	21	22	23	24
Fuzzified low PEEP with fewer linguistic terms	5	5	6	7	8	8	9	8	10	10	11	12	12	13	14	18.134	20	19	20	21	22	23	24
Fuzzified low PEEP with more linguistic terms	6.7	8.31	6	7	10.89	10.39	9	13.14	11.96	13.14	11	14.64	14.64	13	15.55	20.39	20.75	19	20	21	22	23	24

Figure 4.10: A graph showing the relationship between the FiO_2, ARDSNet low PEEP, fuzzified low PEEP with fewer linguisitc terms, and fuzzified low PEEP with more linguisitc terms

4.2 Design and Simulation of a Physician Based Fuzzy Neural System for Ventilator Adjustments in ARDS Patients to Ensure Lung Protection

The training of data attained from the ARDSNET PEEP protocol algorithms, for both the high-PEEP and low-PEEP, was done using the neuro fuzzy designer application in MATLAB software, and later simulated using Simulink. The minimal training error attained was 1.4499×10^{-5} with 20 epochs.

A) **High-PEEP**

i) High-PEEP rule viewer

The rule viewer for the high-PEEP algorithm in Figure 4.11 shows that after inserting the parameters of inspired fraction of oxygen (FiO_2) and non-fuzzified PEEP as 0.3 and 5 respectively, the output (fuzzified PEEP) is 5 as per the ARDSNet protocol [Force et al., 2012a]. The remaining obtained fuzzified outputs are shown in Table 4.5. There are two inputs: FiO_2 and non-fuzzified high-PEEP; and one output: fuzzified high-PEEP. The fuzzified high-PEEP is the same as the non-fuzzified high-PEEP after training; implying that the algorithm mimics the non-fuzzified high-PEEP values.

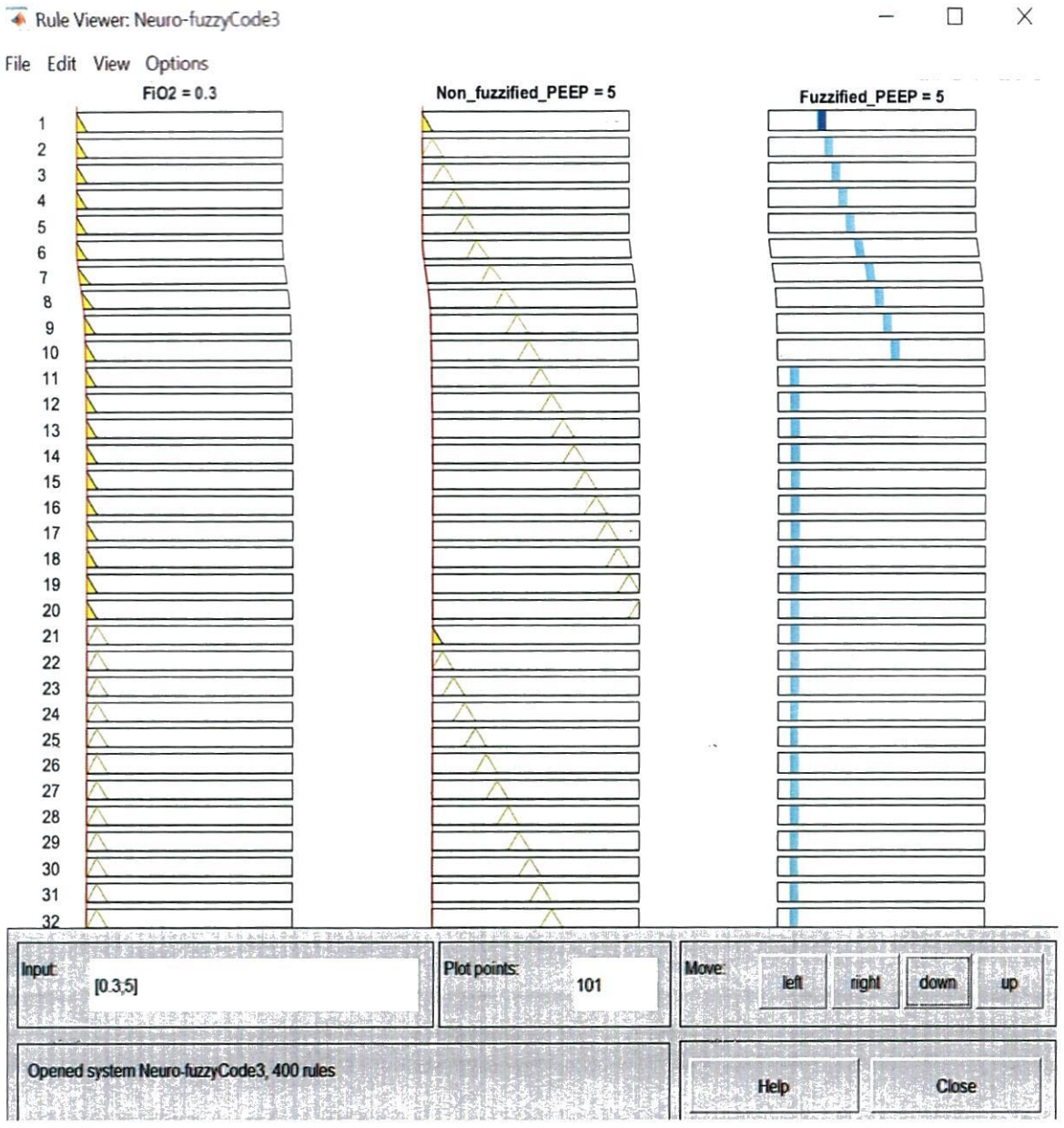


Figure 4.11: High-PEEP rule viewer for $FiO_2 = 0.3$ and non-fuzzified PEEP = 5, giving an output of fuzzified PEEP = 5

Table 4.5: Comparison between non-fuzzified high-PEEP and fuzzified high-PEEP [Brower et al., 2004, Sahetya et al., 2017b]

Input variables		**Output variables**
FiO_2	**Non-fuzzified PEEP**	**Fuzzified PEEP**
0.3	5	5
0.3	6	6
0.3	7	7
0.3	8	8
0.3	9	9
0.3	10	10
0.3	11	11
0.3	12	12
0.3	13	13
0.3	14	14
0.4	14	14
0.4	15	15
0.4	16	16
0.5	16	16
0.5	17	17
0.5	18	18
0.6	18	18
0.6	19	19
0.6	20	20
0.7	18	18
0.7	19	19
0.7	20	20
0.8	20	20
0.8	21	21
0.8	22	22
0.9	22	22
1.0	22	22
1.0	23	23
1.0	24	24

ii) **High PEEP graph**

Figure 4.12 shows a graph displaying the two input parameters: FiO_2 (yellow in colour) and general range of PEEP (blue in colour), and one output: fuzzified high-PEEP (orange in colour). The general range of PEEP shows the recommended range of PEEP during ventilation, which increases step-wise from 5 to 24, then repeats for the different values of FiO_2 (that is: 0.3 to 1). The fuzzified high-PEEP changes with respect to the ARDSNet protocol.

The graph shows that below 0.3 of FiO_2, fuzzified high-PEEP is zero, since the ARDSNet protocol does not define the PEEP in that range; however, the PEEP changes for $0.3 \leq FiO_2 \leq 1$.

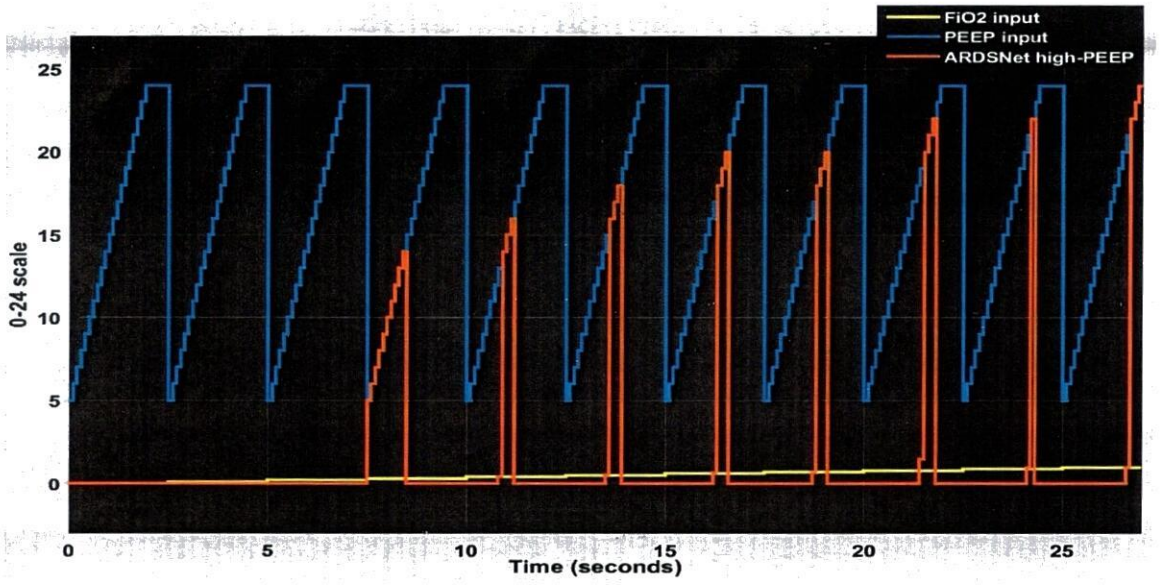


Figure 4.12: Graph showing the relationship between the two input parameters: FiO_2 (yellow in colour) and general range of PEEP (blue in colour), with one output: fuzzified high-PEEP (orange in colour)

iii) **High-PEEP surface view**

Figure 4.13 shows the surface view of the two inputs: FiO_2 and non-fuzzified high-PEEP, and one output: fuzzified high-PEEP, trained using the neuro fuzzy designer. As the values of FiO_2 increase, so does the non-fuzzified high-PEEP and fuzified high-PEEP. The surface view shows that the neuro algorithm mimics the non-fuzzified high-PEEP values from the ARDSNet high PEEP protocol.

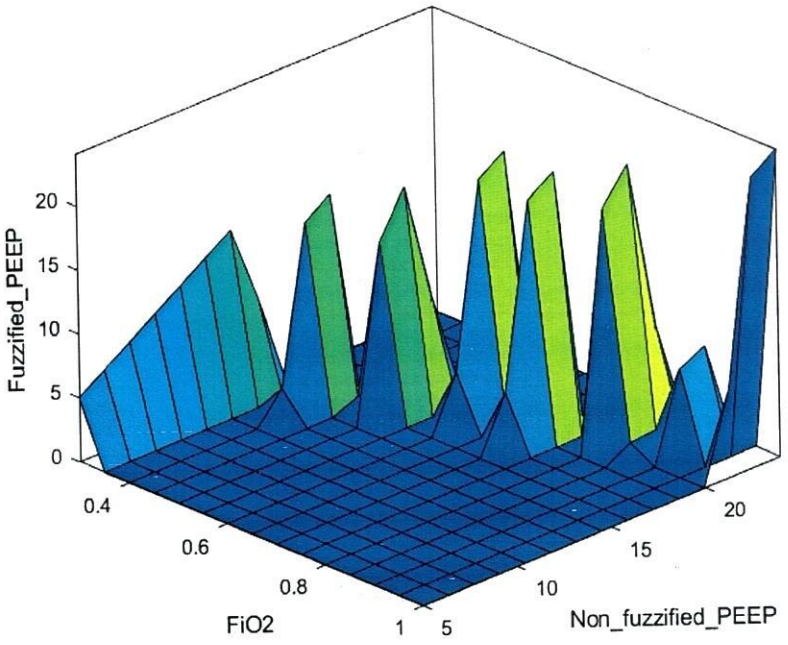


Figure 4.13: Surface view for the two inputs: FiO_2 and non-fuzzified high-PEEP, and one output: fuzzified high-PEEP

B) **Low-PEEP**

i) **Low-PEEP rule viewer**

The rule viewer for the low-PEEP algorithm in Figure 4.14 shows that the output (Fuzzified PEEP = 5) of low-PEEP rule viewer is the same as the high-PEEP rule

viewer after inserting the parameters of FiO_2 and non-fuzzified PEEP as 0.3 and 5 respectively, which is as well defined in the low ARDSNet low-PEEP protocol table. The remaining obtained outputs of PEEP as FiO_2 varies are shown in Table 4.6.

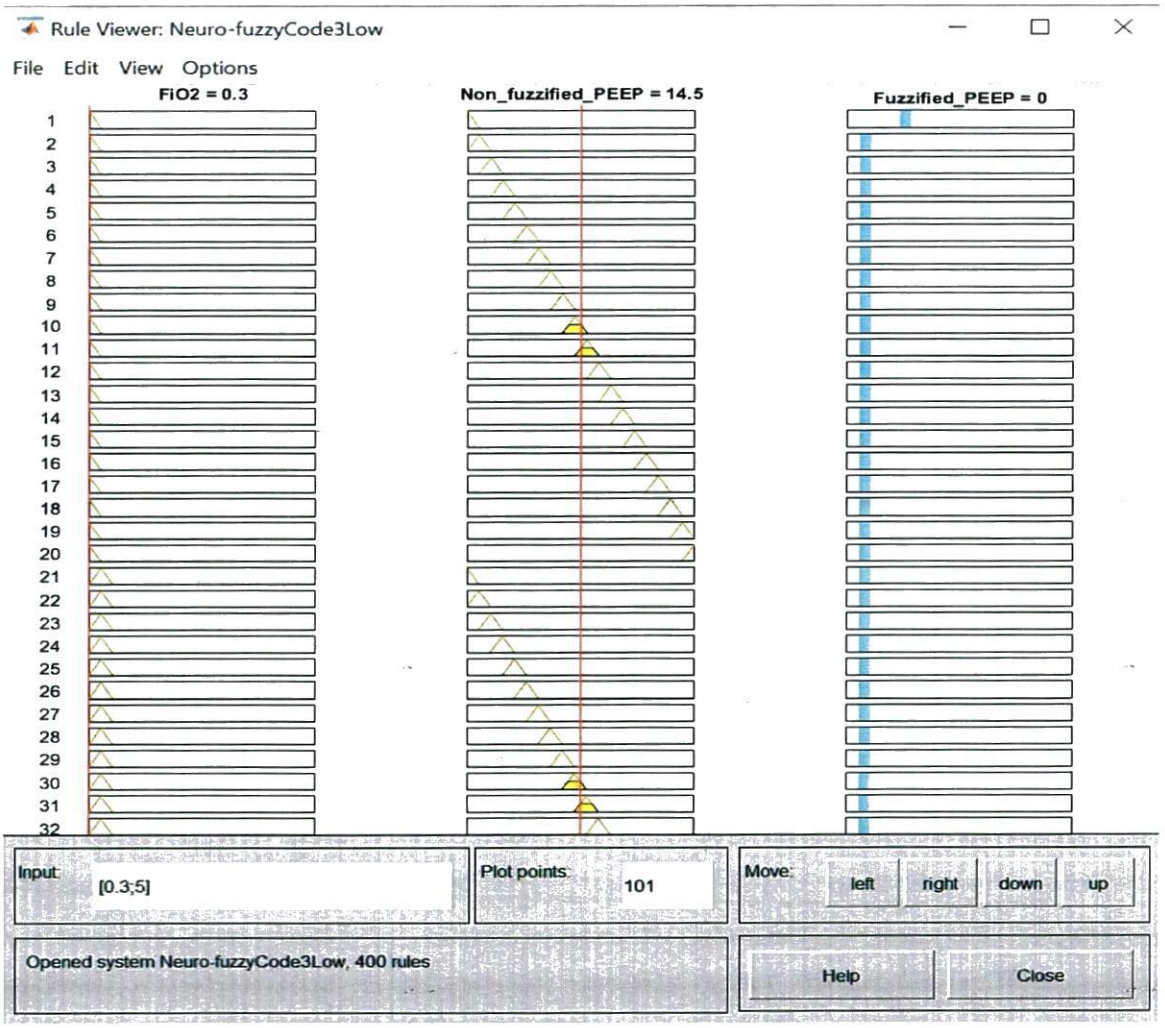


Figure 4.14: Low-PEEP rule viewer for $FiO_2 = 0.3$ and non-fuzzified PEEP = 5, giving an output of fuzzified PEEP = 5

Table 4.6: Comparison between non-fuzzified low-PEEP and fuzzified low-PEEP [Brower et al., 2004, Sahetya et al., 2017b]

Input variables		Output variables
FiO_2	**Non-fuzzified PEEP**	**Fuzzified PEEP**
0.3	5	5
0.4	5	5
0.4	6	6
0.4	7	7
0.4	8	8
0.5	8	8
0.5	9	9
0.5	10	10
0.6	10	10
0.7	10	10
0.7	11	11
0.7	12	12
0.8	12	12
0.8	13	13
0.8	14	14
0.9	18	18
1.0	18	18
1.0	19	19
1.0	20	20
1.0	21	21
1.0	22	22
1.0	23	23
1.0	24	24

ii) **Low-PEEP graph**

Figure 4.15 shows a graph displaying the two input parameters: FiO_2 (yellow in colour) and general range of PEEP (blue in colour), and the one output:

fuzzified low-PEEP (orange in colour). The general range of PEEP shows the recommended range of PEEP during ventilation, which increases step-wise from 5 to 24, then repeats for the different values of FiO_2 (that is: 0.3 to 1) as explained for the high-PEEP graph. The graph shows that below 0.3 of FiO_2, fuzzified low-PEEP is also zero, as it is for the case of high-PEEP, since the ARDSNet low-PEEP protocol does not define the PEEP in that range; however, the low-PEEP changes for $0.3 \leq FiO_2 \leq 1$.

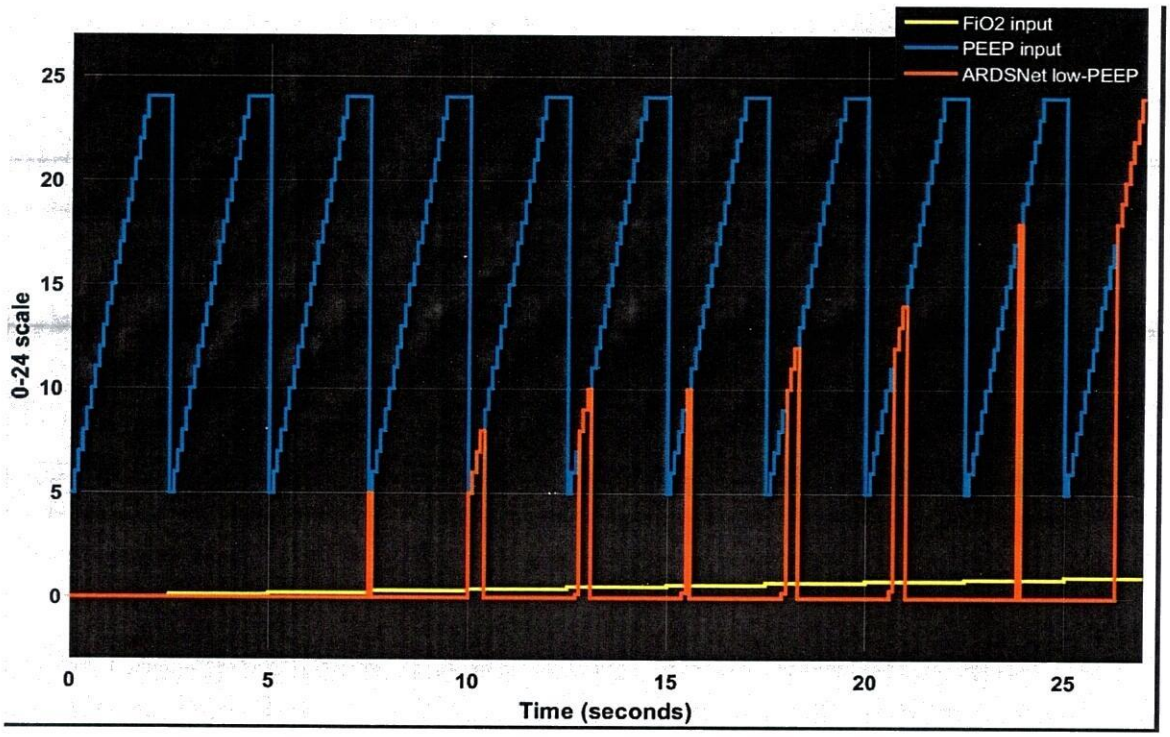


Figure 4.15: Graph showing the relationship between the two input parameters: FiO_2 (yellow in colour) and general range of PEEP (blue in colour), with one output: fuzzified low-PEEP (orange in colour)

iii) Low-PEEP surface view

Figure 4.16 shows the surface view of the two inputs: FiO_2 and non-fuzzified

low-PEEP, and one output: fuzzified low-PEEP. It shows that as the values of the FiO_2 increase so does the non-fuzzified low-PEEP, which in-turn corresponds to the fuzzified low-PEEP.

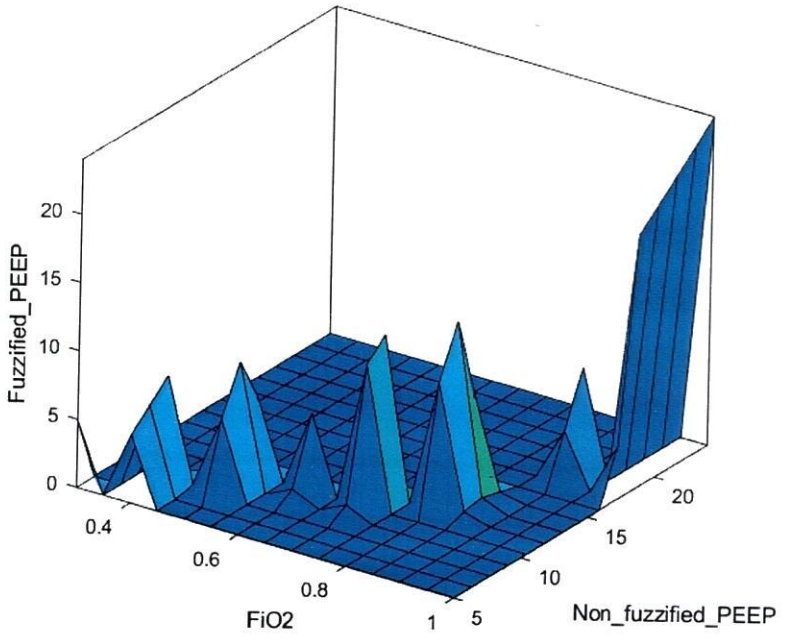


Figure 4.16: Surface view for the two inputs: FiO_2 and non-fuzzified low-PEEP, and one output: fuzzified low-PEEP

4.3 Build a Feed-in Imaging Model to Detect Lung and Brain Scans using Convolutional Neural Netwo

A) **Lung**

i) **Lung confusion matrix**

The confusion matrix attained from the lung-trained model is shown in Table 4.7, for three classes: corona virus diseases 2019 (COVID19), healthy lungs (Normal), and pneumonia, with accuracies of: 97.45%, 97.52%, and 91.5% respectively.

Table 4.7: Lung CNN confusion matrix

	COVID19	**Normal**	**Pneumonia**
COVID19	0.9745	0.0078	0.0177
Normal	0.0154	0.9752	0.0094
Pneumonia	0.0184	0.0666	0.9150

To calculate for overall lung-trained model accuracy, let True Positive be TP, True Negative be TN, False Positive be FP, and False Negative be FN [Powers, 2011]. Therefore, for respective lung classes;

$TP_{(COVID19)} = 0.9745$

$TP_{(Normal)} = 0.9752$

$TP_{(Pneumonia)} = 0.9150$

$$TN_{(COVID19)} = (0.9752 + 0.0094 + 0.0666 + 0.9150) = 1.9662$$

$$TN_{(Normal)} = (0.9745 + 0.0177 + 0.0184 + 0.9150) = 1.9256$$

$$TN_{(Pneumonia)} = (0.9745 + 0.0078 + 0.0154 + 0.9752) = 1.9729$$

$$FP_{(COVID19)} = (0.0078 + 0.0177) = 0.0255$$

$$FP_{(Normal)} = (0.0154 + 0.0094) = 0.0248$$

$$FP_{(Pneumonia)} = (0.0184 + 0.0666) = 0.0850$$

$$FN_{(COVID19)} = (0.0154 + 0.0184) = 0.0338$$

$$FN_{(Normal)} = (0.0078 + 0.0666) = 0.0744$$

$$FN_{(Pneumonia)} = (0.0177 + 0.0094) = 0.0271$$

From the formulars of precision, recall/ sensitivity, and F1-score in Equation 3.5, Equation 3.6, and Equation 3.7 respectively, the values are shown in Table 4.8.

Table 4.8: Lung CNN performance measurement values

	Precision	**Recall**	**F1-score**
COVID19	0.97	0.97	0.97
Normal	0.98	0.93	0.95
Pneumonia	0.92	0.97	0.94

Therefore,

$$Accuracy_{(Lung-model)} = \frac{TP + TN}{TP + TN + FP + FN} * 100\% \tag{4.1}$$

$$Accuracy_{(Lung-model)} = \frac{8.7294}{9} * 100\% \tag{4.1a}$$

$$= 97\% \tag{4.1b}$$

ii) **Lung accuracy and error graph**

The key for Figure 4.18 and Figure 4.19 is shown in Figure 4.17.

The lung data was trained on 7 epochs with 280 iterations per epoch, and the validation was done at a frequency of 100 iterations. The final validation accuracy attained was 97% and training error loss of 0.0014.

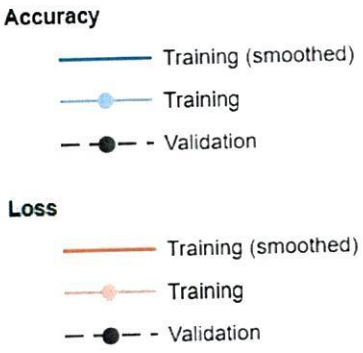


Figure 4.17: Accuracy and error graph key

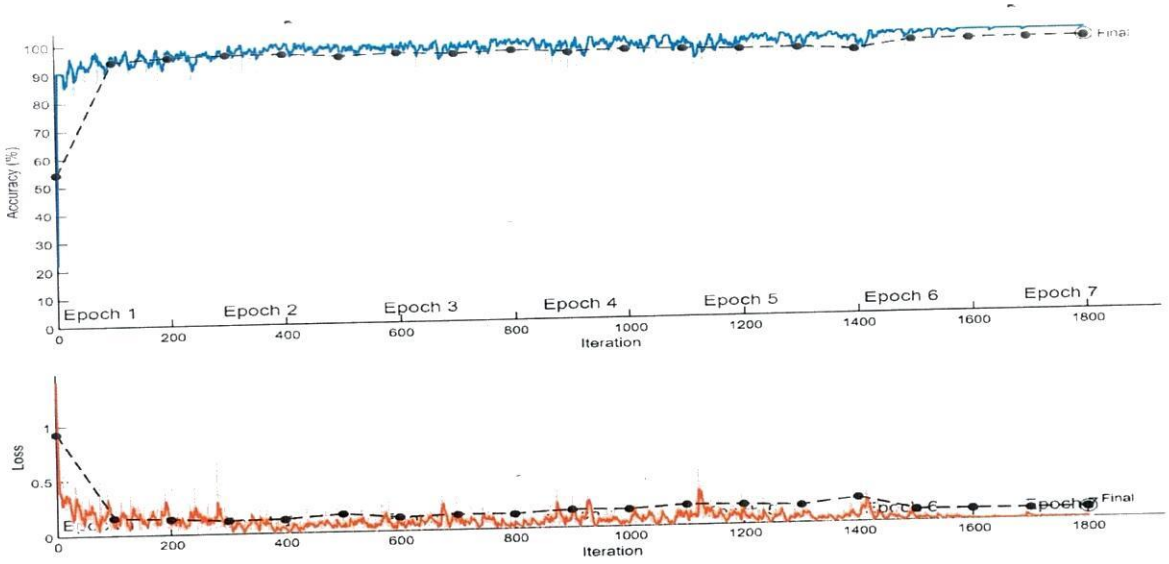


Figure 4.18: Accuracy and loss curves for three lung conditions

B) **Brain**

i) **Brain confusion matrix**

The confusion matrix attained from the brain-trained model is shown in Table 4.9 for three classes: Acute ischemic stroke, healthy brain (control), and Intracranial hemorrhage with accuracy of: 97.18%, 93.18%, and 99.4% respectively.

Table 4.9: Brain CNN confusion matrix

	Acute ischemic	**Control**	**Intracranial hemorrhage**
Acute ischemic	0.9718	0.0282	0
Control	0.0682	0.9318	0
Intracranial hemorrhage	0.0060	0	0.9940

To calculate for brain-trained model accuracy, let True Positive be TP, True

Negative be TN, False Positive be FP, and False Negative be FN [Powers, 2011].

$$TP_{(Acute-ischemic)} = 0.9718$$

$$TP_{(Control)} = 0.9318$$

$$TP_{(Intracranial-hemorrhage)} = 0.9940$$

$$TN_{(Acute-ischemic)} = (0.9318 + 0 + 0 + 0.9940) = 1.9258$$

$$TN_{(Control)} = (0.9718 + 0 + 0.0060 + 0.9940) = 1.9718$$

$$TN_{(Intracranial-hemorrhage)} = (0.9718 + 0.0282 + 0.0682 + 0.9318) = 2$$

$$FP_{(Acute-ischemic)} = (0.0282 + 0) = 0.0282$$

$$FP_{(Control)} = (0.0682 + 0) = 0.0682$$

$$FP_{(Intracranial-hemorrhage)} = (0.0060 + 0) = 0.0060$$

$$FN_{(Acute-ischemic)} = (0.0682 + 0.0060) = 0.0742$$

$$FN_{(Control)} = (0.0282 + 0) = 0.0282$$

$$FN_{(Intracranial-hemorrhage)} = (0 + 0) = 0$$

From the formulars of precision, recall/ sensitivity, and F1-score, the values are shown in Table 4.10.

Table 4.10: Brain CNN performance measurement values

	Precision	Recall	F1-score
Acute-ischemic	0.97	0.93	0.95
Control	0.93	0.97	0.95
Intracranial hemorrhage	0.99	1	1

Therefore,

$$Accuracy_{(Brain-model)} = \frac{8.7952}{9} * 100\% \tag{4.1a}$$

$$= 98\% \tag{4.1b}$$

ii) **Brain accuracy and error graphs**

The brain data was trained on 6 epochs with 62 iterations per epoch, and the validation was done at a frequency of 10 iterations. The final validation accuracy attained was 98% and training error loss of 0.0005 as shown in Figure 4.19.

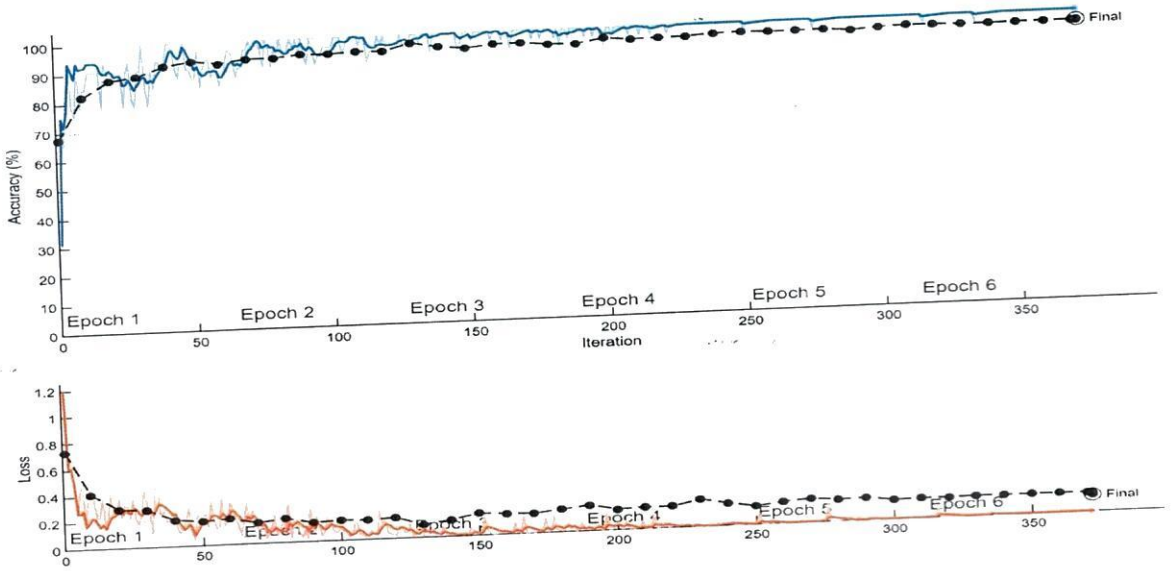


Figure 4.19: Accuracy and loss curves for three brain conditions

4.4 Design and Simulation of an Intelligent System to Test and Validate Patient Ventilator Synchrony and Lung Protection using Real-time Medical Imagi and Fuzzy Expert System

Using Equation 3.10, recommended values for healthy lungs are: 0.5 - 2.5 cm $H_2O/l/s$ for airway resistance, 0.2 l/cm H_2O for lung compliance [Scanlan et al., 1990]. For simulation of healthy lung, healthy airway resistance of 0.5 cm $H_2O/l/s$ and healthy lung compliance of 0.2 l/cm H_2O were used, forming Equation 4.2. The results are displayed in Figure 4.20, with positive end expiratory pressure (PEEP) of 5 cm H_2O. The recommended lung residual volume (RV) of 0.8 l and recommended total lung capacity (TLC) of 5 l were attained [Williams et al., 2010, Lofrese et al., 2023]. Figure 4.21 displays the results with PEEP of 15 cm H_2O, showing the RV of 2.5 l and TLC of 5 l. PEEP of 15 cm H_2O indicates the need to lower PEEP values for healthy lungs. This is due to the fact that the RV increases with increase in PEEP, which affects the lungs given that there is more air left in the lungs.

$$H_{(s)} = \frac{0.2s}{0.1s + 1} \tag{4.2}$$

The flow figures for both Figure 4.20 and Figure 4.21 show that air is completely released from the lungs, and the lungs are at rest before the next inspiration.

For simulation of sick lung, sick airway resistance of 6 cm $H_2O/l/s$ and sick lung compliance of 0.1 l/cm H_2O were used, forming Equation 4.3. The results are displayed in Figure 4.22 with PEEP of 5 cm H_2O, showing the lung RV of 0.5 l and TLC of 2.5

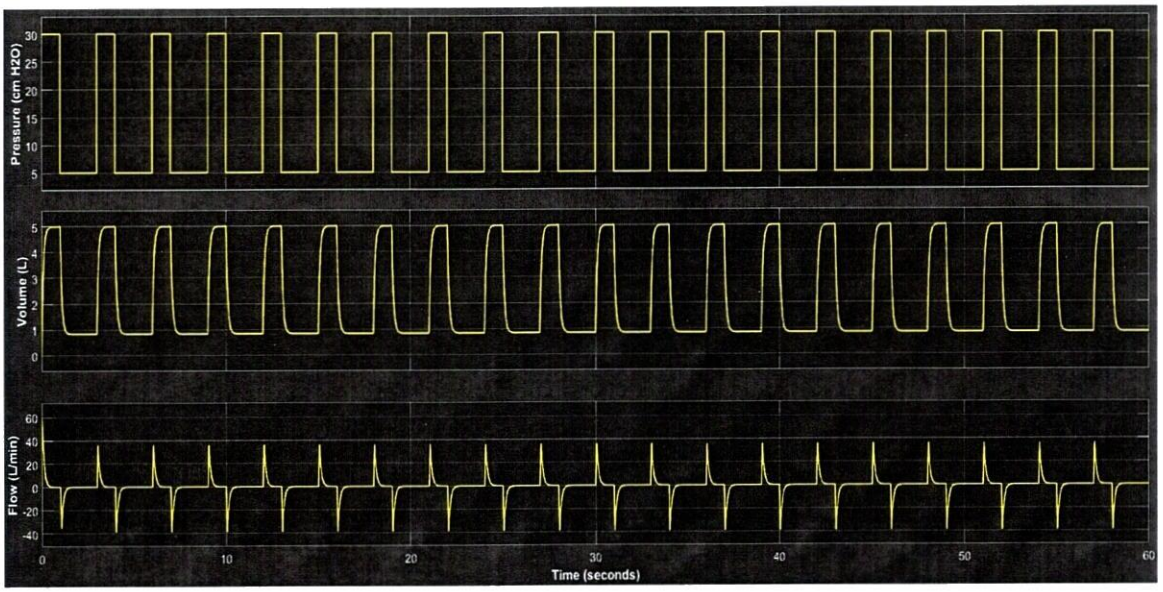


Figure 4.20: Ventilator waveforms for healthy lungs with PEEP of 5 cm H_2O

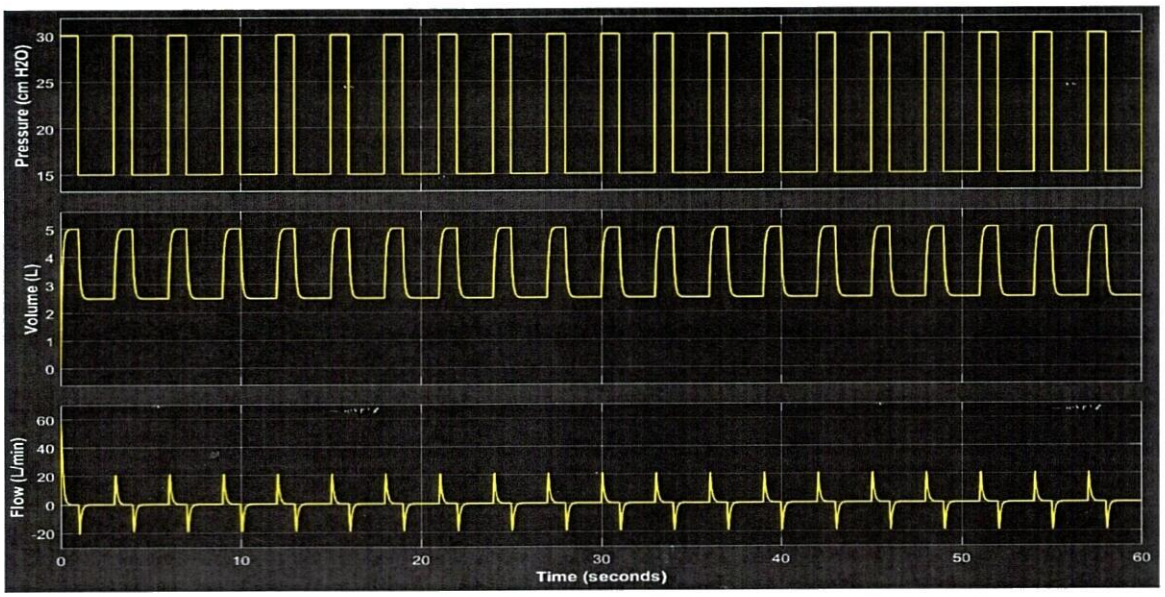


Figure 4.21: Ventilator waveforms for healthy lungs with PEEP of 15 cm H_2O

l. Figure 4.23 with PEEP of 15 cm H_2O, showing the RV of 1.4 l and TLC of 2.5 l; indicating the need to increase PEEP for sick lungs since the RV decreases with lower PEEP.

$$H_{(s)} = \frac{0.1s}{0.6s + 1} \tag{4.3}$$

Flow graph shows that for Figure 4.22, there is more air left in the lungs before the next inspiration, and when PEEP is increased in Figure 4.23, little air is left in the lungs after expiration.

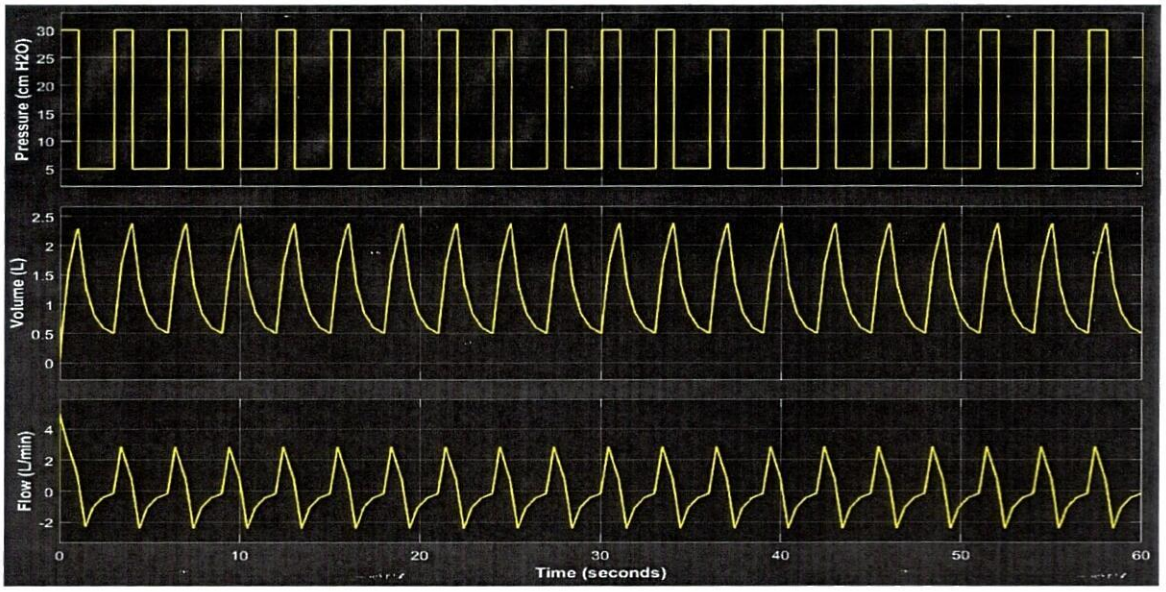


Figure 4.22: Ventilator waveforms for sick lungs with PEEP of 5 cm H_2O

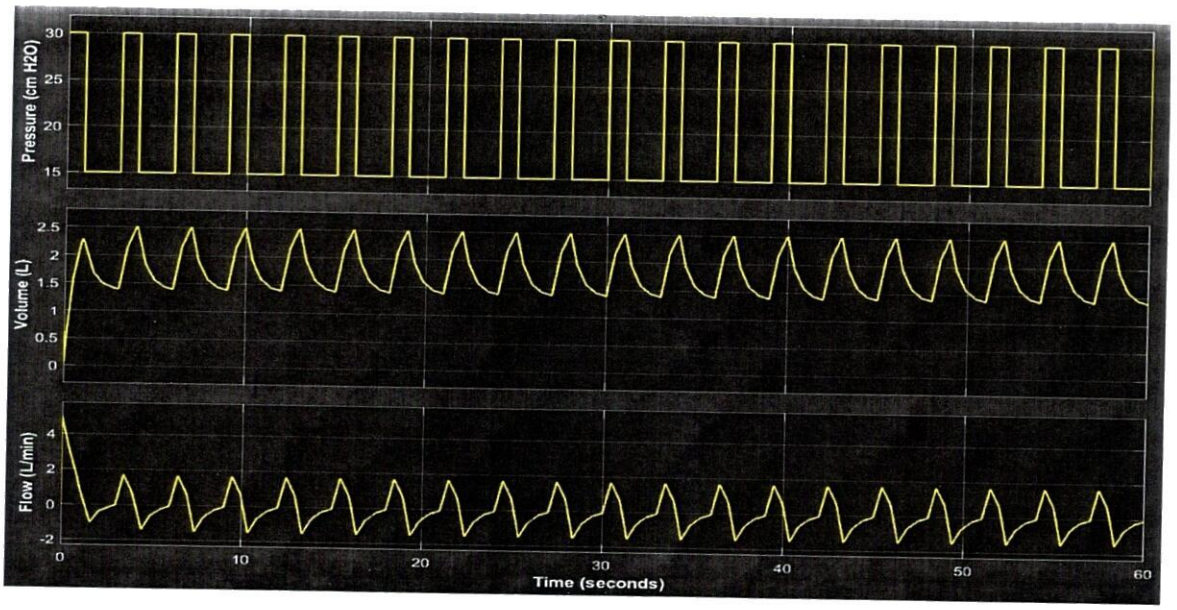


Figure 4.23: Ventilator waveforms for sick lungs with PEEP of 15 cm H_2O

For simulation of recovering lung, recovering airway resistance of 4 cm $H_2O/l/s$ and recovering lung compliance of 0.15 l/cm H_2O were used, forming Equation 4.4. The results are displayed in Figure 4.24 with PEEP of 5 cm H_2O, showing the lung RV of 0.7 l and TLC of 3.8 l. Figure 4.25 with PEEP of 15 cm H_2O, shows the RV of 2.0 l and TLC of 3.9 l; indicating the need to decrease PEEP for recovering lungs since the RV increases with increasing PEEP. Therefore, as the lungs recover, there is need to lower the PEEP to avoid rupture/ over expansion of lungs.

$$H_{(s)} = \frac{0.15s}{0.4s + 1} \tag{4.4}$$

Flow graph in Figure 4.24 shows that all inhaled air is exhaled and lungs rest before the next inspiration. However, with higher PEEP as shown in Figure 4.25, RV increases beyond recommended range, and flow reduces.

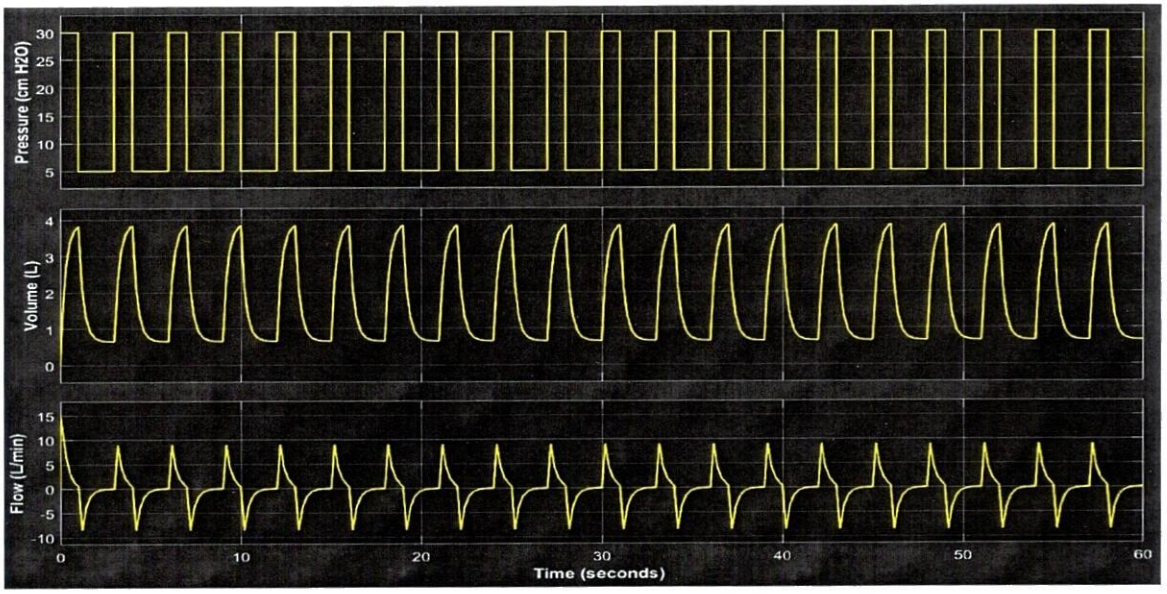


Figure 4.24: Ventilator waveforms for recovering lungs with PEEP of 5 cm H_2O

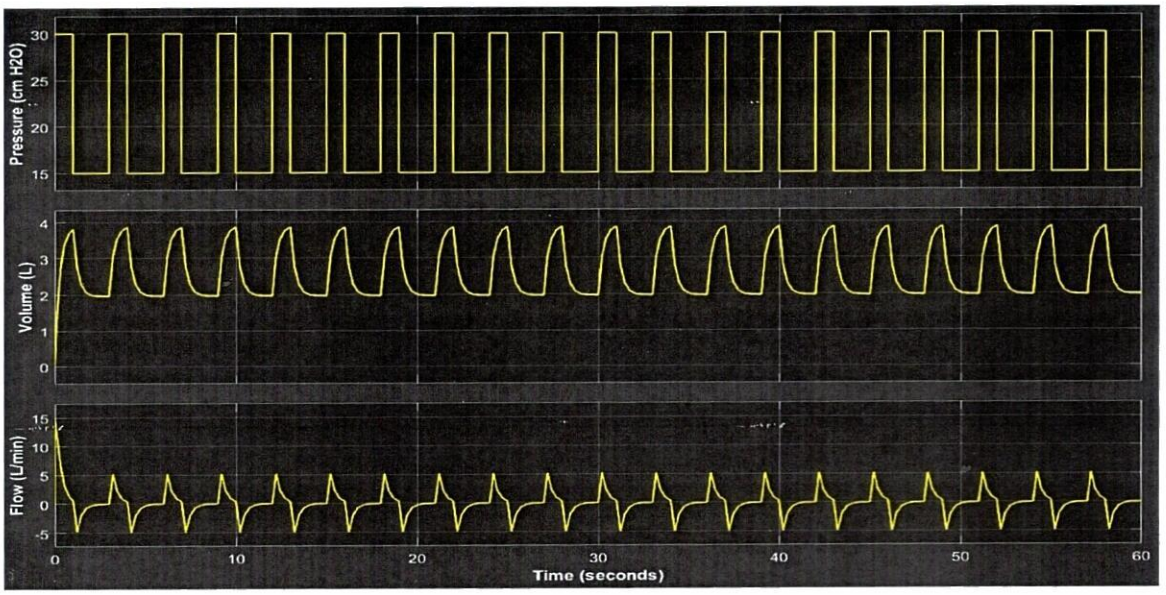


Figure 4.25: Ventilator waveforms for recovering lungs with PEEP of 15 cm H_2O

The air left in the lung before the next inspiration, indicates that the patient's lungs do not have enough power to excel out the inhaled gas. When the PEEP is increased for the sick and recovering lungs, the gas that remains in the lungs is minimal or none, indicating that the lungs are recovering or have fully recovered to excel the inhaled gas. The RV and TLC is low for sick and recovering lungs if low PEEP is used, and increase for higher PEEP. Therefore, for the healthy lungs, lower PEEP of 5 cm H_2O is recommended; for sick and recovering lungs, higher PEEP is recommended to improve on the RV and TLC of the patient's lungs.

For general testing with different brain conditions, fraction of inspired oxygen (FiO_2) = 0.4 and PEEP = 16 were used, and if the lung had pneumonia condition, the incremental high-PEEP algorithm is selected by the image-fuzzified based system, and PEEP of 18 is suggested. If the lung has corona virus disease 2019 (COVID-19), then decremental high-PEEP algorithm is selected and suggestion of PEEP = 15 is given. If FiO_2 = 0.5, PEEP = 10, and if the lung was normal with a brain scan of intracranial hemorrhage or acute ischemic stroke condition, the incremental low-PEEP algorithm is selected and 13.14 suggestion of the PEEP is given. If the brain is healthy, then decremental low-PEEP is selected and suggestion of PEEP = 8 is given, with an alarm such that the patient can be on ventilation as the brain is being operated on. The system is therefore, able to protect lungs by using lower PEEP adjustment protocols for recovering lungs, and higher PEEP for sick lungs. Patient ventilator synchrony is attained since the PEEP is adjusted based on the amount of oxygen in the blood, measured by the FiO_2, and the system is then able to support the patient depending on the demand.

Chapter 5

Conclusions and recommendations

5.1 Conclusion

Physicians in most hospitals are few and the number of patients with respiratory failures/ difficulties are on the rise. This comes with human errors caused by some physicians especially when they are overwhelmed with a lot of work, which may lead to inaccurancy or delay in the adjustments made on the mechanical ventilators. The need for use of the fuzzy logic method to guide the physicians is not new, but the application of the fuzzy logic and in combination with the neural fuzzy method, in adjustment of the inspired fraction of oxygen (Fi_2O) and positive end expiratory pressure (PEEP) ventilator parameters is new, with a purpose of reducing the physician's time spent in thinking on what parameters to control/ adjust on the ventilator, especially during an emergency. The fuzzy algorithms also decrease the possibility of having ventilator inevitable human errors; hence, ensuring lung protection, and reduction in time spent by physicians in making decisions on the ventilator adjustments that base on the patient's responses. Therefore, the fuzzy logic can be used to guide the physicians on what parameters to adjust during the ventilation, at minimal possible time, and increase the possibility of patient survival due to reduction of human errors.

Fuzzy logic systems adjust the PEEP values, fuzzy neural network was further used to compare the output of the PEEP algorithms with the acute respiratory distress syndrome network (ARDSNet) PEEP values. The fuzzy neural network increases the accuracy and reduces the time spent comparing the fuzzy logic algorithm output and the ARDSNet PEEP values, by using the trained neural network to mimic the Berlin ARDSNet PEEP values.

The convolutional neural network (CNN) was further used to classify the different brain and lung conditions, so as to add a variable/ alarm to already exisiting ventilator variables. The model produced high performance accuracy, able to differentiate the complex medical scans. The CNN algorithm is able to improve the efficiency of the ventilators by determining the cause of the failure or difficulty in breathing, in case the lungs are fully functioning, which can be due to a problem originating from the brain during the ventilation. The early intervention is good for patients with diseases that need urgent treatment such as: the fluid build-up in the brain, the rupture of the blood vessel in the brain, and damage of brain cells.

A single lung compartment transfer function was derived and used to test the simulation of the fuzzy-image based system, with trained fuzzified PEEP and CNN algorithms connected to the derived lung transfer function. The pressure, volume, and flow graphs show that there is improvement of the lung residual volume (RV) and total lung capacity (TLC) with adjustment of PEEP for sick patients, to attain the recommended lung RV and TLC for health lungs.

Therefore, the efficiency of physicians that operate on the mechanical ventilators, especially during emergency times, can now be improved by not necessarily increasing the number of the physicians, but by adding the fuzzy-image reasoning to the mechanical ventilator

systems, to help in providing suggestions to the physician(s). A time trigger of 20 breaths per minute was used for this study to easily identify the presence of air in the lungs after expiration, which is more effective than the breath trigger setting. The limitations of the system are: images trained were not enough, especially the brain medical scans; the lung transfer function is static, implying that it is hard to determine the improvement or decline of the lung functionality; the trained multi-algorithms increase the need of computational power which further increases the response-time of the intelligent fuzzified system.

5.2 Recommendations

In order to improve this system, the following recommendations may be considered:

(1) collection of more brain and lung medical images, for both CNN training and improving the performance of the algorithms.

(2) use of patient simulator to test the algorithm suggestions for lung protection and oxygenation.

(3) employing the algorithms to a computer with more computational processing power to further decrease the system response time.

References

H. Aguirre-Bermeo, M. Bottiroli, S. Italiano, F. Roche-Campo, J. A. Santos, M. Alonso, and J. Mancebo. Pressure support ventilation and proportional assist ventilation during weaning from mechanical ventilation. *Med Intensiva*, 38:363–370, 08 2014. doi: https://doi: 10.1016/j.medin.2013.08.003.

M. Ahishali, A. Degerli, M. Yamac, S. Kiranyaz, M. E. H. Chowdhury, K. Hameed, T. Hamid, R. Mazhar, and Gabbouj M. Advance warning methodologies for covid-19 using chest x-ray images. *IEEE Access*, 9:41052–41065, 2021. doi: https://doi.org/10.1109/ACCESS.2021.3064927.

Michael G. Allison, Michael C. Scott, Kami M. Hu, Michael D. Witting, and Michael E. Winters. High initial tidal volumes in emergency department patients at risk for acute respiratory distress syndrome. *Journal of Critical Care*, 30(2):341–343, 2015. ISSN 0883-9441. doi: https://doi.org/10.1016/j.jcrc.2014.12.004. URL `https://www.sciencedirect.com/science/article/pii/S0883944114004948`.

Raouf S. Amin. Chapter 14 - chronic respiratory failure. In Victor Chernick, Thomas F. Boat, Robert W. Wilmott, and Andrew Bush, editors, *Kendig's Disorders of the Respiratory Tract in Children (Seventh Edition)*, pages 243–258. W.B. Saunders, Philadelphia, seventh edition edition, 2006. ISBN 978-0-7216-3695-5. doi: https://doi.org/10.1016/B978-0-7216-3695-5.50018-3. URL `https://www.sciencedirect.com/science/article/pii/B9780721636955500183`.

JM. Arnal, M. Saoli, and A. Garnero. Airway and transpulmonary driving pressures and mechanical powers selected by intellivent-asv in passive, mechanically ventilated icu patients. *Heart Lung*, 4:427–434, 06 2020. doi: 10.1016/j.hrtlng.2019.11.001.

MC. Bachmann, C. Morais, G. Bugedo, A. Bruhn, A. Morales, E. Borges, JB. Costa, and J. Retamal. Electrical impedance tomography in acute respiratory distress syndrome. *Crit Care*, 22, October 2018. doi: 10.1186/s13054-018-2195-6.

Wang D. Bai Y. Fundamentals of fuzzy logic control — fuzzy sets, fuzzy rules and defuzzifications. in: Bai y., zhuang h., wang d. (eds) advanced fuzzy logic technologies in industrial applications. *Advances in Industrial Control. Springer, London*, 2006. doi: https://doi.org/10.1007/978-1-84628-469-4$_$2.

Sabrina Setembre Batah and Alexandre Todorovic Fabro. Pulmonary pathology of ards in covid-19: A pathological review for clinicians. *Respiratory Medicine*, 176:106239, 2021. ISSN 0954-6111. doi: https://doi.org/10.1016/j.rmed.2020.106239. URL `https://www.sciencedirect.com/science/article/pii/S0954611120303796`.

Jason H. Bates and Bradford J. Smith. Ventilator-induced lung injury and lung mechanics. *Annals of translational medicine*, 6, 06 2018. doi: 10.21037/atm.2018.06.29. URL `https://doi.org/10.21037/atm.2018.06.29`.

Thomas Bein, Salvatore Grasso, Onnen Moerer, Michael Quintel, Claude Guerin, Maria Deja, Anita Brondani, and Sangeeta Mehta. The standard of care of patients with ards: ventilatory settings and rescue therapies for refractory hypoxemia. *Intensive Care Medicine*, 42, 04 2016. doi: 10.1007/s00134-016-4325-4.

D. B. Bernstein, B. Nguyen, G. B. Allen, and J. H. Bates. Elucidating the fuzziness in physician decision making in ards. *J Clin Monit Comput.*, 27:357–363, 2013.

Reena M Bhatt, Howard W Clark, Massimo Girardis, and Stefano Busani. Exogenous pulmonary surfactant in covid-19 ards. the similarities to neonatal rds suggest a new

scenario for an 'old' strategy. *BMJ Open Respiratory Research*, 8(1), 2021. doi: 10.1136/bmjresp-2020-000867. URL `https://bmjopenrespres.bmj.com/content/8/1/e000867`.

Pratik Bhowal, Subhankar Sen, Jin Hee Yoon, Zong Woo Geem, and Ram Sarkar. Choquet integral and coalition game-based ensemble of deep learning models for covid-19 screening from chest x-ray images. *IEEE Journal of Biomedical and Health Informatics*, 2021.

E. Bialais, X. Wittebole, L. Vignaux, J. Roeseler, M. Wysocki, J. Meyer, G. Reychler, D. Novotni, T. Sottiaux, PF. Laterre, and P. Hantson. Closed-loop ventilation mode (intellivent®-asv) in intensive care unit: a randomized trial. *Minerva Anestesiol*, pages 657–668, 03 2016.

F. Bobillo, M. Calvo-Flores, J. Gomez-Romero, and U. Straccia. Joining godel and zadeh fuzzy logics in fuzzy description logics. *International Journal of Uncertainty, Fuzziness and Knowledge-Based Systems*, 20:475–508, 8 2012. doi: 10.1142/S0218488512500249.

M. Briel, M. Meade, A. Mercat, R. G. Brower, D. Talmor, S. D. Walter, A. S. Slutsky, E. Pullenayegum, Q. Zhou, D. Cook, L. Brochard, M. R. Jean-Christophe, F. Lamontagne, N. Bhatnagar, T. E. Stewart, and G. Guyatt. Higher vs lower positive end-expiratory pressure in patients with acute lung injury and acute respiratory distress syndrome: Systematic review and meta-analysis. *The journal of the American Medical Association (JAMA)*, 303:865–873, 3 2010. doi: 10.1001/jama.2010.218.

Timothy Bristle, Shawn Collins, Ian Hewer, and Kevin Hollifield. Anesthesia and critical care ventilator modes: Past, present, and future. *AANA journal*, 82:387–400, 10 2014.

R. G. Brower, P. N. Lanken, N. MacIntyre, M.A. Matthay, A. Morris, M. Ancukiewicz, D. Schoenfeld, B.T. Thompson, National Heart Lung, and Blood Institute ARDS Clinical Trials Network. Higher versus lower positive end-expiratory pressures in

patients with the acute respiratory distress syndrome. *N Engl J Med*, 351:327–336, 2004.

J. J. Buckley and Y. Hayashi. Fuzzy input-output controllers are universal approximators. *Fuzzy Sets and Systems*, 58:273–278, 9 1993. doi: https://doi.org/10.1016/0165-0114(93)90503-A.

C. Bureau, M. Decavèle, S. Campion, Marie-Cécile Nierat, Julien Mayaux, Elise Morawiec, Mathieu Raux, Thomas Similowski, and Alexandre Demoule. Proportional assist ventilation relieves clinically significant dyspnea in critically ill ventilated patients. *Ann. Intensive Care*, 11, 12 2021. doi: https://doi.org/10.1186/s13613-021-00958-7.

D. Campbell and J. Brown. The electrical analogue of lung. *Brit. J. Anaesth.*, 35, 1963.

A. A. Carrillo and C.J. López-Herce. Parameters of mechanical ventilation. *An Pediatr (Barc)*, 59:67–74, 2003.

A.R. Carvalho and W.A. Zin. Respiratory system dynamical mechanical properties: modeling in time and frequency domain. *Biophys Rev*, 3:71–84, 2011. doi: https://doi.org/10.1007/s12551-011-0048-5.

M. J. Cawley. Mechanical ventilation: a tutorial for pharmacists. *Pharmacotherapy*, 27: 250–266, 2 2007. doi: 10.1592/phco.27.2.250. PMID: 17253915.

R. L. Chatburn, M. El-Khatib, and E. Mireles-Cabodevila. A taxonomy for mechanical ventilation: 10 fundamental maxims. *Respir Care*, 59:1747–1763, 11 2014. doi: 10.4187/respcare.03057.

Robert L. Chatburn and Eduardo Mireles-Cabodevila. *Design and function of mechanical ventilators*. Oxford University Press, Oxford, UK, 04 2016. ISBN 9780191810398. doi: 10.1093/med/9780199600830.003.0092. URL `https://oxfordmedicine.com/view/10.1093/med/9780199600830.001.0001/med-9780199600830-chapter-92`.

M.E.H. Chowdhury, T Rahman, A. Khandakar, R. Mazhar, M.A. Kadir, Z.B. Mahbub, K.R. Islam, M.S. Khan, A. Iqbal, N. Al-Emadi, M.B.I. Reaz, and M. T. Islam. Can ai help in screening viral and covid-19 pneumonia? *IEEE Access*, 8:132665 – 132676, 2020.

J. T. Cleophas and H. A. Zwinderman. Fuzzy logic. *Statistics Applied to Clinical Studies, Springer*, 2012.

F. Collino, F. Rapetti, F. Vasques, G. Maiolo, T. Tonetti, F. Romitti, J. Niewenhuys, T. Behnemann, L. Camporota, G. Hahn, V. Reupke, K. Holke, P. Herrmann, E. Duscio, F. Cipulli, O. Moerer, J. J. Marini, M. Quintel, and L. Gattinoni. Positive end-expiratory pressure and mechanical power. *Anesthesiology*, 130:119–130, 1 2019. doi: 10.1097/ALN.0000000000002458.

C.A. Del-Negro, G. D. Funk, and J. L. Feldman. Breathing matters. *Nature reviews. Neuroscience*, 19:351–367, 2018. doi: https://doi.org/10.1038/s41583-018-0003-6.

C. R. Dennison, P. A. Mendez-Tellez, W. Wang, P. J. Pronovost, and D. M. Needham. Barriers to low tidal volume ventilation in acute respiratory distress syndrome: survey development, validation, and results. *Crit Care Med.*, 35:2747–2754, 12 2007.

Z. Isa F. Shukri. Experts' judgment-based mamdani-type decision system for risk assessment. *Mathematical Problems in Engineering*, 9:1–13, 11 2021. doi: 10.1155/2021/6652419.

Eddy Fan, Daniel Brodie, and Arthur S. Slutsky. Acute respiratory distress syndrome: Advances in diagnosis and treatment. *JAMA*, 319:698–710, 2018. doi: https://doi:10.1001/jama.2017.21907.

N.D. Ferguson, E. Fan, L. Camporota, M. Antonelli, A. Anzueto, R. Beale, L. Brochard, R. Brower, A. Esteban, L. Gattinoni, A. Rhodes, A. S. Slutsky, J. Vincent, G. D.

Rubenfeld, B. T. Thompson, and V. M. Ranieri. The berlin definition of ards: an expanded rationale, justification, and supplementary material. *Intensive Care Med*, 38: 1573–1582, 1 2012. doi: https://doi.org/10.1007/s00134-012-2682-1.

Juan Carlos Figueroa García, Christian Servin, and Vladik Kreinovich. Centroids beyond defuzzification. In Barnabás Bede, Martine Ceberio, Martine De Cock, and Vladik Kreinovich, editors, *Fuzzy Information Processing 2020*, pages 407–412, Cham, 2022. Springer International Publishing. ISBN 978-3-030-81561-5.

ARDS Definition Task Force, V.M. Ranieri, G.D. Rubenfeld, B.T. Thompson, N.D. Ferguson, E. Caldwell, E. Fan, L. Camporota, and A.S. Slutsky. Acute respiratory distress syndrome: the berlin definition. *JAMA*, 23:2526–2533, 06 2012a. doi: doi: 10.1001/jama.2012.5669.

ARDS Definition Task Force, V.M. Ranieri, G.D. Rubenfeld, B.T. Thompson, N.D Ferguson, E. Caldwell, E. Fan, L. Camporota L, and A.S. Slutsky. Acute respiratory distress syndrome: the berlin definition. *JAMA*, 307:2526–2533, June 2012b. doi: https://doi:10.1001/jama.2012.5669.

The ARDS Definition Task Force. Acute respiratory distress syndrome: the berlin definition. *JAMA*, 307:2526–253, 2012.

S. A. Forman and V. A. Chin. General anesthetics and molecular mechanisms of unconsciousness. *International anesthesiology clinics*, 46:43–53, 2008. doi: https://doi.org/10.1097/AIA.0b013e3181755da5.

N. R. Frank, H. A. Lyons, A. A. Siebens, and T. F. Nealon. Pulmonary compliance in patients with cardiac disease. *The American Journal of Medicine*, 22:516 – 523, 1957. doi: https://doi.org/10.1016/0002-9343(57)90106-7.

P. D. Wendel Garcia, D. A. Hofmaenner, S. D. Brugger, C. T. Acevedo, J. Bartussek, G. Camen, P. R. Bader, G. Bruellmann, J. Kattner, C. Ganter, R. A. Schuepbach, and

P. K. Buehler. Closed-loop versus conventional mechanical ventilation in covid-19 ards. *J Intensive Care Med*, 36:1184–1193, 10 2021.

L. Gattinoni, E. Carlesso, L. Brazzi, and P. Caironi. Positive end-expiratory pressure. *Curr Opin Crit Care*, 16:39–44, 2 2010. doi: 10.1097/MCC.0b013e3283354723.

L. Gonzalez-De La Fuente, A. Nieto-Reyes, and P. Teran. Statistical depth for fuzzy sets. *Fuzzy Sets and Systems*, 443:58–86, 8 2022. doi: https://doi.org/10.1016/j.fss.2021.09.015.

Giacomo Grasselli, Tommaso Tonetti, Alessandro Protti, Thomas Langer, Massimo Girardis, Giacomo Bellani, John Laffey, Gianpaolo Carrafiello, Luca Carsana, Chiara Rizzuto, Alberto Zanella, Vittorio Scaravilli, Giacinto Pizzilli, Domenico Luca Grieco, Letizia Di Meglio, Gennaro de Pascale, Ezio Lanza, Francesco Monteduro, Maurizio Zompatori, Claudia Filippini, Franco Locatelli, Maurizio Cecconi, Roberto Fumagalli, Stefano Nava, Jean-Louis Vincent, Massimo Antonelli, Arthur S Slutsky, Antonio Pesenti, V Marco Ranieri, Alfredo Lissoni, Nicola Rossi, Amedeo Guzzardella, Carlo Valsecchi, Fabiana Madotto, Francesca Bevilacqua, Marco Di Laudo, Lorenzo Querci, and Carmen Seccafico. Pathophysiology of covid-19-associated acute respiratory distress syndrome: a multicentre prospective observational study. *The Lancet Respiratory Medicine*, 8(12):1201–1208, 2020. ISSN 2213-2600. doi: https://doi.org/10.1016/S2213-2600(20)30370-2. URL `https://www.sciencedirect.com/science/article/pii/S2213260020303702`.

C. Guerin and J. C. Richard. Measurement of respiratory system resistance during mechanical ventilation. *Intensive Care Med*, 33:1046–1049, 04 2007. doi: https://doi.org/10.1007/s00134-007-0652-9.

H Guler and F. Ata. The comparison of manual and labview-based fuzzy control on

mechanical ventilation. *Journal of Engineering in Medicine*, 9:916–925, 2014. doi: 10.1177/0954411914550513.

Josef Guttmann, Luc Eberhard, Gunther Wolff, Wolfgang Bertschmann, Julius Zeravik, and Michael Adolph. Maneuver-free determination of compliance and resistance in ventilated ards patients. *Chest*, 102(4):1235–1242, 1992. ISSN 0012-3692. doi: https://doi.org/10.1378/chest.102.4.1235. URL `https://www.sciencedirect.com/science/article/pii/S0012369216343124`.

J. Joris Hage and Romy J. Brinkman. Andreas vesalius' understanding of pulmonary ventilation. *Respiratory Physiology and Neurobiology*, 231:37–44, 2016. ISSN 1569-9048. doi: https://doi.org/10.1016/j.resp.2016.05.015. URL `https://www.sciencedirect.com/science/article/pii/S1569904816300921`.

Liming Hao, Shuai Ren, Yan Shi, Na Wang, Yixuan Wang, Zujin Luo, Fei Xie, Meng Xu, Jian Zhang, and Maolin Cai. A novel method to evaluate patient-ventilator synchrony during mechanical ventilation. *Complexity*, 2020:1–15, 2020. doi: https://doi.org/10.1155/2020/4828420.

Maud Hoofs, Rob Hagmeijer, and Marieke L. Duiverman. Inspired oxygen fraction during non-invasive ventilation: the influence of flow rates, masks, exhalation ports and ventilatory settings. *European Respiratory Journal*, 52(suppl 62), 2018. ISSN 0903-1936. doi: 10.1183/13993003.congress-2018.PA2377. URL `https://erj.ersjournals.com/content/52/suppl_62/PA2377`.

M. Hssayeni. Computed tomography images for intracranial hemorrhage detection and segmentation. *PhysioNet*, 78, 2019. doi: doi:10.13026/w8q8-ky94.

Mohammad Jaber, Lara Hamawy, Mohamad Hajj-Hassan, Mohamad Abou Ali, and Abdallah Kassem. Matlab/simulink mathematical model for lung and ventilator. In

2020 32nd International Conference on Microelectronics (ICM), pages 1–5, 2020. doi: 10.1109/ICM50269.2020.9331820.

Shazia M. Jamil and Roger G. Spragg. Chapter 4 - acute lung injury: Acute respiratory distress syndrome. In PETER J. PAPADAKOS, BURKHARD LACHMANN, and Laraine Visser-Isles, editors, *Mechanical Ventilation*, pages 28–41. W.B. Saunders, Philadelphia, 2008. ISBN 978-0-7216-0186-1. doi: https://doi.org/10.1016/B978-0-7216-0186-1.50008-9. URL `https://www.sciencedirect.com/science/article/pii/B9780721601861500089`.

Z. Jin and B. K. Bose. Evaluation of membership functions for fuzzy logic controlled induction motor drive. *IEEE 2002 28th Annual Conference of the Industrial Electronics Society (IECON)*, 1:229–234, 11 2002. doi: 10.1109/IECON.2002.1187512.

R. John. Fuzzy sets and knowledge representation. in: Szczepaniak p.s., lisboa p.j.g., kacprzyk j. (eds) fuzzy systems in medicine. *Studies in Fuzziness and Soft Computing*, 41, 2000. doi: https://doi.org/10.1007/978-3-7908-1859-8$_4$.

Gavin M. Joynt. Chapter 7 - severe acute respiratory syndrome (sars). In PETER J. PAPADAKOS, BURKHARD LACHMANN, and Laraine Visser-Isles, editors, *Mechanical Ventilation*, pages 61–66. W.B. Saunders, Philadelphia, 2008. ISBN 978-0-7216-0186-1. doi: https://doi.org/10.1016/B978-0-7216-0186-1.50011-9. URL `https://www.sciencedirect.com/science/article/pii/B9780721601861500119`.

M. Juventin, V. Ghibaudo, J. Granget, C. Amat, E. Courtiol, and N. Buonviso. Respiratory influence on brain dynamics: the preponderant role of the nasal pathway and deep slow regime. *Pflugers Arch.*, 475:23–35, January 2023. doi: 10.1007/s00424-022-02722-7.

Robert M Kacmarek. The mechanical ventilator: Past, present, and future. *Respiratory*

Care, 56(8):1170–1180, 2011. ISSN 0020-1324. doi: 10.4187/respcare.01420. URL `http://rc.rcjournal.com/content/56/8/1170`.

J. Kacprzyk. Fuzzy sets and fuzzy systems: A brief introduction. in: Szczepaniak p.s., lisboa p.j.g., kacprzyk j. (eds) fuzzy systems in medicine. *Studies in Fuzziness and Soft Computing*, 41, 2000. doi: https://doi.org/10.1007/978-3-7908-1859-8$_1$.

Daniel Kermany, Kang Zhang, and Michael Goldbaum. Labeled optical coherence tomography (oct) and chest x-ray images for classification. *Mendeley Data*, V2, 2018. doi: 10.17632/rscbjbr9sj.2.

A. Kessinger and PG. Rigby. Hemorrhage and heat stroke. *Geriatrics*, 25:115–118, July 1970.

Christopher King, Dhwani Sahjwani, A Brown, Saad Feroz, Paula Cameron, Erik Osborn, Mehul Desai, Svetolik Djurkovic, Aditya Kasarabada, Rachel Hinerman, James Lantry, Oksana Shlobin, Kareem Ahmad, Vikramjit Khangoora, Shambhu Aryal, A Collins, Alan Speir, and Steven Nathan. Outcomes of mechanically ventilated patients with covid-19 associated respiratory failure. *PLoS One*, 15, 11 2020. doi: doi: 10.1371/journal.pone.0242651.

A.C. Koumbourlis and E.K. Motoyama. Lung mechanics in covid-19 resemble respiratory distress syndrome, not acute respiratory distress syndrome: could surfactant be a treatment? *Am J Respir Crit Care Med*, 202:624–626, 2020. doi: doi:10.1164/rccm.202004-1471LE.

V. Kumar, R. Kumar, and M. Kumar. Recent advances in low-cost, portable automated resuscitator systems to fight covid-19. *Health Technol.*, 12:181–191, 2022. doi: https://doi.org/10.1007/s12553-021-00629-4.

J. Laffey and B. Kavanagh. Ventilation with lower tidal volumes as compared with

traditional tidal volumes for acute lung injury. *The New England journal of medicine*, 343:813–814, 10 2000. doi: 10.1056/NEJM200009143431113.

Y. Lambat, N. Ayres, L. Maglaras, and M. A. Ferrag. A mamdani type fuzzy inference system to calculate employee susceptibility to phishing attacks. *Applied Sciences*, 19: 3–19, 9 2021. doi: 11. 1. 10.3390/app11199083.

Olivier Lamouret, Laure Crognier, Fanny Vardon Bounes, Jean-Marie Conil, Caroline Dilasser, Thibaut Raimondi, Stéphanie Ruiz, Antoine Rouget, Clement Delmas, Thierry Seguin, Vincent Minville, and Bavakure Georges. Neurally adjusted ventilatory assist (nava) versus pressure support ventilation: Patient-ventilator interaction during invasive ventilation delivered by tracheostomy. *Critical Care*, 23, 12 2019. doi: 10.1186/s13054-018-2288-2.

François Lellouche and Laurent Brochard. Advanced closed loops during mechanical ventilation (pav, nava, asv, smartcare). *Best Practice and Research Clinical Anaesthesiology*, 23(1):81–93, 2009. ISSN 1521-6896. doi: https://doi.org/10.1016/j.bpa.2008.08.001. URL `https://www.sciencedirect.com/science/article/pii/S1521689608000815`. Information Technology in Anaesthesia and Critical Care.

Henry Lewith and Jaideep J. Pandit. Lung ventilation and the physiology of breathing. *Surgery (Oxford)*, 38(5):233–239, 2020. ISSN 0263-9319. doi: https://doi.org/10.1016/j.mpsur.2020.03.005. URL `https://www.sciencedirect.com/science/article/pii/S0263931920300491`.

Z. Liu, X. Di, L. Zhong, Z. Su, B. Xu, X. Zhang, Z. Liang, G. Zhao, and Z. Hu. Clinical application of adaptive minute ventilation + intellicycle ventilation mode in patients with mild-to-moderate acute respiratory distress syndrome. pages 20–25, 01 2020. doi: 10.3760/cma.j.cn121430-20191012-00004.

JJ Lofrese, C. Tupper, D. Denault, and SL. Lappin. Physiology, residual volume. *Treasure Island (FL): StatPearls Publishing*, 11, 01 2023.

Sharon Lozano, K Moeller, Claudius Stahl, and Josef Guttmann. Autopilot-bt: an approach towards automatic mechanical ventilation. *Critical Care - CRIT CARE*, 11, 03 2007. doi: 10.1186/cc5326.

Y. Mao, O. Bajinka, Z. Tang, X. Qiu, and Y. Tan. Lung-brain axis: Metabolomics and pathological changes in lungs and brain of respiratory syncytial virus-infected mice. *J Med Virol.*, 94:5885–5893, December 2022. doi: 10.1002/jmv.28061.

M. Marlena, G. Norbert, K. Aneta, and K. Konrad. Different defuzzification methods in guimbal cabri g2 helicopter takeoff possibility evaluation. *Transport Problems*, 13: 27–38, 6 2018. doi: 10.20858/tp.2018.13.2.3.

PJ Martinez-Pitre, BR Sabbula, and Cascella M. Restrictive lung disease. *Treasure Island (FL): StatPearls Publishing*, July 2023.

M. Meade, D. Cook, G. Guyatt, A. Slutsky, Y. Arabi, D. Cooper, A. Davies, L. Hand, Q. Zhou, L. Thabane, P. Austin, S. Lapinsky, A. Baxter, J. Russell, Y. Skrobik, J. Ronco, and T. Stewart. Ventilation strategy using low tidal volumes, recruitment maneuvers, and high positive end-expiratory pressure for acute lung injury and acute respiratory distress syndrome. *The journal of the American Medical Association (JAMA)*, 299:637–645, 2 2008. doi: 10.1001/jama.299.6.637.

IM. Mehedi, HSM. Shah, M. Ubaid, R. Mansouri, and M. Bettayeb. Adaptive fuzzy sliding mode control of a pressure-controlled artificial ventilator. *Journal of Healthcare Engineering*, 4, 2021. doi: 10.1155/2021/1926711.

JS. MEYER. Ischemic cerebrovascular disease (stroke). clinical investigation and management. *JAMA*, 183:237–240, January 1963. doi: 10.1001/jama.1963.03700040039009.

Takashi Mitsuishi. Definition of centroid method as defuzzification. *Formalized Mathematics*, 30(2):125–134, 2022. doi: doi:10.2478/forma-2022-0010. URL `https://doi.org/10.2478/forma-2022-0010`.

N. Mogharreban and L. Dilalla. Comparison of defuzzification techniques for analysis of non-interval data. *Annual Conference of the North American Fuzzy Information Processing Society (NAFIPS)*, pages 257–260, 6 2006. doi: 10.1109/NAFIPS.2006.365418.

J. Monicka, N. O. Sekhar, and K. Kumar. Performance evaluation of membership functions on fuzzy logic controlled ac voltage controller for speed control of induction motor drive. *International Journal of Computer Applications*, 13:8–12, 1 2011. doi: 13. 10.5120/1778-2451.

Jacopo P. Mortola. How to breathe? respiratory mechanics and breathing pattern. *Respiratory Physiology and Neurobiology*, 261:48–54, 2019. ISSN 1569-9048. doi: https://doi.org/10.1016/j.resp.2018.12.005. URL `https://www.sciencedirect.com/science/article/pii/S1569904818303161`.

J.F. Murray. The structure and function of the lung. *Int J Tuberc Lung Dis.*, 14:391–396, April 2010.

S. Nafday, R. Green, J. Lin, Ian Ochshorn, and Ian R Holzman. Is there an advantage of using pressure support ventilation with volume guarantee in the initial management of premature infants with respiratory distress syndrome? a pilot study. *J Perinatol*, 25:193–197, 2005. doi: https://doi.org/10.1038/sj.jp.7211233.

The Acute Respiratory Distress Syndrome Network. Ventilation with lower tidal volumes as compared with traditional tidal volumes for acute lung injury and the acute respiratory distress syndrome. *The New England journal of medicine*, 342:1301–1308, 1 2000.

L. Ney and W. Kuebler. Ventilation with lower tidal volumes as compared with traditional tidal volumes for acute lung injury. *The New England journal of medicine*, 343:812–813, 9 2000.

B. Nguyen, D. B. Bernstein, and J. H. Bates. Controlling mechanical ventilation in acute respiratory distress syndrome with fuzzy logic. *Journal of critical care*, 29:551–556, 8 2014. doi: https://doi.org/10.1016/j.jcrc.2014.03.009.

C.R. Olsen, F.C. Hale, and R. Elsner. Mechanics of ventilation in the pilot whale. *Respiration Physiology*, 7(2):137–149, 1969. ISSN 0034-5687. doi: https://doi.org/10.1016/0034-5687(69)90001-2. URL `https://www.sciencedirect.com/science/article/pii/0034568769900012`.

A. Omar, A. Aous, and S. Balasem. Comparison between the effects of different types of membership functions on fuzzy logic controller performance. *International Journal of Emerging Engineering Research and Technology*, 3:76–83, 3 2015.

E. Ortiz-Prado, J. F. Dunn, J. Vasconez, D. Castillo, and G. Viscor. Partial pressure of oxygen in the human body: a general review. *American journal of blood research*, 9: 1–14, 2019.

Rolando Peralta, Sara Andino, and Stephen Perrig. Patient machine interface for the control of mechanical ventilation devices. *Brain sciences*, 3:1554–1568, 12 2013. doi: 10.3390/brainsci3041554.

T. Pettenuzzo, A. Boscolo, A. De Cassai, N. Sella, F. Zarantonello, P. P. Pasin, L. Laura, G. Landoni, and P. Navalesi. Higher versus lower positive end-expiratory pressure in patients without acute respiratory distress syndrome: a meta-analysis of randomized controlled trials. *Critical Care*, 25:1–11, 12 2021. doi: 10.1186/s13054-021-03669-4.

T. Pham, L. J. Brochard, and A. S. Slutsky. Mechanical ventilation: State of the art. *Mayo Clin Proc.*, 92:1382–1400, 9 2017. doi: 10.1016/j.mayocp.2017.05.004. PMID: 28870355.

D. Powers. Evaluation: From precision, recall and f-measure to roc, informedness, markedness and correlation. *J. Mach. Learn. Technol*, 2:2229–3981, 01 2011. doi: 10.9735/2229-3981.

D. Purohit, AK. Ahirwar, A. Sakarde, P. Asia, and Gopal N. Covid-19 and lung pathologies. *Horm Mol Biol Clin Investig.*, 42:435–443, August 2021. doi: 10.1515/hmbci-2020-0096.

T. Rahman, A. Khandakar, Y. Qiblawey, A. Tahir, S. Kiranyaz, S.B.A. Kashem, M.T. Islam, S.A. Maadeed, S.M. Zughaier, M.S. Khan, and M.E. Chowdhury. Exploring the effect of image enhancement techniques on covid-19 detection using chest x-ray images. *Computers in Biology and Medicine, Elsevier*, 132, 2021. doi: https://doi.org/10.1016/j.compbiomed.2021.104319.

Chiara Riforgiato, Denise Battaglini, Chiara Robba, and Paolo Pelosi. Chapter 4 - mechanical ventilation—peep. In Hemanshu Prabhakar, editor, *Essentials of Evidence-Based Practice of Neuroanesthesia and Neurocritical Care*, pages 33–42. Academic Press, 2022. ISBN 978-0-12-821776-4. doi: https://doi.org/10.1016/B978-0-12-821776-4.00004-4. URL `https://www.sciencedirect.com/science/article/pii/B9780128217764000044`.

A. F. Roldan Lopez de Hierro, M. A. Tiscar, C. Roldan, and et al. A fuzzy methodology for approaching fuzzy sets of the real line by fuzzy numbers. *Fuzzy Sets and Systems*, 435:55–77, 5 2022. doi: https://doi.org/10.1016/j.fss.2021.08.024.

L. Rondeau, R. Ruelas, L. Levrat, and M. Lamotte. A defuzzification method respecting the fuzzification. *Fuzzy Sets and Systems*, 86:311–32, 3 1997. doi: https://doi.org/10.1016/S0165-0114(95)00399-1.

T.J. Ross. Membership functions, fuzzification and defuzzification. in: Szczepaniak p.s.,

lisboa p.j.g., kacprzyk j. (eds) fuzzy systems in medicine. *Studies in Fuzziness and Soft Computing*, 41, 2000. doi: https://doi.org/10.1007/978-3-7908-1859-8$_3$.

S. K. Sahetya, E. C. Goligher, and R. G. Brower. Fifty years of research in ards. setting positive end-expiratory pressure in acute respiratory distress syndrome. *Am J Respir Crit Care Med.*, 195:1429–1438, 6 2017a. doi: 10.1164/rccm.201610-2035CI.

Sarina K. Sahetya, Christopher Mallow, Jonathan E. Sevransky, Greg S. Martin, Timothy D. Girard, Roy G. Brower, William Checkley, and Society of Critical Care Medicine Discovery Network Critical Illness Outcomes Study Investigators. Association between hospital mortality and inspiratory airway pressures in mechanically ventilated patients without acute respiratory distress syndrome: a prospective cohort study. *Critical Care*, 23:367, 11 2019. doi: https://doi.org/10.1186/s13054-019-2635-y.

S.K. Sahetya, E.C. Goligher, and R.G. Brower. Fifty years of research in ards. setting positive end-expiratory pressure in acute respiratory distress syndrome. *Am J Respir Crit Care Med.*, 195:1429–1438, 6 2017b. doi: 10.1164/rccm.201610-2035CI.

N. Sameena, A. Afshar, and B. Ranjit. Effect of different defuzzification methods in a fuzzy based load balancing application. *International Journal of Computer Science Issues*, 8:261–267, 9 2011.

Catherine SH Sassoon. Triggering of the ventilator in patient-ventilator interactions. *Respiratory Care*, 56(1):39–51, 2011. ISSN 0020-1324. doi: 10.4187/respcare.01006. URL `http://rc.rcjournal.com/content/56/1/39`.

Craig L Scanlan, Robert L Wilkins, James K Stoller, Albert J Heuer, and William F Galvin. *Egan's Fundamentals of Respiratory Care.* The C.V. Mosby Company, 1990.

Andreas Schulze. Chapter 32 - proportional assist ventilation and respiratory mechanical unloading in infants. In Steven M. Donn and Sunil K. Sinha, editors, *Manual of*

Neonatal Respiratory Care (Second Edition), pages 216–221. Mosby, Philadelphia, second edition edition, 2006. ISBN 978-0-323-03176-9. doi: https://doi.org/10.1016/B978-032303176-9.50037-4. URL https://www.sciencedirect.com/science/article/pii/B9780323031769500374.

Christer Sinderby, Paolo Navalesi, Jennifer Beck, Yoanna Skrobik, Norman Comtois, Sven Friberg, Stewart Gottfried, and Lilia Lindström. Neural control of mechanical ventilation in respiratory failure. *Nature medicine*, 5:1433–1436, 01 2000. doi: 10.1038/71012.

D. Sinha and E. R. Dougherty. Fuzzification of set inclusion: Theory and applications. *Fuzzy Sets and Systems*, 55:15–42, 4 1993. doi: https://doi.org/10.1016/0165-0114(93)90299-W.

Sunil K. Sinha and Steven M. Donn. Chapter 31 - pressure support ventilation. In Steven M. Donn and Sunil K. Sinha, editors, *Manual of Neonatal Respiratory Care (Second Edition)*, pages 212–215. Mosby, Philadelphia, second edition edition, 2006. ISBN 978-0-323-03176-9. doi: https://doi.org/10.1016/B978-032303176-9.50036-2. URL https://www.sciencedirect.com/science/article/pii/B9780323031769500362.

A. Srivastava, A. Sood, S. P. Joy, and J. Woodcock. Principles of physics in surgery: the laws of flow dynamics physics for surgeons - part 1. *The Indian journal of surgery*, 71:182–187, 2009. doi: https://doi.org/10.1007/s12262-009-0064-x.

E. Straszecka. Defining membership functions. in: Szczepaniak p.s., lisboa p.j.g., kacprzyk j. (eds) fuzzy systems in medicine. *Studies in Fuzziness and Soft Computing*, 41, 2000. doi: https://doi.org/10.1007/978-3-7908-1859-8$_2$.

S. Sud, J. O. Friedrich, N. K. J. Adhikari, E. Fan, N. D., Ferguson, G. Guyatt, and M. O. Meade. Comparative effectiveness of protective ventilation strategies for moderate and

severe acute respiratory distress syndrome. *A Network Meta-Analysis. Am J Respir Crit Care Med*, 203:1366–1377, 06 2021. doi: doi: 10.1164/rccm.202008-3039OC.

P. Tamburrano, F. Sciatti, E. Distaso, L. Di-Lorenzo, and R. Amirante. Validation of a simulink model for simulating the two typical controlled ventilation modes of intensive care units mechanical ventilators. *Applied Sciences*, 4, 2022. doi: https://doi.org/10.3390/app12042057.

N. Tamiloli, J. Venkatesan, G. Vinay, P. Sai, S. Irfan, T. Sampathkumar, and D. Jayabalakrishnan. Comparison of sugeno-type and mamdani-type fuzzy inference systems for end milling process. *AIP Conference Proceedings*, 1, 10 2021. doi: 2395. 040012. 10.1063/5.0068445.

B. Tasci and I. Tasci. Deep feature extraction based brain image classification model using preprocessed images: Pdrnet. *Biomedical Signal Processing and Control*, 78, 2022. doi: https://doi.org/10.1016/j.bspc.2022.103948.

S. Thaker and V. Nagori. Analysis of fuzzification process in fuzzy expert system. *Procedia Computer Scienc*, 132:1308–1316, 6 2018. doi: https://doi.org/10.1016/j.procs.2018.05.047.

M. Tobin and C. Manthous. Mechanical ventilation. *Am J Respir Crit Care Med*, 196:3–4, 7 2017. doi: 10.1164/rccm.1962P3. PMID: 28707967.

M. J. Tobin. Physiologic basis of mechanical ventilation. *Ann Am Thorac Soc*, 15:49–52, 2 2018. doi: 10.1513/AnnalsATS.201705-417KV. PMID: 29461885.

Martin J. Tobin. Principles and practice of mechanical ventilation, third edition. *McGraw-Hill Companies*, 2013. URL `http://accessanesthesiology.mhmedical.com/book.aspx?bookID=520`.

K. Uchida. Respiratory rate as a factor in lung injury-not just what you set, but how you set. *Anesthesiology*, pages 351–353, April 2023.

Mian Zain Urfy and Jose I. Suarez. Chapter 17 - breathing and the nervous system. In José Biller and José M. Ferro, editors, *Neurologic Aspects of Systemic Disease Part I*, volume 119 of *Handbook of Clinical Neurology*, pages 241–250. Elsevier, 2014. doi: https://doi.org/10.1016/B978-0-7020-4086-3.00017-5. URL https://www.sciencedirect.com/science/article/pii/B9780702040863000175.

David Williams, Anna Kenyon, and Dawn Adamson. Chapter ten - physiology. In Phillip Bennett and Catherine Williamson, editors, *Basic Science in Obstetrics and Gynaecology (Fourth Edition)*, pages 173–230. Churchill Livingstone, fourth edition edition, 2010. ISBN 978-0-443-10281-3. doi: https://doi.org/10.1016/B978-0-443-10281-3.00014-2. URL https://www.sciencedirect.com/science/article/pii/B9780443102813000142.

Jay M. Wilson and John W. DiFiore. Chapter 7 - respiratory physiology and care. In Arnold G. Coran, editor, *Pediatric Surgery (Seventh Edition)*, pages 109–122. Mosby, Philadelphia, seventh edition edition, 2012. ISBN 978-0-323-07255-7. doi: https://doi.org/10.1016/B978-0-323-07255-7.00007-6. URL https://www.sciencedirect.com/science/article/pii/B9780323072557000076.

Wang Xiaosong, Peng Yifan, Lu Le, Lu Zhiyong, Bagheri Mohammadhadi, and Summers Ronald. Chestx-ray8: Hospital-scale chest x-ray database and benchmarks on weakly-supervised classification and localization of common thorax diseases. *IEEE CVPR*, pages 3462–3471, 2017.

X Yang, Y Yu, and J Xu. Clinical course and outcomes of critically ill patients with sars-cov-2 pneumonia in wuhan, china: a single-centered, retrospective, observational

study. *The Lancet Respiratory Medicine*, 8:475–481, 2020. doi: https://doi.org/10.1016/s2213-2600(20)30079-5.

Koichi Yuki, Miho Fujiogi, and Sophia Koutsogiannaki. Covid-19 pathophysiology: A review. *Clinical Immunology*, 215:108427, 2020. ISSN 1521-6616. doi: https://doi.org/10.1016/j.clim.2020.108427. URL `https://www.sciencedirect.com/science/article/pii/S152166162030262X`.

L.A. Zadeh. Fuzzy sets, information and control. *Information Control*, 8:353–388, 1 1965.

H. Zhu and K. Moller. Ventilator control based on a fuzzy-neural network approach. pages 747 – 750, 06 2008. doi: 10.1109/ICBBE.2008.182.

Appendix

A) FUZZY SET RULES

Table 1: FiO_2 and low-PEEP Fuzzy set rules

1. If (FiO_2 is F1) and (PEEP is HP1) then (Change in PEEP is Increase)
2. If (FiO_2 is F1) and (PEEP is HP2) then (Change in PEEP is Increase)
3. If (FiO_2 is F1) and (PEEP is HP3) then (Change in PEEP is Increase)
4. If (FiO_2 is F1) and (PEEP is HP4) then (Change in PEEP is Increase)
5. If (FiO_2 is F1) and (PEEP is HP5) then (Change in PEEP is Increase)
6. If (FiO_2 is F1) and (PEEP is HP6) then (Change in PEEP is Increase)
7. If (FiO_2 is F1) and (PEEP is HP7) then (Change in PEEP is Increase)
8. If (FiO_2 is F1) and (PEEP is HP8) then (Change in PEEP is Increase)
9. If (FiO_2 is F2) and (PEEP is HP1) then (Change in PEEP is Increase)
10. If (FiO_2 is F2) and (PEEP is HP2) then (Change in PEEP is Maintain)
11. If (FiO_2 is F2) and (PEEP is HP3) then (Change in PEEP is Increase)
12. If (FiO_2 is F2) and (PEEP is HP4) then (Change in PEEP is Increase)
13. If (FiO_2 is F2) and (PEEP is HP5) then (Change in PEEP is Increase)
14. If (FiO_2 is F2) and (PEEP is HP6) then (Change in PEEP is Increase)
15. If (FiO_2 is F2) and (PEEP is HP7) then (Change in PEEP is Increase)
16. If (FiO_2 is F2) and (PEEP is HP8) then (Change in PEEP is Increase)
17. If (FiO_2 is F3) and (PEEP is HP1) then (Change in PEEP is Increase)
18. If (FiO_2 is F3) and (PEEP is HP2) then (Change in PEEP is Increase)
19. If (FiO_2 is F3) and (PEEP is HP3) then (Change in PEEP is Maintain)
20. If (FiO_2 is F3) and (PEEP is HP4) then (Change in PEEP is Increase)
21. If (FiO_2 is F3) and (PEEP is HP5) then (Change in PEEP is Increase)
22. If (FiO_2 is F3) and (PEEP is HP6) then (Change in PEEP is Increase)
23. If (FiO_2 is F3) and (PEEP is HP7) then (Change in PEEP is Increase)

Table 2: FiO_2 and low-PEEP Fuzzy set rules continuation

24. If (FiO_2 is F3) and (PEEP is HP8) then (Change in PEEP is Increase)
25. If (FiO_2 is F4) and (PEEP is HP1) then (Change in PEEP is Increase)
26. If (FiO_2 is F4) and (PEEP is HP2) then (Change in PEEP is Increase)
27. If (FiO_2 is F4) and (PEEP is HP3) then (Change in PEEP is Increase)
28. If (FiO_2 is F4) and (PEEP is HP4) then (Change in PEEP is Maintain)
29. If (FiO_2 is F4) and (PEEP is HP5) then (Change in PEEP is Increase)
30. If (FiO_2 is F4) and (PEEP is HP6) then (Change in PEEP is Increase)
31. If (FiO_2 is F4) and (PEEP is HP7) then (Change in PEEP is Increase)
32. If (FiO_2 is F4) and (PEEP is HP8) then (Change in PEEP is Increase)
33. If (FiO_2 is F5) and (PEEP is HP1) then (Change in PEEP is Increase)
34. If (FiO_2 is F5) and (PEEP is HP2) then (Change in PEEP is Increase)
35. If (FiO_2 is F5) and (PEEP is HP3) then (Change in PEEP is Increase)
36. If (FiO_2 is F5) and (PEEP is HP4) then (Change in PEEP is Increase)
37. If (FiO_2 is F5) and (PEEP is HP5) then (Change in PEEP is Maintain)
38. If (FiO_2 is F5) and (PEEP is HP6) then (Change in PEEP is Increase)
39. If (FiO_2 is F5) and (PEEP is HP7) then (Change in PEEP is Increase)
40. If (FiO_2 is F5) and (PEEP is HP8) then (Change in PEEP is Increase)
41. If (FiO_2 is F6) and (PEEP is HP1) then (Change in PEEP is Increase)
42. If (FiO_2 is F6) and (PEEP is HP2) then (Change in PEEP is Increase)
43. If (FiO_2 is F6) and (PEEP is HP3) then (Change in PEEP is Increase)
44. If (FiO_2 is F6) and (PEEP is HP4) then (Change in PEEP is Increase)
45. If (FiO_2 is F6) and (PEEP is HP5) then (Change in PEEP is Increase)
46. If (FiO_2 is F6) and (PEEP is HP6) then (Change in PEEP is Maintain)
47. If (FiO_2 is F6) and (PEEP is HP7) then (Change in PEEP is Increase)
48. If (FiO_2 is F6) and (PEEP is HP8) then (Change in PEEP is Increase)
49. If (FiO_2 is F7) and (PEEP is HP1) then (Change in PEEP is Increase)
50. If (FiO_2 is F7) and (PEEP is HP2) then (Change in PEEP is Increase)
51. If (FiO_2 is F7) and (PEEP is HP3) then (Change in PEEP is Increase)
52. If (FiO_2 is F7) and (PEEP is HP4) then (Change in PEEP is Increase)
53. If (FiO_2 is F7) and (PEEP is HP5) then (Change in PEEP is Increase)
54. If (FiO_2 is F7) and (PEEP is HP6) then (Change in PEEP is Increase)
55. If (FiO_2 is F7) and (PEEP is HP7) then (Change in PEEP is Maintain)
56. If (FiO_2 is F7) and (PEEP is HP8) then (Change in PEEP is Increase)
57. If (FiO_2 is F8) and (PEEP is HP1) then (Change in PEEP is Increase)
58. If (FiO_2 is F8) and (PEEP is HP2) then (Change in PEEP is Increase)
59. If (FiO_2 is F8) and (PEEP is HP3) then (Change in PEEP is Increase)
60. If (FiO_2 is F8) and (PEEP is HP4) then (Change in PEEP is Increase)

Table 3: FiO_2 and low-PEEP Fuzzy set rules continuation

61. If (FiO_2 is F8) and (PEEP is HP5) then (Change in PEEP is Increase)
62. If (FiO_2 is F8) and (PEEP is HP6) then (Change in PEEP is Increase)
63. If (FiO_2 is F8) and (PEEP is HP7) then (Change in PEEP is Increase)
64. If (FiO_2 is F8) and (PEEP is HP8) then (Change in PEEP is Maintain)
65. If (FiO_2 is F9) and (PEEP is HP1) then (Change in PEEP is Increase)
66. If (FiO_2 is F9) and (PEEP is HP2) then (Change in PEEP is Increase)
67. If (FiO_2 is F9) and (PEEP is HP3) then (Change in PEEP is Increase)
68. If (FiO_2 is F9) and (PEEP is HP4) then (Change in PEEP is Increase)
69. If (FiO_2 is F9) and (PEEP is HP5) then (Change in PEEP is Increase)
70. If (FiO_2 is F9) and (PEEP is HP6) then (Change in PEEP is Increase)
71. If (FiO_2 is F9) and (PEEP is HP7) then (Change in PEEP is Increase)
72. If (FiO_2 is F9) and (PEEP is HP8) then (Change in PEEP is Increase)
73. If (FiO_2 is F1) and (PEEP is HP9) then (Change in PEEP is Increase)
74. If (FiO_2 is F2) and (PEEP is HP9) then (Change in PEEP is Increase)
75. If (FiO_2 is F3) and (PEEP is HP9) then (Change in PEEP is Increase)
76. If (FiO_2 is F4) and (PEEP is HP9) then (Change in PEEP is Increase)
77. If (FiO_2 is F5) and (PEEP is HP9) then (Change in PEEP is Increase)
78. If (FiO_2 is F6) and (PEEP is HP9) then (Change in PEEP is Increase)
79. If (FiO_2 is F7) and (PEEP is HP9) then (Change in PEEP is Increase)
80. If (FiO_2 is F8) and (PEEP is HP9) then (Change in PEEP is Increase)
81. If (FiO_2 is F9) and (PEEP is HP9) then (Change in PEEP is Maintain)

Table 4: FiO_2 and high-PEEP Fuzzy set rules

1. If (FiO_2 is F1) and (PEEP is HP1) then (Change in PEEP is Increase)
2. If (FiO_2 is F1) and (PEEP is HP2) then (Change in PEEP is Increase)
3. If (FiO_2 is F1) and (PEEP is HP3) then (Change in PEEP is Increase)
4. If (FiO_2 is F1) and (PEEP is HP4) then (Change in PEEP is Increase)
5. If (FiO_2 is F1) and (PEEP is HP5) then (Change in PEEP is Increase)
6. If (FiO_2 is F1) and (PEEP is HP6) then (Change in PEEP is Increase)
7. If (FiO_2 is F1) and (PEEP is HP7) then (Change in PEEP is Increase)

Table 6: FiO_2 and high-PEEP Fuzzy set rules continuation

43. If (FiO_2 is F6) and (PEEP is HP3) then (Change in PEEP is Increase)
44. If (FiO_2 is F6) and (PEEP is HP4) then (Change in PEEP is Increase)
45. If (FiO_2 is F6) and (PEEP is HP5) then (Change in PEEP is Maintain)
46. If (FiO_2 is F6) and (PEEP is HP6) then (Change in PEEP is Increase)
47. If (FiO_2 is F6) and (PEEP is HP7) then (Change in PEEP is Increase)
48. If (FiO_2 is F6) and (PEEP is HP8) then (Change in PEEP is Increase)
49. If (FiO_2 is F7) and (PEEP is HP1) then (Change in PEEP is Increase)
50. If (FiO_2 is F7) and (PEEP is HP2) then (Change in PEEP is Increase)
51. If (FiO_2 is F7) and (PEEP is HP3) then (Change in PEEP is Increase)
52. If (FiO_2 is F7) and (PEEP is HP4) then (Change in PEEP is Increase)
53. If (FiO_2 is F7) and (PEEP is HP5) then (Change in PEEP is Increase)
54. If (FiO_2 is F7) and (PEEP is HP6) then (Change in PEEP is Maintain)
55. If (FiO_2 is F7) and (PEEP is HP7) then (Change in PEEP is Increase)
56. If (FiO_2 is F7) and (PEEP is HP8) then (Change in PEEP is Increase)
57. If (FiO_2 is F8) and (PEEP is HP1) then (Change in PEEP is Increase)
58. If (FiO_2 is F8) and (PEEP is HP2) then (Change in PEEP is Increase)
59. If (FiO_2 is F8) and (PEEP is HP3) then (Change in PEEP is Increase)
60. If (FiO_2 is F8) and (PEEP is HP4) then (Change in PEEP is Increase)
61. If (FiO_2 is F8) and (PEEP is HP5) then (Change in PEEP is Increase)
62. If (FiO_2 is F8) and (PEEP is HP6) then (Change in PEEP is Increase)
63. If (FiO_2 is F8) and (PEEP is HP7) then (Change in PEEP is Maintain)
64. If (FiO_2 is F8) and (PEEP is HP8) then (Change in PEEP is Increase)
65. If (FiO_2 is F9) and (PEEP is HP1) then (Change in PEEP is Increase)
66. If (FiO_2 is F9) and (PEEP is HP2) then (Change in PEEP is Increase)
67. If (FiO_2 is F9) and (PEEP is HP3) then (Change in PEEP is Increase)
68. If (FiO_2 is F9) and (PEEP is HP4) then (Change in PEEP is Increase)
69. If (FiO_2 is F9) and (PEEP is HP5) then (Change in PEEP is Increase)
70. If (FiO_2 is F9) and (PEEP is HP6) then (Change in PEEP is Increase)
71. If (FiO_2 is F9) and (PEEP is HP7) then (Change in PEEP is Increase)
72. If (FiO_2 is F9) and (PEEP is HP8) then (Change in PEEP is Maintain)

Table 7: Rules for high-PEEP algorithm 1 system

1. If (FiO_2 is F10) and (High-PEEP is HP1) then (Change-in-PEEP is Increase)
2. If (FiO_2 is F10) and (High-PEEP is HP2) then (Change-in-PEEP is Increase)
3. If (FiO_2 is F10) and (High-PEEP is HP3) then (Change-in-PEEP is Increase)
4. If (FiO_2 is F10) and (High-PEEP is HP4) then (Change-in-PEEP is Increase)
5. If (FiO_2 is F10) and (High-PEEP is HP5) then (Change-in-PEEP is Increase)
6. If (FiO_2 is F10) and (High-PEEP is HP6) then (Change-in-PEEP is Increase)
7. If (FiO_2 is F10) and (High-PEEP is HP7) then (Change-in-PEEP is Increase)
8. If (FiO_2 is F10) and (High-PEEP is HP8) then (Change-in-PEEP is Maintain)
9. If (FiO_2 is F9) and (High-PEEP is HP8) then (Change-in-PEEP is Decrease)
10. If (FiO_2 is F9) and (High-PEEP is HP7) then (Change-in-PEEP is Maintain)
11. If (FiO_2 is F8) and (High-PEEP is HP7) then (Change-in-PEEP is Decrease)
12. If (FiO_2 is F8) and (High-PEEP is HP6) then (Change-in-PEEP is Maintain)
13. If (FiO_2 is F7) and (High-PEEP is HP6) then (Change-in-PEEP is Decrease)
14. If (FiO_2 is F7) and (High-PEEP is HP5) then (Change-in-PEEP is Maintain)
15. If (FiO_2 is F6) and (High-PEEP is HP5) then (Change-in-PEEP is Decrease)
16. If (FiO_2 is F6) and (High-PEEP is HP4) then (Change-in-PEEP is Maintain)
17. If (FiO_2 is F5) and (High-PEEP is HP4) then (Change-in-PEEP is Decrease)
18. If (FiO_2 is F5) and (High-PEEP is HP3) then (Change-in-PEEP is Maintain)
19. If (FiO_2 is F4) and (High-PEEP is HP3) then (Change-in-PEEP is Decrease)
20. If (FiO_2 is F4) and (High-PEEP is HP2) then (Change-in-PEEP is Maintain)
21. If (FiO_2 is F3) and (High-PEEP is HP2) then (Change-in-PEEP is Decrease)
22. If (FiO_2 is F3) and (High-PEEP is HP1) then (Change-in-PEEP is Maintain)
23. If (FiO_2 is F2) and (High-PEEP is HP1) then (Change-in-PEEP is Maintain)
24. If (FiO_2 is F1) and (High-PEEP is HP1) then (Change-in-PEEP is Maintain)

Table 8: Rules for low-PEEP algorithm 1 system

1. If (FiO_2 is F10) and (Low-PEEP is HP1) then (Change-in-PEEP is Increase)
2. If (FiO_2 is F10) and (Low-PEEP is HP2) then (Change-in-PEEP is Increase)
3. If (FiO_2 is F10) and (Low-PEEP is HP3) then (Change-in-PEEP is Increase)
4. If (FiO_2 is F10) and (Low-PEEP is HP4) then (Change-in-PEEP is Increase)
5. If (FiO_2 is F10) and (Low-PEEP is HP5) then (Change-in-PEEP is Increase)
6. If (FiO_2 is F10) and (Low-PEEP is HP6) then (Change-in-PEEP is Increase)
7. If (FiO_2 is F10) and (Low-PEEP is HP7) then (Change-in-PEEP is Increase)
8. If (FiO_2 is F10) and (Low-PEEP is HP8) then (Change-in-PEEP is Maintain)
9. If (FiO_2 is F9) and (Low-PEEP is HP8) then (Change-in-PEEP is Decrease)
10. If (FiO_2 is F9) and (Low-PEEP is HP7) then (Change-in-PEEP is Maintain)
11. If (FiO_2 is F8) and (Low-PEEP is HP7) then (Change-in-PEEP is Decrease)
12. If (FiO_2 is F8) and (Low-PEEP is HP6) then (Change-in-PEEP is Maintain)
13. If (FiO_2 is F7) and (Low-PEEP is HP6) then (Change-in-PEEP is Decrease)
14. If (FiO_2 is F7) and (Low-PEEP is HP5) then (Change-in-PEEP is Maintain)
15. If (FiO_2 is F6) and (Low-PEEP is HP5) then (Change-in-PEEP is Decrease)
16. If (FiO_2 is F6) and (Low-PEEP is HP4) then (Change-in-PEEP is Maintain)
17. If (FiO_2 is F5) and (Low-PEEP is HP4) then (Change-in-PEEP is Decrease)
18. If (FiO_2 is F5) and (Low-PEEP is HP3) then (Change-in-PEEP is Maintain)
19. If (FiO_2 is F4) and (Low-PEEP is HP3) then (Change-in-PEEP is Decrease)
20. If (FiO_2 is F4) and (Low-PEEP is HP2) then (Change-in-PEEP is Maintain)
21. If (FiO_2 is F3) and (Low-PEEP is HP2) then (Change-in-PEEP is Decrease)
22. If (FiO_2 is F3) and (Low-PEEP is HP1) then (Change-in-PEEP is Maintain)
23. If (FiO_2 is F2) and (Low-PEEP is HP1) then (Change-in-PEEP is Maintain)
24. If (FiO_2 is F1) and (Low-PEEP is HP1) then (Change-in-PEEP is Maintain)